Division of Pharmaceutical Chemistry and Technology
Faculty of Pharmacy
University of Helsinki
Finland

Transdermal Iontophoresis – Delivery Control by Ion-Exchange Fibers and Nanocarriers

by

Kristina Malinovskaja-Gomez

ACADEMIC DISSERTATION

To be presented, with the permission of the Faculty of Pharmacy of the University of Helsinki, for public examination in Auditorium 1, Infocenter Korona (Viikinkaari 11), on October 7th 2016, at 12.00 noon.

Helsinki 2016

Supervisors Professor and Dean Jouni Hirvonen
Division of Pharmaceutical Chemistry and Technology
Faculty of Pharmacy
University of Helsinki
Finland

Docent Timo Laaksonen
Division of Pharmaceutical Biosciences
Faculty of Pharmacy
University of Helsinki
Finland

Reviewers Professor Reinhard Neubert
Department of Pharmaceutical Technology and Biopharmaceutics
Institute of Pharmacy
Martin Luther University of Halle-Wittenberg
Germany

Associate Professor Johan Engblom
Research Center for Biointerfaces
Faculty of Health and Society
Malmö University
Sweden

Opponent Professor Yogeshvar N. Kalia
School of Pharmaceutical Sciences
University of Geneva
Switzerland

ISBN 978-951-51-2441-8 (Paperback)
ISBN 978-951-51-2442-5 (PDF)
ISSN 2342-3161 (Print)
ISSN 2342-317X (Online)

Hansaprint Oy
Turenki 2016

ABSTRACT

Malinovskaja-Gomez., 2016. **Transdermal iontophoresis – delivery control by ion-exchange fibers and nanocarriers.**

Dissertationes Scholae Doctoralis Ad Sanitatem Investigandam Universitatis Helsinkiensis, 61/2016, pp. 76
ISBN 978-951-51-2441-8 (Paperback), ISBN 978-951-51-2442-5 (PDF, http://ethesis.helsinki.fi), ISSN 2342-3161

Biological variation and poor transport efficacy are the major concerns in the development of novel iontophoretic drug delivery systems for the transdermal administration of therapeutics. One possibility to overcome these limitations would be to load the drug in interest into a reservoir system such as ion-exchange fibers or nanocarriers prior administration. More precise and homogenous control of drug release and the following transdermal iontophoretic permeation could be obtained as the transdermal device/patch would determine the rate of drug transfer instead of the skin, leading to smaller inter- and intrasubject variability. In addition, the range of molecules delivered by iontophoresis can be expanded as charges could be imparted to neutral drugs by encapsulating them in charged drug carriers. Other benefits raising from such combined systems include enhanced drug transport into or across the skin, improved drug stability and decreased local side effects on skin.

The aim of this thesis was to study *in vitro* the applicability of systems that combine iontophoresis and either drug-loaded ion-exchange fibers or nanocarriers for the controlled transdermal delivery of therapeutics.

Firstly, drug reservoirs based on cation-exchange fibers were utilized to retard drug release and provide additional control into transdermal transport of a small molecular drug and a peptide. The drug release kinetics could be modified by the choice of the fiber type or the ionic composition of the external solution. The application of pulsed current iontophoresis instead of conventional constant current led to increased transport efficiency of a cationic hydrophobic peptide that has a tendency to adsorb into skin and inhibit electroosmosis as its main transport mechanism. In addition, drug delivery systems combining iontophoresis and nanoencapsulation into polymeric nanoparticles or lipid vesicles for the controlled transdermal delivery of lipophilic or hydrophilic model compound were developed and tested. Although the obtained nanocarriers were considered as suitable for transdermal iontophoretic administration, regarding the colloidal properties, stability and release kinetics, no clear advantage was observed with respect to drug permeation from free drug formulation. Throughout the thesis, the impact of formulation parameters and current type on drug transport efficiency was monitored. Iontophoretic transdermal drug delivery from polymeric nanoparticle-based formulations but not from lipid vesicular nanocarriers was improved by the application of pulsed current.

In conclusion, binding the drug molecules prior iontophoresis into reservoir based on ion-exchange material or nanocarriers is a promising approach to be utilized in controlled transdermal delivery, although the comprehensive evaluation of full potential of such systems tailored for specific drug warrants further investigation in the future.

ACKNOWLEDGEMENTS

This work was carried out at the Division of Pharmaceutical Chemistry and Technology, Faculty of Pharmacy, University of Helsinki during the years of 2011-2016.

I gratefully acknowledge all the funding sources that made my doctoral thesis possible, including Estonian Ministry of Education and Research and Finnish Ministry of Education and Culture.

I express my warmest gratitude to my supervisor professor Jouni Hirvonen for giving me a chance to join his research group at the University of Helsinki and introducing me his world of transdermal iontophoresis, for positive attitude and endless optimism during these years.

I would also like to thank my second supervisor, Docent Timo Laaksonen for his trust and valuable discussions. He was always available when help or encouragement was needed.

A special acknowledgement to my supervisors in Germany and Spain, professor Marc Schneider, Hagar Labouta, Maria J. Garrido and Socorro Espuelas for their hospitality and sincere cooperation. Also, I wish to thank all the other co-authors for their generous contribution to this work.

Professor Reinhard Neubert and professor Johan Engblom are sincerely thanked for reviewing this thesis and providing valuable suggestions for its improvement.

My deepest gratitude to Dr. Silvia Pescina from University of Pavia for her useful tips on skin preparation and iontophoretic experiments, professor Lasse Murtomäki for the expertise on ion-exchange, Dr. Mardiyanto for the training on the preparation of polymeric nanoparticles, and Tatu Lajunen on the liposomes.

I am grateful to all the colleagues of Departement of Pharmaceutical Chemistry and Technology and Centre of Drug Research for the pleasant and friendly working atmosphere. I wish to thank especially Tiina, Päivi, Ruzica, Sreevani, Peng and Heli for wonderful funny moments and for making me feel like at home in Finland.

I would also like to express my warmest gratitude to my Estonian friends (Ines, Eleri, Piret E., Liis, Jaana, Piret R.) for their friendship and taking my mind out of the work from time to time.

I thank my parents, Anne and Valeri, for their understanding and trust in me to stubbornly follow my own path.

Finally, my warmest thanks to my dear husband José David for his unconditional love and support, and to my little girl, Maite, for being the sunshine of my life.

Helsinki, September 2016

Kristina Malinovskaja-Gomez

To Ana Maite

CONTENTS

LIST OF ORIGINAL PUBLICATIONS

This thesis is based on the following publications:

I **Malinovskaja K**, Laaksonen T, Kontturi K, Hirvonen J. Ion-exchange and iontophoresis-controlled delivery of apomorphine. Eur J Pharm Biopharm. 2013; 83(3): 477-84.

II **Malinovskaja K**, Laaksonen T, Hirvonen J. Controlled transdermal delivery of leuprorelin by pulsed iontophoresis and ion-exchange fiber. Eur J Pharm Biopharm. 2014; 88(3): 594-601.

III **Malinovskaja-Gomez K**, Labouta H I, Schneider M, Hirvonen J, Laaksonen T. Transdermal iontophoresis of flufenamic acid loaded PLGA nanoparticles. Eur J Pharm Sci. 2016; 89: 154-162.

IV **Malinovskaja-Gomez K**, Espuelas S, Garrido M. J, Hirvonen J, Laaksonen T. Transdermal iontophoretic drug delivery from various liposome-encapsulated formulations. Submitted manuscript, 2016.

The publications are referred to in the text by their roman numerals. The papers I-III are reprinted with the kind permission of Elsevier.

ABBREVIATIONS AND SYMBOLS

A	surface area
ACN	acetonitrile
AC	alternating current
BA^+	benzalkonium cation
cap	loading capacity
c_d	molar concentration of drug ion
c_i	molar concentration of ion
c_{ss}	steady-state concentration
CL	clearence
D	diffusion coefficient
DC	direct current
DDAB	dimethyldiooctadecylammonium bromide
DODAP	1,2- dioleoyl-3-dimethylammonium propane
DOSPER	(1,3-dioleoyloxy-2-(6-carboxyspemyl) propylamide (tetraammonium tetraacetate)
DOTAP	1,2- dioleoyl-3-trimethylammonium propane
DMAP	1-ethyl-3-(3-dimethylaminopropyl)-carbodiimide
E	iontophoretic enhancement factor
F	Faraday constant
FA	5-fluoresceineamine
FA-PLGA	5-fluoresceineamine-bound poly(lactic-co-glycolic acid)
FFA	flufenamic acid
HEPES	4-(2-hydroxyethyl)-1-piperazineethanesulphonic acid
HPLC	high performance liquid chromatography
I	current
$I\%$	percent of ionization
J_{EO}	electroosmotic flux
$J_{iontophoresis}$	iontophoretic steady-state flux
$J_{passive,}$ J_P	passive flux
J_{ss}	steady-state flux
LHRH	luteinizing-hormone-releasing hormone
$\log P_{oct}$	octanol/water partition coefficient
MeOH	methanol
MRM	multiple reaction monitoring
MW	molecular weight
MWCO	molecular weight cut off
$[n^+]$	molar amount of extracting electrolyte (counter-ion) which is based on the loaded amount of model compound
NSAID	non-steroidal anti-inflammatory drug
PC	pulsed current
PDI	polydispersity index
pKa	dissociation constant

PLGA	poly(lactic-co-glycolic acid)
PVA	polyvinyl alcohol
Q	cumulative amount
R	gas constant
SD	standard deviation
SEM	standard error of the mean
Smopex®-101	styrene sulphonic acid grafted polypropylene fiber
Smopex®-102	acrylic acid grafted polypropylene fiber
T	absolute temperature
TEA^+	tetraethylammonium cation
TQ-S	triplequadrupole mass spectrometer
UPLC-ESI-MS	ultra-performance liquid chromatography combined with electrospray ionization mass spectrometry
T_n, t_d	transport number
z	valence
z_d	charge number (valence) of drug ion
z_i	charge number (valence) of ion
μ	chemical potential
μ_d	mobility of drug ion
μ_i	mobility of ion
ϕ	electrical potential

1 INTRODUCTION

Transdermal drug delivery route is an appealing alternative to minimize and avoid the limitations linked to oral and parenteral administration of therapeutics (Thomas and Finnin, 2004). It can overcome problems related to poor gastrointestinal absorption, hepatic first-pass metabolism, and variable bioavailability. In addition, patient compliance can be improved by reducing the frequency of the dosing due to the continuous input of the drug. However, since the approval of the first transdermal drug delivery system (TDDS) in 1979, this mode of administration has been clinically realized only for a limited number of drugs (less than two dozen) owing to the formidable barrier properties of the outermost layer of skin, the *stratum corneum* (Naik et al., 2000). Therefore, only extremely potent therapeutics possessing appropriate balance of hydro-/lipophilicity, small size and no charge are able to pass this layer passively in pharmacologically relevant amounts. In order to overcome the resistant barrier function of the skin and to expand the range of compounds that can be delivered transdermally, a number of strategies have been developed to facilitate the transdermal transport, either by improving the permeability properties of the *stratum corneum* or by providing a driving force acting directly on the drug (Gratieri et al., 2013; Parhi et al., 2012).

Unlike other physical techniques that tend to disrupt the skin barrier during promoting the transdermal flux, iontophoresis acts on the drug molecule itself (Kalia et al., 2004). It applies a mild external electric current (up to 0.5 mA/cm^2) to enhance the permeation of ionized and neutral compounds across biological membranes. The drug dose delivered by iontophoresis is directly proportional to the amount of charge passed through the skin and can be therefore controlled by the electric input of the iontophoretic system: current density, type of the current and the application time of iontophoretic treatment. Neveretheless, iontophoresis does not eliminate passive flux variability and, therefore, does not always achieve true controlled delivery where the rate of drug input is modulated in a precisely controlled manner by a patch or a device (Delgado-Charro and Guy, 2003; Guy and Hadgraft, 1992). Another major limitation is that that only charged and relatively small molecules are predominantly transported by the electrorepulsion mechanism that benefit the most from this enhancement technique.

One possibility to achieve more homogenous and reproducible transdermal drug delivery by iontophoresis would be to load the drug into ion-exchange materials such as ion-exchange fibers or nanocarriers prior to the administration. Once the drug has been gradually released from the fiber/ nanocarriers onto skin surface or into skin, iontophoresis can pump it into deeper skin layers for topical or systemic purposes. The combination of both the systems may provide a constant rate of input into the systemic circulation, resulting in drug transport which is less dependent on skin

variables. In addition, the range of molecules delivered by iontophoresis can be expanded to neutral and large drugs by encapsulating them in charged nanocarriers. Other possible benefits from transdermal drug delivery from drug-loaded ion-exchange fibers or nanocarriers in conjunction with transdermal iontophoresis include enhanced drug transport into or across the skin, improved drug stability and decreased local side effects on the skin.

One of the major concerns in iontophoretic drug delivery is the low transport efficiency of drug molecules. Therefore, it is important to consider the impact of all the various formulation, electrical and biological factors involved in the process (Banga, 2002). A common problem in the development of formulations for iontophoretic drug delivery is the presence of co-ions from the buffering agents that are usually smaller and more mobile than the drug molecules, and will reduce the fraction of the current carried by the drug. Also, the choice of current type can significantly affect the outcome of iontophoresis. The continuous application of direct current iontophoresis is typically considered as the most efficient way of transdermal delivery as the amount of drug transported is directly proportional to the total amount of current passed through the skin. However, problems related to long-term continuous use of direct current (skin polarization, risk of electrochemical burns) could be sometimes overcome by a current delivered in a pulsatile or alternating mode. Another major challenge is the delivery of large or neutral molecules such as peptides that are transported mainly by electroosmosis and are able to inhibit their own transport by neutralizing the negative charge of the skin membrane.

The main goal of this thesis was to study *in vitro* the applicability of a system that combines iontophoresis and drug-loaded ion-exchange fibers or nanocarriers for the controlled transdermal delivery of therapeutics. Firstly, the transdermal delivery of small molecules and peptides were tested from a combined system of ion-exchange fibers and iontophoresis. The changes in mechanisms involved in the iontophoretic transport of cationic peptides were evaluated and different current profiles were tested to increase the transdermal delivery. Secondly, two different types of biocompatible drug-loaded nanocarriers were combined with iontophoresis – polymeric PLGA nanoparticles and liposomes, and the effect of nanoencapsulation was investigated on the model drugs´ permeation across the skin barrier. Throughout the thesis, appropriate strategies to enhance iontophoretic transport efficiency of therapeutics was set as one of the aims, while determining the impact of both formulation parameters and current type on transdermal drug transport.

2 REVIEW OF THE LITERATURE

2.1 Transdermal drug delivery

Transdermal drug delivery is a painless method of delivering drugs systematically by applying a drug formulation onto intact and healthy skin (Guy and Hadgraft, 2002; Williams, 2003). Topical therapy to treat local indications of skin has been practiced for a long period of time. With the approval of first transdermal system in 1979 − scopolamine patch to treat motion sickness (Shaw and Urquhart, 1979) − transdermal drug delivery began to foster as a systemic mode of administration for therapeutics. This delivery mode has a variety of advantages compared to the oral route (Prausnitz and Langer, 2008; Wiedersberg and Guy, 2014). It can overcome problems related to poor gastrointestinal absorption, hepatic first-pass metabolism, and variable bioavailability. Furthermore, it can lead to controlled, continuous administration of the drug, even in the cases of drugs with short biological half-lives. As a result, constant therapeutic plasma concentrations can be achieved and the frequency of the administration can be significantly reduced, improving patient compliance. In the case of toxic effects, the drug input can be terminated, which is particularly indispensable for drugs with narrow therapeutic window. In addition, transdermal systems are non-invasive and can be self-administered, and are therefore an attractive alternative to hypodermic injections, which are painful, generate dangerous medical waste and increase the risk of disease transmission by the needles.

Skin is the largest and most accessible organ in the body with a surface area of about 2 m^2, occupying about 15% of the total body weight of an average person. It is composed of an outermost layer, epidermis, an inner dermis and underlying subdermal tissue (Berti and Lipsky, 1995; Williams, 2003). Epidermis consists predominantly of keratinocytes (95% of cells), Langerhans cells and Merkel cells. The most superficial layer of epidermis, *stratum corneum* (also called as horny layer) is a dead layer of skin with a rigidly arranged "brick and mortar" structure. This least permeable skin layer is the ultimate stage in the differential process of epidermis, consisting of compressed keratin-filled corneocytes ("bricks") anchored in a lipophilic matrix of ceramides, fatty acids, cholesterol and cholesterol esters ("mortar"). Skin appendages, including hair follicles and sebaceous and sweat glands occupy about 0.1 % of skin surface.

The principal barrier to percutaneous absorption resides in the *stratum corneum* and there are two main routes for drug permeation (Fig. 1). The transepidermal pathway through epidermis can take place between the cells (intercellular) or through the cells (transcellular) (Williams, 2003). The contribution of these routes depends on the solubility, partition coefficient and diffusivity of the drug within lipid or protein phases (Farahmand and Maibach, 2009; Hadgraft and Guy, 2002; Vecchia and Bunge, 2002). The intercellular route allows the passage of lipophilic or

nonpolar molecules, while intracellular route allows the transport of hydrophilic or polar solutes. The transappendageal route involves the drug transport through sweat glands and hair follicles. For a long time, skin appendages were not considered to be a significant transdermal penetration route, as they account for only a very small skin surface area. By now it has been well established that the follicular penetration route may be especially relevant for hydrophilic and high molecular weight molecules, as well as for particle-based drug delivery systems or in drug transport by iontophoresis (Craane-van Hinsberg et al., 1995; Knorr et al., 2009).

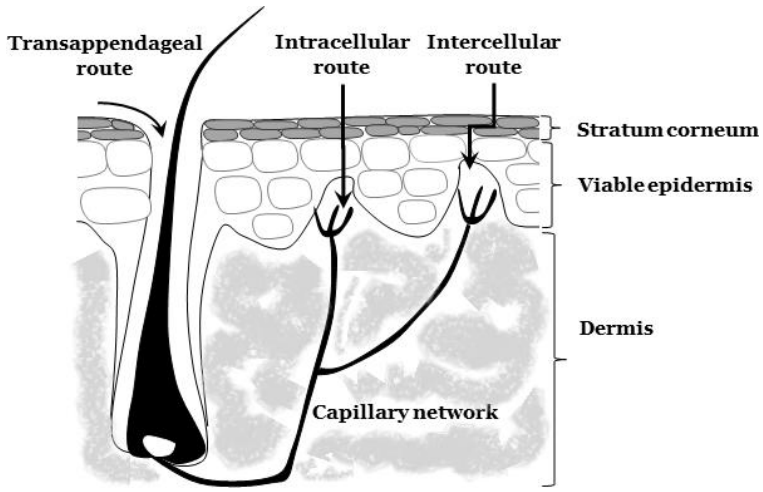

Figure 1. Pathways in transdermal drug delivery.

Although being an attractive alternative to oral and parenteral administration, the clinical use of the transdermal route has remained limited due to the formidable barrier properties of the outermost layer of skin, the *stratum corneum*. The diffusional resistance provided by this layer means that only less than 10 mg of drug can be delivered systematically per day using a reasonable "patch size" area for permeation. Therefore, only a very limited number of molecules are able to pass across this layer passively in therapeutic amounts. For a drug to be a successful transdermal candidate certain criteria need to be met. Firstly, transdermal delivery is suitable only for very potent drugs (Guy, 2010). Secondly, the molecule must possess the necessary physicochemical properties (Table 1) in order to be transported across the *stratum corneum* (Aulton and Taylor, 2013; Naik et al., 2000). For transdermal delivery, the drug molecule must first pass the multiple lipid bilayers between the corneocytes and then the more aqueous environment of the viable epidermis to enter the systemic circulation. Therefore, ideally the the drug molecule should possess both lipoidal and aqueous solubilities: too hydrophilic compunds will not be able to diffuse through *stratum corneum*, while too lipophilic drugs will have problem with clearance into blood circulation. The molecular weight of the drug also impacts dramatically on its transport across the skin as the diffusity across the *stratum corneum* decreases as molecular volume (and hence molecular weight) increases.

Therefore, skin barrier prevents efficiently the entry of larger molecules such as peptide or proteins into body.

Table 1. Physicochemical considerations for passive transdermal drug delivery (modified from Naik et al., 2000).

Molecular weight	400-500 Da
Solubility in water	>1 mg ml^{-1}
Lipophilicity	10 <$K_{o/w}$< 1000
Melting point	< 200 °C
pH of saturated aqueous solution	pH 5-9

The presently approved drugs in the United States and Europe for passive transdermal delivery are presented in Table 2 (Pastore et al., 2015; Wiedersberg and Guy, 2014). The limited number of molecules in this list reflects the major challenge in transdermal drug delivery – the difficulty of finding molecules both with high pharmacological potency and skin permeability.

Table 2. Currently approved transdermally delivered drugs. Modified from Pastore et al., 2015 and Wiedersberg and Guy, 2014.

Drug	Year of approval	Indication
Scopolamine	1979	Motion sickness
Glycerol trinitrate	1981	Angina pectoralis
Clonidine	1984	Hypertension
Estradiol	1986	Female HRT
Fentanyl	1990	Chronic pain
Nicotine	1991	Smoking cessation
Testosterone	1993	Hypogonadism
Estradiol & Norethisterone Acetate	1998	Female HRT
Ethinyl Estradiol & Norelgestromin	2001	Female contraception
Estradiol & Levonorgestrel	2003	Female HRT
Oxybutynin	2003	Overactive bladder
Selegeline	2006	Depression
Methylphenidate	2006	ADHD
Rotigotine	2007	Parkinson´s disease, Restless leg syndrome
Rivastigmine	2007	Alzheimer´s and Parkinson´s disease
Granisetron	2008	Chemotherapy induced emesis
Buprenorphine	2010	Chronic pain

The influence of these physicochemical criteria can also be translated into the Fickian relationship that describes the passive permeation of a compound across the *stratum corneum* that serves as a rate limiting barrier in transdermal drug delivery (Banga, 2002; Naik et al., 2000):

$$J_{ss} = \frac{D*K_{sc/veh}}{h} * \ c_{veh} = K_p \ * c_{veh} \qquad \text{(Eq. 1)}$$

where J_{ss} is the steady-state transdermal flux, D is the diffusion coefficient of the drug, h is the thickness of the skin, $K_{sc/veh}$ is the partition coefficient of the drug between *stratum corneum* and vehicle, c_{veh} is the concentration of the drug in vehicle and K_p is the permeability coefficient of the drug. As seen from this equation, the strategies to increase transdermal bioavailability include increasing the diffusivity of the drug and partitioning in the *stratum corneum*, and increasing the drug concentration in the formulation (Naik et al., 2000; Zhang et al., 2013). Overall, drug absorption from a transdermal delivery system involves the following steps: 1) release from formulation 2) penetration into the *stratum corneum* and permeation/diffusion through it, and 3) partitioning into deeper layers of skin. For most of the formulations, drug partitioning into the *stratum corneum* is the rate limiting step in drug permeation. The major goal in designing controlled transdermal delivery systems is that the patch/device, not the skin, would control the rate of drug transport across the skin, leading to more reproducible and safer drug delivery (Guy and Hadgraft, 1992; Shaw et al., 1976; Shaw and Theeuwes, 1985).

2.2 Enhancement of transdermal permeation

2.2.1 Passive and active enhancement techniques

In order to overcome the formidable barrier function of the skin and to expand the range of compounds that can be delivered transdermally, a number of strategies have been developed to increase transport across or into the skin by enhancing the permeability properties of the *stratum corneum* (passive penetration enhancement) or providing a driving force acting directly on the drug (active penetration enhancement) itself (Herwadkar and Banga, 2012; Parhi et al., 2012).

Passive enhancement techniques include the use of prodrugs or chemical enhancers.

- The basis of the pro-drug approach is the modification of the initial therapeutic entity by the addition of promoiety in order to facilitate its permeation, although being designed later to yield the parent drug after enzymatic or chemical release (Sloan and Wasdo, 2007). Due to the lipid-aqueous biphasic structure of skin, the prodrugs need to incorporate functional groups in the promoiety that will increase not only the lipid but also the aqueous solubility (Sloan and Wasdo, 2003).

- The most extensively investigated enhancement strategy involves the use of chemical enhancers which facilitate drug permeation into the systemic circulation by reversely compromising the barrier function of *stratum corneum.* Examples of commonly used chemical enhancers include alcohols, polyalcohols, pyrrolidones, sulphoxides, essential oils, fatty acids, surfactants, terpenes etc. Most of them have mixed mode of action, such as: increased fluidity of *stratum corneum* lipid bilayers, disruption or extraction of intercellular lipids, interactions with intercellular proteins, increased thermodynamic activity of the drug or increased *stratum corneum* hydration (Thong et al., 2007; Walters and Hadgraft, 1993). The major problem that constrains the use of these substances is that the increased permeation enhancement activity is typically closely correlated with skin irritation. Therefore, a great deal of research continues to identify generally regarded as safe (GRAS) substances with permeation-enhancing effects or to develop new enhancers with reduced toxicity (Akimoto et al., 2001; Karande et al., 2005).
- Newer innovative approaches with supramolecular structures, such as vesicular systems, dendrimers and microemulsions, have also been utilized to improve dermal or transdermal drug delivery. These systems do not only increase skin permeability but also drug partitioning into the skin (Cheng et al., 2007; Khan et al., 2015; Kogan and Garti, 2006).

Active enhancement methods for transdermal delivery use some kind of external energy as a driving force for drug transport across skin or physical disruption the *stratum corneum* (Gratieri et al., 2013; Mitragotri, 2013). These approaches allow a broader class of therapeutics to be administered effectively across the skin, including peptides, proteins and oligonucleotides that are typically large and polar/charged. In addition, the active methods have the ability to provide more controlled and reproducible delivery compared to the passive techniques, leading to smaller inter- and intrasubject variability.

- The most evolved of these technologies, iontophoresis, uses a mild electric current (0.5 mA/cm^2 or less) to facilitate the transport of charged and polar molecules across the skin. Unlike all the other enhancement strategies, iontophoresis acts on the molecule itself by repelling the drug molecules as a result of an electrical potential gradient across the skin (Gratieri and Kalia, 2013). The drug dose delivered can be directly controlled by the current density, duration and profile of the current application.
- Electroporation utilizes short-term (10 μs - 500 ms) high-voltage (50-1500 V) pulses to create transient aqueous pathways in the lipid bilayer of the skin (Denet et al., 2004; Prausnitz, 1999). Although *in vitro* this technique has been demonstrated to be more effective than iontophoresis, clinical and toxicological data of transdermal electroporation *in vivo* has remained limited.

- Sonophoresis (or phonophoresis) refers to the use of ultrasound (sound of frequency greater than 20 kHz) to compromise the barrier properties of skin. Ultrasound enhances drug transport by combined mechanisms of thermal, mechanical and chemical changes in skin tissue and formation of small gaseous pockets (cavitation) within cells (Azagury et al., 2014; Oberli et al., 2014). Commonly used frequencies in sonophoresis can be separated as low-frequency sonophoresis (LFS; frequency 20-200 kHz) and high-frequency sonophoresis (HFS; frequency 0.7-16 MHz). The permeation enhancement by sonophoresis is dependent on the length of ultrasound pulse and energy dose.
- Microneedles are small micron-sized needles that are able to painlessly disrupt the barrier of skin and create pores, resulting in increased drug penetration (Ita, 2015; Prausnitz, 2004; van der Maaden et al., 2012). Drugs can be delivered either by applying a drug patch at the treated site ("poke and patch" approach), coating the drug onto microneedles ("coat and poke" approach), encapsulating the drug into biodegradable microneedles ("poke and release" approach), or by injecting the drug through hollow microneedles ("poke and flow" approach). One of the most attractive applications of the microneedle arrays is to utilize them in vaccination, especially, in self-vaccination strategies.
- High-velocity jet injectors provide a needless alternative to traditional injections by painlessly administering small molecules or proteins with a device which delivers either powders or liquids into the skin at high velocity (100-200 m/s). Either compressed gas or spring is used as a power source for jet injectors and drugs can be administered either intradermally, subcutaneously or intramuscularly, depending on the velocity of jet and the diameter of the orifice of the device (Hogan et al., 2015; Stachowiak et al., 2009).
- Thermal ablation is a method that facilitates the entry of drugs through skin by heating the surface of skin, causing a depletion of *stratum corneum* at the heating site (Shahzad et al., 2015). Methods such as laser or radiofrequency can be applied to result in thermal ablation. In radiofrequency thermal ablation skin is exposed to high frequency alternating current (100-500 kHz) that causes ionic vibrations in the skin, leading ablation of cells in that region (Levin et al., 2005; Sintov et al., 2003). Laser ablation uses deposition of optical energy that leads to evaporation of water and formation of small channels in skin barrier (Sklar et al., 2014). P.L.E.A.S.E.® technology based on fractional laser technology has been successfully utilized even in the percutaneous delivery of therapeutic proteins and in transcutaneous immunization with protein antigens (Weiss et al., 2012; Yu et al., 2011).

2.2.2 Iontophoresis

Iontophoresis is based on the general principle that like charges repel and opposite charges attract each other (Fig. 2). Typically, two electrode chambers are placed on the skin, and on the application of iontophoretic current the drug is repelled from the electrode of the same polarity as the charge of the drug (active electrode) and is driven across the *stratum corneum* towards the electrode of opposite polarity (counter-electrode). The idea of using electric current in drug delivery dates back already to the mid-18th century (Helmstadter, 2001). One of the first well described experiments of medication transfer by electricity across skin originates from 1879, when German Hermann Munk exposed rabbits to an electrified strychnine solution for 20-25 minutes, followed by spontaneous cramps.

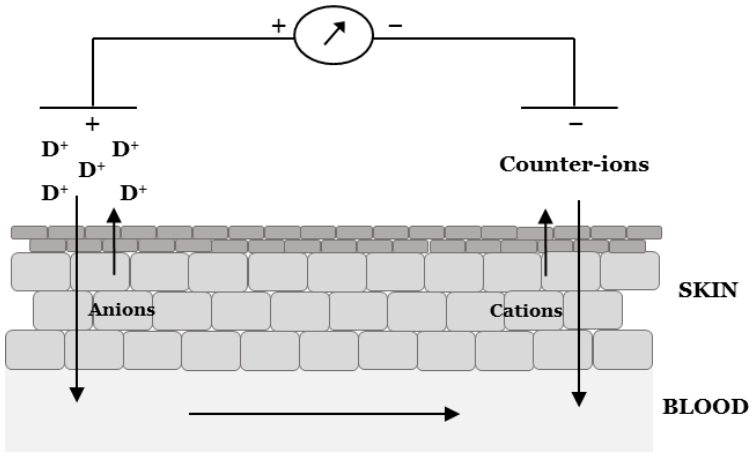

Figure 2. Schematic diagram of the transdermal iontophoretic delivery of a positively charged drug (D^+).

Along with the benefits applicable to passive transdermal delivery (bypassing hepatic metabolism and higher patient compliance), the additional advantages that iontophoretic delivery offers can be summarized as follows (Bodde et al., 1989; Kalia et al., 2004; Sieg and Wascotte, 2009; Singh et al., 1995):

- Delivery of both unionized and ionized drugs
- Suitable both for topical or systemic delivery of drugs
- Better control over the drug dose delivered
- Control over drug administration kinetics, enabling continuous or pulsatile delivery
- Minor skin membrane disruption and irritation
- Enhanced delivery of polar and high molecular weight compounds
- Easy termination of drug delivery in the case of toxicity with very potent drugs
- Reduced inter- and intrasubject variability

The main limitation for iontophoresis resides in the fact that this enhancement approach is restricted mainly to drugs that can be formulated in an ionized form, as for neutral molecules the only iontophoretic transport mechanism would be electroosmosis, which is much less effective than electrorepulsion (Pikal, 2001). Also, although mostly related to operator error or incorrect choice of electrodes and/or formulation composition, cutaneous adverse effects such as skin erythema, burns and pain have been observed occasionally (Curdy et al., 2001). Another risk is that material defects in the iontophoretic system could lead to toxic systemic effects with drugs of narrow therapeutic index (Prescrire, 2009). In addition, iontophoretic devices are typically more expensive than conventional topical preparations (Roustit et al., 2014).

Iontophoresis facilities transdermal drug delivery by three main mechanisms (Hirvonen, 2005):

1) Electrorepulsion (also called electromigration) that is the ordered movement of ions in the presence of applied electric field. Typically it is considered the most important transport mechanism but only charged molecules will benefit from that.

2) Electroosmosis (also called convective solvent flow) is the flow of water across the skin caused by the movement of charges across a membrane under electric current (Kalia et al., 2004). Application of electric field across a charged membrane induces the movement of counter-ions that try to neutralize the membrane charge. Under physiological conditions the skin is negatively charged (pI=4-4.5) and acts as a cation-selective membrane (Marro et al., 2001). Therefore, electroosmosis contributes to the flux of positively charged and uncharged molecules but opposes negatively charged molecules (Burnette and Ongpipattanakul, 1987). Also, since the electrical mobility decreases with increasing molecular weight, it has been hypothesized that the electrotransport of larger molecules such as peptides and proteins is predominantly driven by electroosmosis (Kalia et al., 2004).

3) Enhanced passive permeability of the skin by the flow of electric current, although typically the passive diffusion is considered negligible in the total flux of drug.

Therefore, the total iontophoretic flux (J_i) of a compound *i* across the skin during iontophoresis is the sum of electrorepulsion (J_R), electroosmosis (J_{EO}), and passive diffusion (J_P) contributions:

$$J_i = J_R + J_{EO} + J_P \qquad \text{(Eq. 2)}$$

In more detail, the iontophoretic flux of a compound can be described by Nernst-Planck equation (Finkelstein and Mauro, 2011):

$$J_i = \underbrace{-D_i \frac{dc_i}{dx}}_{\text{Passive diffusion}} - \underbrace{\frac{z_i F}{RT} c_i D_i \frac{d\Phi}{dx}}_{\text{Electrorepulsion}} + \underbrace{\upsilon^c c_i}_{\text{Convective flux}} \qquad \text{(Eq. 3)}$$

where D_i is the diffusion coefficient of the compound i, c_i its concentration, z_i its charge number, F is the Faraday constant, R is the gas constant, T is the absolute temperature, ϕ is the electrical potential and v^c is the solvent velocity.

The efficiency of the drug transport by iontophoresis can be described by a transport number (t_d) that reflects the proportion of the current carried by the drug, as compared to other migrating species in formulation, and is determined by its mobility (μ_d), charge (z_d) and concentration (c_d) (Phipps and Gyory, 1992):

$$t_d = \frac{\mu_d * z_d * c_d}{\sum_i \mu_i * z_i * c_i} \quad \text{(Eq. 4)}$$

The outcome of iontophoretic delivery of solutes into or across the skin can be affected by a number of variables, including physicochemical properties of the drug, formulation parameters, electrical parameters and biological parameters. These variables are summarized in Table 3 (Banga, 2002; Kalia et al., 2004).

Table 3. Variables affecting iontophoretic drug delivery (Banga, 2002; Kalia et al., 2004).

Physicochemical properties of the drug	Drug formulation	Electrical parameters	Biological parameters
Molecular weight	pH	Electrode material	Condition of skin
Charge	Co-ions	Current density	Age
Lipophilicity	Ionic strength	Duration of application	Site
Concentration		Current profile	Skin pH
		Polarity of electrode	Inta- and intersubject variability

Different current profiles have been utilized in transdermal iontophoretic drug delivery. In most cases, iontophoresis is conducted with direct constant current (DC; polarity and density are kept constant) in continuous manner as for most compounds the amount of drug molecules delivered is directly proportional to the total amount of current passed across the skin. However, long-term treatment with DC may lead to skin polarization that operates against the applied electrical field and may greatly decrease the magnitude of effective current across the skin (Lawler et al., 1960). This could be avoided when the current is delivered in a periodic manner (pulsed current; PC) that allows the skin to depolarize during the "off periods" of the pulse, so that no residual charges remain in the skin by the start of the next pulse (Zakzewski et al., 1992). Another limiting factor for both in the use of DC and PC iontophoresis is the accumulation of small ions (H^+ and OH^-) on the electrodes that may cause electrochemical burns at long application times or when inappropriate electrode design is used (Howard et al., 1995). The periodic reversal of current polarity during the iontophoresis (alternating current; AC) has shown to avoid it by maintaining the same electrochemical environment of the solution surrounding the electrodes. AC can also reduce flux drift and skin to skin variability compared to conventional DC iontophoresis (Zhu et al., 2002).

Iontophoresis has been demonstrated to be an effective method to be used in the areas of physical therapy, diagnostic applications, treatment of hyperhidrosis with tap water, and transcutaneous delivery of drugs such as local anaesthetics, opioid analgesics and anti-inflammatory agents (Hirvonen, 2005; Kalia et al., 2004). Table 4 presents the iontophoretic systems for topical and transdermal drug delivery that have currently been approved by drug authorities. In addition to these more established applications, iontophoresis is being currently screened for a wide range of therapeutics, including for cardiovascular, central nervous system and endocrinological applications (Roustit et al., 2014; Sieg and Wascotte, 2009).

The first iontophoretic transdermal system (ITS) approved for systemic drug delivery was IONSYS® for the administration of opiod analgetic fentanyl (Sinatra, 2005). This was a true improvement compared to passive patch, extending the applicability of transdermal drug delivery to acute pain management, and allowing patients to self-administer pre-programmed doses of fentanyl non-invasively through the use of iontophoretic technology. The first-generation fentanyl ITS was an integrated one-piece system; however, corrosion was detected in a small number of systems that could trigger the self-activation of the system, and possibly lead to fentanyl overdose. Therefore, a second-generation system was designed to separate the drug unit from the electronic circuit of the controller during manufacture and storage, and snapped together immediately prior to the application to the patient by a healthcare professional. This new design eliminated the issue of corrosion that was originally seen with the first-generation system, ensuring safe operation with high reliability (Joshi et al., 2016).

Table 4. Currently approved iontophoretic systems for topical and transdermal drug delivery. Based on Roustit et al., 2014.

System	Year of approval	Drug/analyte	Systemic/topical	Indication
Zecuity®	2013	Sumatriptan	Systemic	Migraine
Ionsys®	2006	Fentanyl	Systemic	Postoperative pain
Lidosite®	2004	Epinefrine + lidocaine	Local	Local anesthesia

2.2.3 Iontophoretic delivery of peptide drugs

Peptides are playing an increasingly important role in modern therapy because of their high potency and specificity (McCrudden et al., 2013). However, due to their extensive gastrointestinal metabolism, they are not suitable for oral delivery and are nowadays administered almost exclusively by either subcutaneous, intramuscular or intravenous injections. Although parental administration serves the therapeutical purpose, this invasive method of drug administration has several shortcomings, such as pain and discomfort and reduced patients` compliance. Therefore, the transdermal delivery route offers a potential alternative for continuous and more patient-friendly drug delivery (Thomas and Finnin, 2004). However, the physicochemical properties

of peptides − high molecular weight, charge at physiological pH and hydrophilic nature − render them inappropriate for passive transdermal delivery.

Utilization of iontophoretic enhancement to administer peptide drugs transdermally is an attractive opportunity but also a great challenge (Gratieri et al., 2011; Green, 1996; Herwadkar and Banga, 2011). In addition to facilitated permeation of drug and more precise control over delivery, faster therapy onset and offset times, iontophoresis allows to customize the current profile to mimic endogenous secretion profile of the peptide – *e.g.* by applying current in intermittent or pulsatile modes. At the same time, one of the biggest limitations is still the low transport efficiency by iontophoresis, and sometimes more invasive/effective methods might be needed (Guy, 1996). Other hurdles that need to be overcome include the high vulnerability of peptidic drugs to proteolytic enzymes in skin and blood, short-half life, immunogenicity, and tendency to aggregate, adsorb to surfaces or denaturate before reaching the target in body.

Another factor to be considered is that the electrotransport of large molecules such as peptides and proteins is predominantly driven by electroosmosis and not by electrorepulsion, as the electrical mobility of species decreases with increasing molecular weight (Guy et al., 2000). Typically, the iontophoretic flux of compounds increases proportionally with current density and concentration. However, certain cationic hydrophobic peptides (*e.g.* LHRH and somatostatin analogues) have behaved unexpectedly during iontophoretic delivery (Delgado-Charro et al., 1995; Hoogstraate et al., 1994; Lau et al., 1994; Lu et al., 1993; Schuetz et al., 2005c). It has been shown that peptides containing adjacent cationic and lipophilic residues are able to associate to the negatively charged groups of the skin (Hirvonen et al., 1996). This could result in the neutralization of the membrane to a varying extent, causing a significant reduction in the normal anode-to cathode electroosmotic flow and also in the peptide transport. The magnitude of such electroosmotic inhibition is usually dependent on the amount of peptide in the skin, and therefore, the effect is often pronounced at higher applied current densities and increased peptide concentrations. In several cases, this problem has been overcome by the application of PC iontophoresis instead of traditional DC. Improved delivery with PC as compared to DC has been reported with vasopressin (Singh et al., 1998), buserelin (Knoblauch and Moll, 1993), nafarelin (Raiman et al., 2004) and insulin (Chien et al., 1989) due to the enhancement of electroosmotic solvent flow and improved drug stability.

2.3 Ion-exchange fibers

2.3.1 General aspects

Ion-exchange materials are insoluble polymers that have the ability to exchange counter-ions within external liquid phases surrounding them (Harland, 1994;

Helfferich, 1995). Typically they consist of polymeric backbone (polystyrene or polymethacrylic polymers) onto which acidic or basic ion-exchange groups have been grafted. The ion-exchange materials can be either cation- or anion-exchangers, depending on whether they contain negatively or positively charged groups. Within both categories the ion-exchangers can be further classified as strong or weak exchangers, depending on their affinity for the soluble counter-ions. Ion-exchange materials containing sulfonate ($–SO_3^-$) and phosphorate acid ($–PO_3^-$) groups and those containing tetraammonium ($–NR^{3+}$) basic groups are strongly acidic and strongly basic exchangers, respectively. Materials containing phenolic (–OH) groups and primary and secondary amine ($–NH_2$, –NRH) groups are weakly acidic and weakly basic exchangers, respectively. Carboxyl groups ($–COO^-$) and tertiary amine ($–NR_2$) groups take a medium position between strong and weak acidic and basic exchangers, respectively. Therefore, the exchangeable mobile counter-ions in cation-exchange materials are cations and in anion-exchange materials anions. A small amount of mobile ions with the charge of the same sign as the ion-exchanger (co-ions) can also be present in the ion-exchanger.

Physically the ion-exchange materials are available in various morphologies, including macroreticular resins, fibers, gels and membranes (Harland, 1994; Helfferich, 1995). The oldest and still the most used ion-exchange materials are ion-exchange resins that are first prepared as small spherical polymeric beads (0.5-1.2 mm in diameter) that are then chemically modified to introduce the acid or base functionality (Anand et al., 2001; Elder, 2005). The beads consist of three-dimensional network of hydrocarbon chains that are inter-connected covalently by cross-linking. The degree of cross-linking is controlled by the percent of cross-linking agent such as divinylbenzene (DVB) used during copolymerization. Although the ion-exchange resins are insoluble in all physiological media, the fraction of cross-linkage determines to what extent the resin can swell and shrink. The very first ion-exchange resin was prepared in 1935 by Adams and Holmes, and since then the ion-exchange resins have paved their way for various applications in industries such as pharmaceutical, food processing, chemical synthesis, biomedical, water treatment and chromatography.

The concept of developing fibrous ion-exchangers (ion-exchange fibers) was first reported over 40 years ago by Economy and co-workers (Economy et al., 2002). Unlike ion-exchange resins, the fibers do not have crosslinked polymeric framework (Ekman, 1994). Typically, the backbone of the fibers consists of hydrophobic polymer chains (*e.g.* polypropylene, polyethylene) onto which the positively or negatively charged groups are grafted (Fig. 3). Fibrous ion-exchange materials have several advantages over conventional ion-exchange units (Economy et al., 2002; Kosandrovich and Soldatov, 2012; Sundell et al., 1995; Yuan et al., 2014). Ion-exchange fibers are fabricated in the form of felts or fabrics where the contact efficiency with the media is improved. Due to the non-crosslinked network and higher surface area of the fiber compared to resin, higher rates of ion-exchange can be obtained. Other benefits include good mechanical strength, chemical inertness of

the framework, easier loading of large molecules, possibility to achieve high loading capacity and versatility provided by the fibrous form.

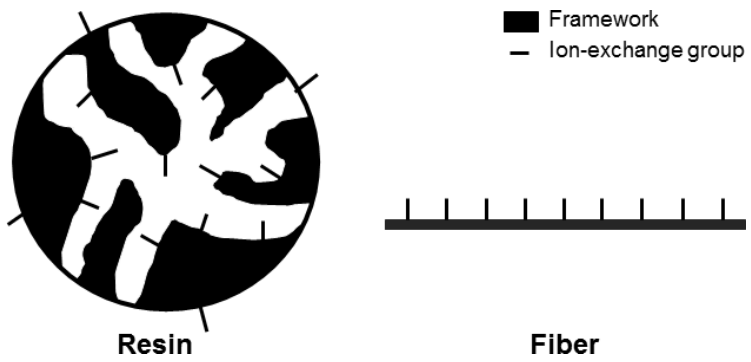

Figure 3. The distinction in structure between ion-exchange resin and fiber.

2.3.2 Theory of ion-exchange

An ion-exchange reaction may be defined as the reversible stoichiometric interchange of ions between a solid phase (the ion-exchanger) and a solution phase, the ion exchanger being insoluble in the medium in which the exchange is carried out (Harland, 1994; Helfferich, 1995). Most importantly, electroneutrality is preserved at all times in both the exchanger and external solution phases, and this in turn requires that counter-ions are exchanged in equivalent amounts. A cation-exchange and anion-exchange reactions may be represented as following:

Cation-exchange reaction: $M^-A^+ + B^+ \longleftrightarrow M^-B^+ + A^+$

Anion-exchange reaction: $M^+A^- + B^- \longleftrightarrow M^+B^- + A^-$

The kinetics of ion-exchange process combines both diffusion and chemical reaction kinetics and is dependent on the physical nature of the ion-exchange material (Harland, 1994; Helfferich, 1995; Lito et al., 2012; Yuan et al., 2014). As in ion-exchange resins, the ion-exchange takes place in the pores and channels of the resin, the diffusion of counter-ions is frequently the rate-determining step in ion-exchange processes, occurring simultaneously in both the ion-exchanger and in the solution. Therefore, the kinetics of ion-exchange resin can be controlled by either interparticle diffusion (film diffusion) or intraparticle diffusion (particle diffusion) or, in intermediate cases, by a combination of both the steps. Controversially, due to the nonporous framework of ion-exchange fibers, the ion-exchange is inclined to be controlled by an ionic reaction process instead of a diffusion process.

According to a theory proposed by Bauman and Eichorn, the driving force for the ion-exchange is Donnan potential, *i.e.* the electrical potential difference between the ion-exchanger and the external liquid phase (Gregor, 1951; Helfferich, 1995; Philipse and Vrij, 2011). The created Donnan potential leads to the interchange of mobile counter-ions between these two phases until the equality of electrical potentials is reached for each ion (Donnan equilibrium). This equilibrium of the ion-exchange reaction between the ion-exchanger and external solution phases results both from electrostatic and hydrophobic interactions (Helfferich, 1995; Kankkunen, 2002; Ramirez et al., 2002). The electrostatic interactions can be expressed by electrical partition coefficient:

$$K_e = exp\left(\frac{-z_i F \phi_D}{RT}\right) \quad \text{(Eq. 5)}$$

where F is the Faraday constant, R gas constant, and T the absolute temperature. ϕ_D is defined as the Donnan potential, *i.e.* the electrical potential difference between the ion-exchanger and the solution phase. For cation-exchange materials $\phi_D < 0$ and $K_e > 0$ and for anion exchangers $\phi_D > 0$ and $K_e < 0$. Similarly, the chemical partition coefficient can be determined as:

$$K_c = exp\left[\frac{\left(\mu_i^0 - \overline{\mu}_i^0\right)}{RT}\right] \quad \text{(Eq. 6)}$$

where μ_i^0 and $\overline{\mu}_i^o$ stand for the standard chemical potential of the ion in the external liquid and ion-exchanger phases, respectively. The chemical partition coefficient depends on the hydrophobicity of the counter-ion. The more hydrophobic the counter-ion, the larger is the value of K_c ($K_c > 1$). As the chemical partition coefficient is also dependent on moisture content of the material, for hydrophilic drugs the value of K_c can be <1. Taken together, the total ion-exchange equilibrium constant is a product of both of electric and hydrophobic interactions:

$$K = K_e K_c \quad \text{(Eq. 7)}$$

2.3.3 Applications of ion-exchangers in drug delivery

Ion-exchange materials have a variety of pharmaceutical applications in oral, nasal, and ophthalmic or transdermal drug delivery systems, either as an excipient or pharmacologically active ingredient (Anand et al., 2001; Elder, 2005; Guo et al., 2009).

Taste masking

At the pH of saliva (6.8) the drug-ion-exchange resin complex remains intact, so the bitter taste of the drug cannot be sensed. Once the complex enters the gastrointestinal tract, the environment changes to acidic and drug is released. Examples of successful taste masking include polyacrylic cation-exchange resins in masking the bitter taste

of diphenhydramine hydrochloride and Carbopol of erythromycin and clarithromycin (Bhise et al., 2008; Lu et al., 1991).

Controlled or sustained release systems

Due to the polymeric (physical control) and ionic (chemical control) properties of ion-exchange materials, the drug-release can be better controlled than by other matrix systems that only possess physical control properties (Anand et al., 2001). Therefore, because of advanced drug-retaining and prevention of dose dumping, these materials have found an important place in the development of controlled and sustained release systems. Variety of different modified release systems, including liquid preparations, microparticles, coated complexes (*e.g.* Pennkinetic systems) and hollow fiber sytems have been designed, utilizing ion-exchange materials (Hussain et al., 1989; Junyaprasert and Manwiwattanakul, 2008; Raghunathan, 1980).

Gastric retentive systems

Prolonged gastric retention time of a drug formulation could significantly improve the bioavailability of drugs that are predominantly absorbed from the stomach. The ion-exchangers have been utilized for that purpose either as floating systems, consisting of a bicarbonate-charged resin that releases carbon dioxide that causes the system to float in stomach (Atyabi et al., 1996) or because of electrostatic interactions with mucin and epithelial cell surface (mucoadhesion) (Jackson et al., 2001).

Stability enhancement

The drug-ion-exchanger complex can sometimes be more stable than the original drug. This approach has been utilized to increase the shelf-life of vitamin B12 and nicotine containing products (Bouchard et al., 1958).

Disintegration enhancement

Ion-exchange resins can be used as tablet disintegrating agents, because of their excellent swelling properties when immersed in water. Weak cation-exchange resin, Amberlite IRP-88 has been widely studied for that purpose (Khan and Rhodes, 1975).

Dissolution enhancement

In the case of poorly soluble ionizable drugs, the release of the drug from drug-ion-exchanger complex can be faster than the rate of dissolution of the solid form of the drug. Therfore, drug-ion-exchanger complexes can be applied to increase the rate dissolution of poorly soluble drugs. Firstly, ion-exchanger resin matrices are relatively hydrophilic and allow fast hydration of the complex. Moreover, the drug is molecularly distributed within the complex and there is no need to overcome crystal lattice energy for dissolution (Guo et al., 2009).

Ophthalmic or nasal DDSs

Ion-exchangers have also found application in ophthalmic drug delivery systems (DDSs). For example, an ophthalmic suspension allowing sustained release of active ingredient (betaxolol hydrochloride), and containing cation-exchange resin Amberlite IRP 69 for enhanced bioadhesion, has been approved to be used in the treatment of glaucoma (Jani et al., 1994). Increased drug bioavailability, ocular comfort and uniform dosing were observed in glaucoma patients. Attempts have been made to deliver nicotine through nasal mucosa from a composition based on drug-ion-exchanger complex. For that purpose, a novel nasal formulation, in the form of a nicotine - Amberlite resin complex powder, was developed to provide an optimal combined pulsatile and sustained nicotine plasma profile for smoking cessation (Cheng et al., 2002).

Ionic strength and pH-responsive membrane bags

Ion-exchange membranes are ion filters of selective permeability that *in vivo* act depending on the pH at the site, ionic strength and drug properties. This principle has been utilized for example in pulsatile and site-specific delivery of gastric acid inhibitors, nitrates, hormone replacement therapy, insulin and immunization (Akerman et al., 1998; Ito et al., 1989).

Implantation devices

Ion-exchange materials can be used to enhance the delivery of water soluble or charged drugs from silicone implantation devices, as they produce additional force that reduces the activation energy for each ion to permeate the membrane (Christy et al., 1979).

Topical applications

The inclusion of ion-exchange resins into topical products, such as ointments, creams, and lotions, has been shown to be advantageous because of their high buffering and adsorption capacity, lack of dermal irritancy, inability to permeate into the skin and flux modification, as the drug-resin complexes act as reservoirs on the skin (Elder, 2005).

Therapeutically active agents

Certain ion-exchange resins have found utility as drugs in their own right. Anion-exchangers cholestyramine and cholestipol are currently used in the treatment of type II and familial hyperlipotroteinemia, lowering low-density lipoprotein cholesterol (LDL-C). They bind and remove bile acids from the gastrointestinal tract that in turn forces the liver to consume more cholesterol in order to produce more bile acids (Goodman et al., 2006). Cation-exchange resins have been utilized in conditions of sodium- and water-retention such as cardiac failure, liver cirrhosis, toxaemia of pregnancy and nephrotic syndrome. Also, in the management of drug poisoning (*e.g.* hyperkalaemia) and hemoperfusion ion-exchange resins have demonstrated their potential (Payne, 1956).

2.4 Nanocarriers for transdermal delivery

2.4.1 General aspects about nanocarriers

Nanotechnology can be defined as a science of engineering of functional systems at the molecular scale (Bamrungsap et al., 2012). As such systems possess unique physical, optical and electronic features, they are attractive for disciplines such as nanomedicine and drug delivery, which try to apply nanotechnogical approaches for the prevention, diagnosis and treatment of diseases. Nano-sized drug delivery systems – nanocarriers – have been developed where drugs are absorbed or conjugated onto the carrier surface, encapsulated inside a polymer/lipid or dissolved within the carrier matrix (Biswajit et al., 2014).

The term "nanoscale" typically refers to particle size below 100 nm, but for the purpose of drug delivery, carriers in the size range of 50-500 nm can be acceptable, depending on their route of administration (Cevc and Vierl, 2010). Due to their small size, new properties arise which have made nanosystems attractive drug delivery platforms for formulation scientists. Firstly, the large surface area helps to bind, adsorb and carry drugs, probes and proteins. Furthermore, bound or encapsulated into the nanocarrier, drugs can be protected from a hostile environment or their unfavorable biopharmaceutical properties can be masked and replaced with the properties of the carrier. In addition, nanocarriers can accumulate preferentially at tumor, inflammatory, and infectious sites due to the enhanced permeability and retention (EPR) effect. The EPR effect includes site-specific characteristics, not associated with normal tissues or organs, thus resulting in increased selective targeting. Based on those features, the application of nanocarriers in drug delivery offer many several benefits, including (1) improvement in drug biodistribution and pharmacokinetics, leading to higher efficacy of drugs; (2) reduction of adverse effects as a consequence of favored accumulation at target sites; (3) improvement in stability of drugs, increasing the range of drugs suitable for administration, and (4) decrease in toxicity by using biocompatible nanomaterials (Bamrungsap et al., 2012; Biswajit et al., 2014)

Although, the primary focus for the use of nanocarriers is placed on the parenteral and peroral applications, other routes such as ocular and transdermal are gaining more attention. Among many others, the nanocarriers most used and investigated in the pharmaceutical field include nanocrystals, polymeric nanoparticles, inorganic nanoparticles, solid lipid nanoparticles, quantum dots, dendrimers, liposomes, microemulsions, protein-based nanoparticles, and hydrogel nanoparticles.

2.4.2 Nanocarriers in skin delivery

In recent years, the transcutaneous utilization of drug-loaded nanocarriers has increasingly gained a lot of attention in order to obtain local drug effect on skin (dermal drug delivery) or systemic drug delivery accompanied by the drug permeation across the skin (transdermal drug delivery). The development of such systems has, in one way or another, addressed the shortcomings of traditional drug delivery systems used for (trans)dermal applications. The most used or investigated nanocarriers for dermal/transdermal drug delivery include liposomes and other vesicular systems, dendrimers, microemulsions, solid lipid nanoparticles and polymeric nanoparticles (Cevc and Vierl, 2010; Khan et al., 2015; Neubert, 2011).

Again the main challenge in the development of such dermal/transdermal systems is how to overcome the tight barrier function of *stratum corneum.* As nanocarriers present a group of highly heterogeneous systems, no straightforward generalizations of intact carrier penetration can be made. The compositions and, with respect to that, the physicochemical properties of the nanocarriers (size, shape, flexibility and surface charge) determine the interactions with the skin barrier. Overall, there are three potential targeting sites for nano-sized carriers, which include the epidermis, skin furrows or the hair follicles (Prow et al., 2011). It is generally agreed that nanocarriers cannot penetrate epidermis and reach deeper layers of skin intact without barrier modification (EC, 2008). There is evidence of some skin penetration for very small particulate carriers (<10 nm), but data of carriers larger than that is controversial and discussion still ongoing. Naturally, in the case of compromised or diseased *stratum corneum*, there might be a potential for bigger particle penetration. Among the lipid-based nanocarrier systems, ultradeformable vesicles (transfersomes) have been reported to invade the skin deep enough to be detected in the systemic circulation (Cevc et al., 2002). It has been claimed that hair follicles could be ideal reservoirs for drug-loaded nanocarriers, since the pilacebaceous unit is more permeable than corneocytes (Lademann et al., 2007). Follicular penetration of both lipid vesicles and polymeric nanoparticles up to 600 mm in size has been reported and it has been suggested that the movement of the hair acts as a geared pump to push the nanocarriers into the hair follicles (Lademann et al., 2009). Approaches such as skin flexing and massage can further increase the penetration depth of nano-sized particulates into hair follicles (Lademann et al., 2007; Tinkle et al., 2003). Taken together, the drug transport by nanocarriers across the skin is a complex process and often a combination of multiple modes, such as release of free drug at the skin/nanocarrier interface, adsorption and fusion of the carrier onto skin surface, penetration of the carrier across the *stratum corneum*, mixing of carrier constituents with skin lipids, increase in drug partitioning into the skin, formation of drug depot in hair follicles or interaction of special chemical composition of nanocarrier with lipid/protein domains of the *stratum corneum*, leading to enhanced permeability (Khan et al., 2015; Schroeter et al., 2010).

The use of topically applied nano-sized carriers have several advantages over the conventional formulations for dermal applications, including readily-tunable chemical and physical features, possibility to protect unstable drugs from degradation/denaturation, decrease in local side effects such as skin irritation, possibility to provide more localized therapeutic effect, and enhancement of cutaneous penetration of the drugs across the skin barrier by increasing the concentration gradient (Zhang et al., 2013). Also, combining of nanotechnology and active enhancement techniques, such as microneedles, electroporation and iontophoresis, are deemed to be the future goal for facilitating even more the transdermal delivery of drugs (Khan et al., 2015). The main limitation in the wider use of nano-sized carrier systems is the overriding concern about the safety of such systems, recognizing the possibility that the non-biodegradable nanocarrier might be taken up and be retained in the reticulo-endothelial system. In addition, there is the environmental burden that needs be considered when it comes to any nanomaterial. Finally, the scale-up of the production of such nanocarriers can be rather complicated and expensive (Prow et al., 2011).

2.4.3 PLGA nanoparticles

Poly(lactic-co-glycolic acid) (PLGA) is a copolymer of polylactic acid (PLA) and polyglycolic acid (PGA) polymers (Fig. 4). It is one of the most widely used polymers for the production of nanoparticles because of its biodegradability by the hydrolysis of the polymer resulting in lactic and glycolic acids which are natural metabolites found in the body. Besides that, the PLGA nanoparticles have other advantages over other polymeric nanocarriers (Danhier et al., 2012; Lai et al., 2014). The high purity of these synthetic polymers makes the preparation of nanoparticles more reproducible. By varying the molecular weight and copolymer ratio, the degradation of the particles can be modified from months to years. By a choice of the preparation method and parameters, hydrophobic or hydrophilic small or macromolecular drugs can be encapsulated, and different physical characteristics can be synthesized for the nanoparticles (size, size distribution, morphology and zeta-potential). Furthermore, the surface properties can be easily modified to impart a targeting ligand or a desired function. Owing to these properties, PLGA has been approved by the US FDA and European Medicine Agency (EMA) to be used on humans in various drug delivery systems.

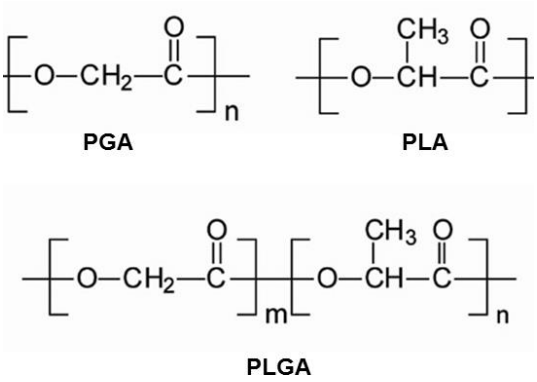

Figure 4. The chemical structure of poly(glycolic acid) (PGA), poly(lactic acid) (PLA), and poly(lactic-co-glycolic acid) (PLGA).

Therefore, biodegradable PLGA nanoparticles have been investigated for sustained and targeted/localized delivery of different compounds (small molecular weight drugs, proteins and peptides, plasmid DNA) in various biomedical applications, such as vaccination, treatment of cancer, cerebral, cardiovascular or inflammatory diseases, or in regenerative medicine (Danhier et al., 2012; Lu et al., 2009). The applications regard mostly parenteral or oral routes, but in the field of transcutaneous drug delivery their potential appears to be rather unexplored.

The rationale behind using polymeric (including PLGA nanoparticles) drug-loaded particles on skin for dermal/transdermal delivery are: (1) effective enhancement of the skin permeation of therapeutics, especially for the poorly water-soluble lipophilic drugs; (2) improvement in the drug stability; (3) decrease in side effects such as skin irritation of applied drugs, and (4) possibility for more localized effect and minimized systemic exposure (Zhang et al., 2013). Most of the reports on the drug-loaded PLGA nanoparticles utilizing transcutaneous route have shown effective delivery of therapeutics for local therapy. Successful dermal delivery by these nanocarriers has been reported for nonsteroidal anti-inflammatory drugs (Abrego et al., 2016; Luengo et al., 2006; Parra et al., 2016; Vega et al., 2013), photosenitisizers (da Silva et al., 2013), corticosteroids (Ozcan et al., 2013) or hairgrowth inducing agents (Tsujimoto et al., 2007). PLGA nanoencapsulation has also demonstrated potential in areas like dermal wound healing therapies (Chereddy et al., 2013; Losi et al., 2013) and transcutaneous vaccination (Mittal et al., 2013). The findings from a study by Raber *et al.* (2014), where the effect of surface modification of PLGA nanoparticles on the nanoparticle uptake into hair follicle was investigated, could be used to optimize drug targeting by that route (Raber et al., 2014). In general, although applicable to local delivery, in order to transport drugs into the deeper layers of skin or for systemic purposes, drug-loaded PLGA particles have to be combined with some active enhancement methods such as microneedles (Zhang et al., 2010), needle-free jet injector (Michinaka and Mitragotri, 2011) or

iontophoresis (Tomoda et al., 2011). Even more, DNA delivery by gene gun from PLGA nanoparticles has been investigated (Lee et al., 2010).

2.4.4 Liposomes

Liposomes are nano-sized vesicles that contain amphipathic phospholipids arranged in one or more bilayers enclosing an equal number of aqueous compartments. Depending on the physicochemical properties, drugs can be intercalated into the lipid bilayer (lipophilic compounds) or in the aqueous core (hydrophilic compounds) (Pierre and Dos Santos Miranda Costa, 2011).

Liposomes have demonstrated great potential as drug carrier systems to be delivered by various routes of administration, including onto skin. Topically administered liposomal formulations can exhibit either a localized effect with augmented deposition of drug on the site of action or they can provide targeted drug delivery through skin appendages (Zhai and Zhai, 2014). Potential advantages of topical liposome use include enhanced drug delivery, solubilization of poorly soluble drugs, drug protection against proteolytic degradation, local skin depot for sustained release, reduction of side-effects and incompatibilities, or the formation of rate-limiting barrier for systemic absorption (Weiner et al., 1994). But at the same time it is generally agreed that conventional liposomes have little or no value as carriers for transdermal delivery as they do not penetrate the skin but rather remain in the upper layers of *stratum corneum* (Pierre and Dos Santos Miranda Costa, 2011). Therefore, specially designed vesicular carriers, such as ethosomes, transfersomes, niosomes, invasomes, polymerosomes etc., have been developed to improve drug permeation through the skin (Fig. 5). The mechanism by which vesicular systems increase the concentration of therapeutics in epidermis or deeper layers of skin are still under investigation. Different mechanisms of action have been proposed, such as free drug permeation after release from the vesicular system, penetration enhancing effects of liposomes, and adsorption/fusion with skin lipids (Schroeter et al., 2010). Discussions are still ongoing whether liposomes or similar vesicles are penetrating skin as intact aggregates or the liposomal lipids are incorporated into the ones of *stratum corneum*.

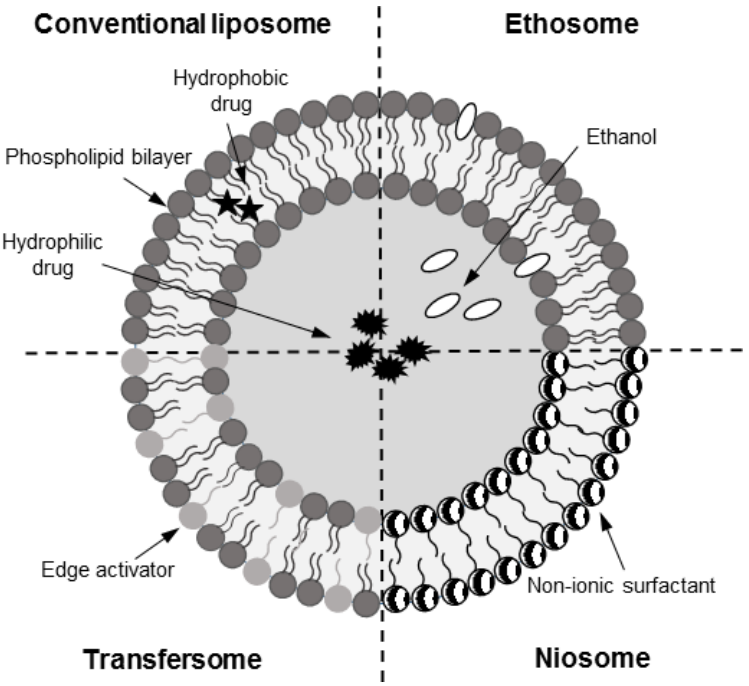

Figure 5. Different types of lipid-based vesicular delivery systems used in transdermal drug delivery.

From the vesicular systems, ethosomes and transfersomes have shown the highest potential in transdermal drug delivery. Ethosomes are flexible, soft liposomes that contain 20-45% of ethanol (Touitou et al., 2000). They have been reported to increase skin permeability by a tentative synergistic "ethanol-ethosome effect" in which ethanol disrupts the organization of *stratum corneum* lipid bilayer, allowing the flexible ethosomes then to penetrate and possibly permeate this layer. Transfersomes (also called as ultradeformable liposomes) are another type of modified liposomes, whose main feature lies in the inclusion of edge activator (surfactant such as sodium cholate, sodium deoxycholate, Span-80, Tween-80) into lipid bilayer, promoting elasticity and deformability (Cevc and Blume, 1992). As the basic driving force for the transfersomes to penetrate the skin was found to be the hydration gradient between skin surface and the inside, non-occlusive conditions are a prerequisite for their barrier penetration. The enhanced transdermal delivery by niosomes, the non-ionic surfactant vesicles, has been proposed as a result of the vesicles mixing with the skin lipids in the intercellular layers (Uchegbu and Vyas, 1998). Invasomes, containing ethanol and terpenes, combine the synergistic effects of both constituents in penetration enhancement (Dragicevic-Curic et al., 2008). Polymersomes are vesicular aggregates containing self-assembling block-co-polymers instead of lipids that have also potential for transdermal delivery because of flexibility, deformability and biocompatibility (Rastogi et al., 2009).

2.5 Benefits from the combined use of transdermal iontophoresis and drug-loaded ion-exchange fibers or nanocarriers

It is generally agreed that iontophoresis provides relatively good control over drug fluxes as drug transport is directly controlled by the current applied. Therefore, iontophoretic treatment may be safe to use even in populations of uncertain barrier maturity such as neonates, premature infants or on compromised skin (Hirvonen, 2005; Sekkat et al., 2001). At the same time, iontophoresis does not eliminate the passive variability, and for some compounds such as nicotine the iontophoretic and passive contributions can be of the same order of magnitude (Brand and Guy, 1995). Another major limitation of iontophoresis lies in the range of molecules (charged molecules mainly) that can benefit from the technique. Large and neutral molecules demonstrate low transport numbers under iontophoretic current as for these drugs convective solvent flow is the main mechanism of electrotransport (Delgado-Charro and Guy, 2003). One possibility to overcome these two limitations would be to load the drug of interest into a reservoir system, such as ion-exchange fibers or nanocarriers, prior to the administration. The rationale behind this approach is that more precise and homogenous control of drug release and the following transdermal iontophoretic permeation could be obtained. Therefore, the transdermal device/patch would determine the rate of drug transfer instead of the skin, the fluxes would be more reproducible, leading to smaller inter- and intrasubject variability (Guy and Hadgraft, 1992). Firstly, the drug would be gradually released from the reservoir/carrier in a predetermined rate (1^{st} flux controlling part). Once released onto the skin surface or into the skin, iontophoretic current (2^{nd} flux controlling part) would pump the drug into the deeper skin layers for topical or systemic applications. In addition, the range of molecules delivered by iontophoresis could be expanded as charges could be imparted to neutral drugs by encapsulating them in charged drug carriers.

While the application of ion-exchange materials as drug delivery vehicles in passive transdermal delivery has proven to be rather unsuccessful (Conaghey et al., 1998), transdermal systems have been developed where iontophoresis has been combined with drug-loaded ion-exchange materials. Charged drug molecules have been electrostatically bound to the ion-exchange groups of ion-exchangers prior to administration and then gradually released by mobile counter-ions and transported across the skin by the iontophoretic current. By the selection of suitable external conditions, ion-exchanger and drug properties (Table 5), the drug release kinetics from the ion-exchange system and drug permeation could easily be optimized to required needs (Hirvonen, 2005). Such systems combining ion-exchange materials and iontophoresis have been successfully utilized in both transscleral (Li et al., 2006) and transdermal iontophoretic drug delivery (Kankkunen et al., 2002b; Xin et al., 2012; Xu et al., 2009). Transdermal drug transport from ion-exchangers under iontophoretic treatment *in vitro* or *in vivo* has been investigated for a variety of

different drugs, including nicotine, beta blockers, NSAIDs, opioids and therapeutics used in the treatment of neurodegenerative diseases (Conaghey et al., 1998; Gao et al., 2014; Jaskari et al., 2000; Kankkunen et al., 2002a; Kankkunen et al., 2002b; Xin et al., 2012; Xin et al., 2014; Xu et al., 2009; Yu et al., 2006). The successful *in vivo* delivery of anti-Alzheimer drug tacrine from cation-exchange fibers has been demonstrated in humans (Kankkunen et al., 2002b).

Table 5. Factors affecting the binding and release of a drug into/from ion-exchanger (Akerman et al., 1998; Helfferich, 1995; Hänninen, 2008; Kankkunen, 2002; Vuorio, 2004)

Properties of the ion-exchanger	Properties of the drug	Properties of the external solution
Ion-exchange capacity	pKa	pH
Nature of ion-exchange groups	Lipophilicity	Ionic strength
Particle size	Size	Temperature
Degree of cross-linking	Solubility	Valence of counter-ions
Preloaded counter-ion	Sterical properties	Concentration of counter-ions
	Concentration in ion-exchanger	Selectivity of counter-ion

Similarly, drug-loaded nanocarriers could be combined with iontophoresis in transdermal delivery. The drug loaded carriers could create a drug reservoir on the surface of the skin and/or in the hair follicles; from this reservoir, the drug would be slowly released to the surface of the skin and into the deeper skin layers; and once released, the iontophoretic current could carry the drug across the skin into the systemic circulation. Although there are many reports on the separate use of nanocarriers and iontophoresis for skin penetration enhancement, the combined use of both the approaches has remained rather unexplored. There are only few reports where transdermal iontophoresis was combined with polymeric nanoparticles (Tomoda et al., 2011, 2012a; Tomoda et al., 2012b), solid lipid nanoparticles (Charoenputtakun et al., 2015; Liu et al., 2008), dendrimers (Mutalik et al., 2013), microemulsions (Boinpally et al., 2004; Kantaria et al., 1999; Sintov and Brandys-Sitton, 2006), nanovesicles (Boinpally et al., 2004; Chen et al., 2009) or liposomes (Essa et al., 2002a, b, 2004; Fang et al., 1999; Han et al., 2004; Kajimoto et al., 2011; Kigasawa et al., 2012; Vutla et al., 1996).

Several advantages over conventional formulations/vehicles have been reported on the iontophoretic drug delivery from the drug-ion-exchange fiber complexes or drug-loaded nanocarriers:

- *Enhanced drug delivery into or across the skin*

Significant improvement of systemic drug permeation has been demonstrated in several studies by combining ion-exchange materials as drug reservoirs (Xin et al., 2012; Xu et al., 2009) or drug-loaded nanocarriers, such as polymeric nanoparticles or lipid vesicles (Essa et al., 2002b; Tomoda et al., 2011; Tomoda et al., 2012b) with iontophoretic treatment. Also higher follicular accumulation of the drug for the

dermal delivery has been reported when iontophoresis has been combined with nanocarriers (Han et al., 2004).

- *Better flux control*

Combining iontophoresis with drug-loaded reservoir or carrier system from where the drug is gradually released at a predetermined rate could lead to more predictable and controlled drug transport, resulting in fluxes less dependent on skin variables.

- *Improved drug stability*

Binding the drug into the ion-exchange material or encapsulating it into nanocarriers could also be used as a strategy to stabilize the drug until it is gradually released into the surrounding solution at the time of the application. This was shown with an easily oxidizing drug levodopa that was attached to ion-exchange fibers in an acidic solution (Kankkunen et al., 2002a) or when enkephalin was incorporated into liposomes (Vutla et al., 1996).

- *Reduced local toxicity*

Due to the enhanced drug delivery, skin irritation could be minimized as shorter application times of the iontophoretic current are needed or the amount of permeation enhancing excipient in the formulation might be reduced for the equivalent drug dose delivered.

- *Possibility to deliver neutral/large molecules by iontophoresis*

Neutral and large molecules that are difficult to deliver by iontophoresis as their transport is dependent on the electroosmosis could be encapsulated into charged nanocarriers in order to improve the transport efficiency. This approach has been utilized with a neutral molecule colchicine or large molecules such as insulin or superoxide dismutase that were encapsulated into cationic liposomes prior to the iontophoretic administration (Kajimoto et al., 2011; Kigasawa et al., 2012; Kulkarni et al., 1996)

- *Entrapment of counter-ions*

Ion-exchange materials can be used in transdermal iontophoretic delivery to capture competing endogenous counter-ions for better drug transport efficiency or pH control over the formulation (Conaghey et al., 1998; Xu et al., 2009).

3 AIMS OF THE STUDY

The main aim of this thesis was to evaluate the potential of the combined use of iontophoresis and drug-loaded ion-exchange reservoir or carrier systems for the controlled transdermal delivery of therapeutics.

More specifically, the aims of the study were:

- To investigate the applicability of drug delivery systems that combine transdermal iontophoresis and ion-exchange fibers as drug reservoirs for the administration of either small molecular compounds or peptides (**I, II**).

- To evaluate the transport mechanisms involved in the iontophoretic drug delivery of peptidic drug leuprorelin acetate (**II**).

- To investigate the applicability of drug delivery systems that combine transdermal iontophoresis and drug nanoencapsulation. More precisely, the goal was to investigate drug transport from charged biocompatible nanocarriers such as PLGA nanoparticles and liposomes (**III, IV**).

- To determine the effect of formulation parameters and current type of the iontophoretic system on the transdermal drug transport (**I, II, III, IV**).

4 EXPERIMENTAL

Complete details of all the materials, equipment and methods used in this work can be found in the respective original publications (**I-IV**).

4.1 Materials (I-IV)

Apomorphine hydrochloride hemihydrate (**I**), flufenamic acid (**III**), diclofenac sodium (**IV**) were obtained from Sigma Chemical Co. (St. Louis, MO, USA), leuprorelin acetate (**II**) from ChemPep® (Wellington, FL, USA) and acetaminophen (**II**) from Hawkins Inc. (Minneapolis, MN, USA). Chemical structures of the model drug compounds and their most important physicochemical properties are given in Table 6.

The cation-exchange fibers Smopex®-101 [-SO_3H ion-exchange groups, styrene sulphonic acid grafted polypropylene fiber] and Smopex®-102 [-COOH ion-exchange groups, acrylic acid grafted polypropylene fiber] were received from Johnson Matthey (**I-II**) (Turku, Finland). The ion-exchange capacities of Smopex®-101 and Smopex®-102 fiber were 4.1 and 6.4 mmol/g, respectively. Poly(lactic-co-glycolic acid) 50:50 (PLGA; Resomer® RG 503H) (**III**) with a molecular weight (MW) of 24,000-38,000 Da, polyvinyl alcohol (PVA; Mowiol® 4-88) (**III**), 5-fluoresceinamine (FA) (**III**), 1-ethyl-3-(3-dimethylaminopropyl)-carbodiimide hydrochloride (DMAP), cholesterol (Chol), Tween-80 (**IV**) and 4-(2-hydroxyethyl)-1-piperazineethanesulphonic acid (HEPES) (**I-IV**) were obtained from Sigma Chemical Co. (St. Louis, MO, USA). Soya phosphatidylcholine (PC; Emulmetik 930) (**IV**) was purchased from Lucas Meyer Cosmetics (Champlan, France) and 1,2-distearoyl-sn-glycero-3-phosphoethanolamine-N-[methoxy(polyethylene glycol)-2000] ammonium salt (DSPE-PEG2000) (**IV**) from Avanti Polar Lipids (Alabaster, AL, US). All other chemicals were at least of analytical grade. Deionized water (≥ 18.2 MΩ/cm of resistance; Millipore, Molsheim, France) was used to prepare all the solutions.

Table 6. Physicochemical properties of the drugs studied.

Drug	MW	pKa	logP_{oct}	Structure/ sequence
Apomorphine hydrochloride (**I**)	312.79	7.2, 8.9	1.76 [a]	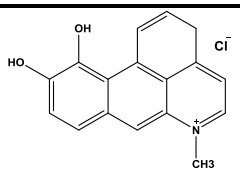
Leuprorelin acetate (**II**)	1209.4	-	1.76 [b]	Pyr-His-Trp-Ser-Tyr-D-Leu-Leu-Arg-Pro-NHEt
Flufenamic acid (**III**)	281.23	3.9	5.62 [c]	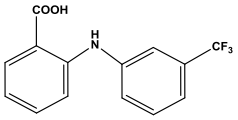
Diclofenac sodium (**IV**)	318.13	4.15	0.92 [d]	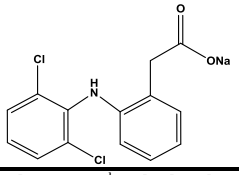

[a] Corresponds to apomorphine base, experimentally determined (Drayton et al., 1990); [b] calculated value (Drugbank); [c] experimentally determined (Moffat, 1986); [d] experimentally determined (Sarveiya et al., 2004).

4.2 Methods (I-IV)

4.2.1 Drug loading into ion-exchange fibers (I-II)

In order to load drugs into Smopex®-101 and Smopex®-102 cation-exchange fibers, 100 mg of fiber (dry content) bundles wrapped into porous gauze (Mesoft®, Mölnlycke Health Care, Gothenburg, Sweden) were prepared. Loading of fibers was conducted with 10 fiber bundles immersed in the same loading solution on a shaker (150 movements/min):

- Loading with apomorphine was performed over 2 consecutive loading periods – initially for 24 h and then the bundles were transferred into fresh loading solution for an additional 24 h (**I**). 50 ml of apomorphine solutions pH3.0 with two different concentrations (0.1% or 0.25%) were used for loading.
- Loading with leuprorelin acetate was conducted for 48 h. 30 ml of 2 mg/ml leuprorelin acetate solution in deionized water pH=7.4 was used as a loading solution (**II**). Prior to loading, the bundles were pre-treated with 30 ml 100 mM NaCl/ 100 mM NaOH mixture for 30 + 30 minutes.

When the effect of NaCl or HCl pre-treatment on the loading extent/ stability of the drug was studied, the bundles were immersed prior to the loading into 100 mM

NaCl for 30 + 30 minutes or 100 mM HCl for 6 + 18 hours (**I**). After each loading period, the unbound compound was washed from each bundle and the washing solutions were combined with the loading solution. The amount of compound loaded into the fiber bundles was determined by HPLC (**I**) or by UPLC-ESI-MS (**II**) as the difference between the amounts of compound in the initial loading solution and in the collected post-loading and washing solution.

4.2.2 Preparation of PLGA nanoparticles (III)

Firstly, 5-fluoresceineamine-bound PLGA (FA-PLGA) was prepared based upon the method described by Horisawa et al. (Horisawa et al., 2002) and Weiss et al. (Weiss et al., 2006). Briefly, 3.07 g PLGA, 0.0583 g FA and 0.0408 g of DMAP were dissolved in 30 ml of acetonitrile and incubated at room temperature for 24 h under gentle stirring and light protection. The resulting FA-PLGA was precipitated by the addition of purified water and separated by centrifugation. The polymer was rinsed from excessive reagents (repeated dissolution in acetone and precipitation with ethanol) and then lyophilized with Alpha 2-4 LSC freeze-dryer (Martin Christ Gefriertrocknungsanlagen GmbH, Osterode am Harz, Germany). FA-PLGA nanoparticles loaded with flufenamic acid (FFA) were prepared by the emulsion diffusion/evaporation technique. In brief, 6 mg of flufenamic acid and 50 mg FA-PLGA were dissolved in 2.5 ml ethyl acetate. This organic solution was added dropwise into 2.5 ml of an aqueous solution of 2% PVA. The mixture was then kept for 1 hour under magnetic stirring at 600 rpm at ambient temperature. The resulting o/w emulsion was homogenized with Branson ultrasonifier S250D (Branson Ultrasonics Co., CT, USA) at 10% amplitude for 30 s. 20 ml of water was added and the emulsion was kept under stirring overnight to evaporate the organic solvent. For reference, standard drug-free FA-PLGA nanoparticles were prepared in the same way. The dispersions were purified using Vivaspin 20 ml ultrafiltration spin column (Sartorius, Goettingen, Germany) using centrifugation at 4000 rpm for 40 min and were further washed three times with deionized water. 1 ml of final formulation used in all the permeation experiments consisted of 17.86 mg FA-PLGA nanoparticles (containing 1 mg of FFA) suspended in 25 mM Hepes buffered saline pH=7.4.

4.2.3 Preparation of liposomes (IV)

Conventional liposomes, pegylated liposomes and transfersomes were prepared by the classic cast film method (Table 7). Briefly, phophatidylcholine (PC), cholesterol (Chol), 1,2-distearoyl-sn-glycero-3-phosphoethanolamine-N-methoxy-polyethylene-glycol-2000 ammonium salt (DSPE-PEG2000) and Tween-80 were dissolved in absolute ethanol in a clean, dry, round-bottom flask. The organic solvent was removed by evaporation for 20 min at 45 °C to obtain homogenous thin lipid film on the inner surface of the flask. The deposited film was then hydrated with 2.5 mg/ml

diclofenac sodium solution (DS) in 10 mM Hepes buffered saline pH=7.4 for 1 h at 45 °C. The resulting vesicles were extruded 11 times through 100 nm polycarbonate membrane at 45 °C.

In order to prepare ethosomes, the lipids and DS were dissolved in absolute ethanol. This mixture was heated to 30 °C ± 1°C in a water bath. Buffer (10 mM Hepes buffered saline pH=7.4), also heated to 30 °C ± 1 °C, was added slowly as a fine stream to the lipid mixture with constant stirring at 700 rpm in a closed vessel. Mixing was continued for an additional 5 minutes, while maintaining the system at 30 °C ± 1 °C. The size of the vesicles was reduced by sonication for 15 s at 15 W, followed by extrusion for 11 times through 100 nm polycarbonate membrane at ambient temperature.

Table 7. Composition of DS lipid vesicles.

Formulation	Composition
Conventional liposomes	90 mM PC 30 mM Chol
Pegylated liposomes	90 mM PC 30 mM Chol 2.5% (mol/mol%) DSPE-PEG2000
Transfersomes	120 mM PC 15% (w/w%) Tween-80
Ethosomes	90 mM PC 30 mM Chol 20% (v/v%) ethanol

4.2.4 Physicochemical characterization of nanocarriers (III-IV)

The colloidal characteristics (hydrodynamic radius, polydispersity index, zeta potential) of the drug-loaded nanocarriers were determined by Malvern Zetasizer Nano (**III-IV**; Malvern Instruments, Malvern, UK). The morphology of the FA-PLGA nanoparticles (**III**) was evaluated by FEI Quanta^{TM} FEG scanning electron microscope (SEM; FEI Company, Hillsboro, OR, USA). The samples were fixed onto a two-sided carbon tape with silicone adhesive and sputtered with platinum for 25 seconds with an Agar sputter device (Agar Scientific Ltd., Essex, UK) prior to imagining.

Drug loading into the nanocarriers was assessed as follows:

- For FA-PLGA nanoparticles, a fixed amount of purified freeze-dried nanoparticles was dissolved in acetone (polymer and drug both soluble) and then methanol was added (only drug soluble) to precipitate the FA-PLGA (**III**). The nanoparticle dispersion was centrifuged to separate the supernatant

and the encapsulated amount of flufenamic acid was determined by HPLC analysis.

- For liposomes, the vesicle-encapsulated diclofenac sodium was separated from the unentrapped drug by ultracentrifugation at 30000 rpm for 6 h at 4 °C (**IV**). After that liposomes were lysed with absolute ethanol and the released diclofenac sodium was quantified by HPLC. The percent of encapsulation efficiency (EE%) was then calculated according to the following equation:

$$EE\% = \frac{amount\ of\ drug\ in\ liposomes}{total\ amount\ of\ drug} \times 100 \qquad \text{(Eq. 8)}$$

4.2.5 Drug release studies (I-IV)

Drug release from cation-exchange fibers (I):
In order to determine apomorphine release from the cation-exchange fibers, the drug-loaded fiber bundles were immersed individually (n=3) into 15 ml of extracting electrolyte solution (NaCl or $CaCl_2$). The molar amount of extracting electrolyte ($[n^+]$) was determined on the basis of the molar amount of the compound bound into the fiber was equal ($1[n^+]$), ten-fold ($10[n^+]$) or hundred-fold ($100[n^+]$) compared to the loaded compound. The release of the bound compound into pure de-ionised water was determined as a control. The release profiles were obtained over 24 h by sampling 100 µl at 1, 5, 15, 30, 45 min and 1, 2, 4, 8, 12 and 24 h. The release experiments were performed at ambient room temperature in amber glass vessels placed on a shaker (180 motions/min).

Drug release from nanocarriers (III-IV):
The drug release studies from drug-loaded FA-PLGA nanoparticles or liposomes were carried out in static Franz diffusion cells through MWCO=3.5 kD (**III**; Fisherbrand; Thermo Fisher Scientific, Waltham, MA, USA) or MWCO=6-8 kD (**IV**; Spectra/Por; Spectrum Laboratories, Rancho Dominquez, CA, USA) regenerated cellulose dialysis membrane. To mimic physiological conditions, the cells were thermostated at 32 °C (**III**) or 37 °C (**IV**). Fixed amount of drug-loaded nanocarrier dispersion in buffer was placed into the donor compartment. Either 10 mM (**IV**) or 25 mM (**III**) HEPES-buffer containing 154 mM NaCl was used both in the donor and receiver compartments. The volume of the receiver compartment was 5 (**IV**) or 12 ml (**III**). 300 µl-sized samples were collected from the receiver compartment at 0.5, 1, 2, 3, 4, 6, 8 and 24 h for analysis and replaced with fresh buffer. In the study with flufenamic acid loaded-FA-PLGA nanoparticles (**III**), the drug release was also determined under different iontophoretic current profiles: 100% constant current, 75% on/25% off pulsed current or 50%+:50%- alternating current (cathodal, 8h, current density 0.5 mA/cm^2, frequency of pulsing 500 Hz).

4.2.6 Stability studies (III-IV)

The stability of the drug-loaded nanocarriers was evaluated as a change in hydrodynamic diameter and polydispersity index (PDI). The stability under iontophoretic current was tracked both for the drug-loaded FA-PLGA nanoparticles and liposomes for 8 h under different iontophoretic current profiles (**III-IV**). Following current profiles were used: 100% constant current (**III-IV**), 75% on/25% off pulsed current (**III-IV**) or 50%+:50%- alternating current (**III**) (cathodal, current density 0.5 mA/cm^2, frequency of pulsing 500 Hz). For flufenamic acid-loaded FA-PLGA nanoparticles, also the stability 1) for 24 h in 25 mM HEPES-buffered saline pH=7.4 and 2) for 8 h in contact with human epidermis or porcine full-thickness skin were determined (**III**). The effects of the buffer and iontophoretic current were studied in small glass vials. Nanoparticle stability when in contact with human epidermis or full-thickness porcine skin was investigated using Franz diffusion cells with either the *stratum corneum* side or the dermal side of the skin membrane facing the upper donor compartment containing the nanoparticle dispersion in buffer.

4.2.7 Preparation of skin (I-IV)

Human skin was obtained from abdominoplasty patients with the approval of the Research Ethic Committee of Saarland in Germany (Ärztekammer des Saarlandes, Dec. 2008) (**III**). Porcine ears were collected from a local abattoir within a few hours of post-mortem and were cleaned under cold running water (**I-IV**). The whole skin was removed carefully from the outer region of the ear and separated from the underlying cartilage with a scalpel and preserved at -20 °C for further use. Epidermal membranes of human (**III**) or porcine skin (**II**) were prepared by heat-separation technique (Schuetz et al., 2005b): pieces of full-thickness skin were soaked in water at 58 °C for 2 min, followed by careful removal of the epidermis from the dermis. The epidermis was then washed with water and used in the *in vitro* studies within 24 hours.

4.2.8 Transdermal *in vitro* permeation experiments (I-IV)

Side-by-side® diffusion cells (I, II):
In vitro permeation studies with the drug-loaded cation-exchange fibers were performed in Side-by-side®-diffusion cells (Laborexin, Helsinki, Finland). Full-thickness porcine skin (**I**) or porcine heat-separated epidermis (**II**) was clamped between two identical halves of diffusion cells. Regenerated cellulose dialysis membrane (MWCO=25 kD) was used as a supportive membrane under the epidermis (Spectrum Laboratories Inc., Rancho Dominquez, CA, USA). The area of exposed skin/epidermis was 0.785 cm^2. To mimic physiological conditions, the cells were thermostated at 37°C by a surrounding socket. 25 mM HEPES-buffer pH=7.4

including 154 mM NaCl was placed in the receiver compartment of the diffusion cells. Drug loaded cation-exchange fibers or drug in solution [apomorphine 1 or 5 mg/ml (**I)** and leuprorelin acetate 1 mg/ml (**II**)] was placed into the donor compartment. Apomorphine donor solution was prepared in 5 mM citrate buffer pH=5, containing 9.51 mM Na^+ (**I**) and leuprorelin acetate donor solution in the same buffer as used in the receiver compartment (**II**). In permeation studies with apomorphine, the donor and receiver buffers contained 0.1% of ascorbic acid to prevent the auto-oxidative breakdown of the drug (**I**). As apomorphine and leuprorelin acetate are positively charged drugs, they were iontophoresed from the anodic compartment. 100 µl- (**II**) or 300 µl-sized (**I**) samples were collected for analysis from the receiver (in experiments with cation-exchange fibers also from the donor) compartment and replaced by fresh buffer at 0.5, 1, 2, 3, 4, 5, 6, 8 (**I, II**), 12 h (**II**) and 24 h (**I, II**).

Franz diffusion cells (III, IV):

In vitro permeation studies with drug-loaded nanocarriers were carried out in static Franz diffusion cells. Pieces of human heat-separated epidermis (**III**) or porcine full-thickness skin (**III, IV**) were clamped between the donor and receiver compartments of the diffusion cells. Regenerated cellulose dialysis membrane (MWCO=3.5 kD) was used as a supportive membrane under the epidermis (Fisherbrand; Thermo Fisher Scientific, Waltham, MA, USA). The area of exposed skin/epidermis was 1.76 cm^2 (**III**) or 0.785 cm^2 (**IV**). To mimic physiological conditions, the cells were thermostated at 32 °C (**III**) or 37 °C (**IV**). 0.5 ml of drug solution [flufenamic acid 1 mg/ml (**III**) and diclofenac sodium 2 mg/ml (**IV**)] or drug loaded nanocarriers – FA-PLGA nanoparticles (**III**) or liposomes (**IV**) with the equivalent amount of drug in buffer – were placed in the donor compartments of the diffusion cells. Either 10 mM (**IV**) or 25 mM (**III**) HEPES-buffer containing 154 mM NaCl was used both in the donor and receiver compartments. The volume of the receiver compartment was 5 (**IV**) or 12 ml (**III**). As flufenamic acid and diclofenac sodium are negatively charged at pH=7.4, they were iontophoresed from the cathodic compartment. 300 µl-sized samples were collected from the receiver compartment at 0.5, 1, 2, 3, 4, 6, 8 and 24 h for analysis and replaced with fresh buffer.

The effect of cations in donor solution (I):

In the permeation studies with apomorphine, in addition to the monovalent Na^+, the effects of divalent Ca^{2+}, trivalent Al^{3+} as well as of two organic cations with higher molecule masses − TEA^+ (tetraethylammonium) and BA^+ (benzalkonium) − were studied. All the salts used were chlorides at a concentration of 154 mM, except for benzalkonium chloride (15.4 mM) that possesses surfactant properties and would be toxic in such a high concentration. In the experiments with other cations besides Na^+, no buffering agents were used in the donor solution.

Determination of electroosmotic drug transport (II):

Acetaminophen is a neutral hydrophilic compound with negligible passive permeability (≈2 nmol/ cm^2*h) (Schuetz et al., 2005c) and upon the application of

iontophoretic current it is driven across the skin predominantly by electroosmosis. Hence, in our studies acetaminophen was included in the donor formulation (15 mM) to report on the electroosmotic transport from anode to cathode. Electroosmotic component of the flux (J_{EO}) was calculated by subtracting the passive flux (J_P) from the total steady-state flux of acetaminophen (J_{SS}):

$$J_{EO} = J_{SS} - J_P \quad \text{(Eq. 9)}$$

Assessment of the epidermal integrity (II, III):
When epidermal sheets were used in permeation experiments, the integrity of the membrane was assessed after the experiment using a colorimetric method: 100 µl of 1% methylene blue solution was added into the donor solution/nanocarrier dispersion. The presence of blue coloration in the receptor within 30 min was either indicative of defective skin barrier or leakage of test substance as a result of improper sealing of the donor and receptor compartments. When the blue coloration was observed, the data obtained from that cell was discarded.

Iontophoretic apparatus (I-IV):
Platinum electrodes were used in all the iontophoretic experiments. During the experiments the electrodes were separated from the donor and receiver compartments by salt-bridges consisting of 1 M KCl gelled with 2% agarose inside silicone tubing (inner diameter 2 mm, length ca. 15 cm). Salt bridges prevented direct contact and possible reactions and/or pH-effects of the drug with the electrodes. The electrolyte that surrounded the electrodes was 2 M KCl. Current was on for 8 h (**I, III, IV**) or 12 h (**II**) (Ministat potentiostat, Sycopel Scientific Ltd., Boldon, UK), whereafter passive flux was followed up to 24 h. Different current profiles – 100% constant direct current (**I-IV**), 75% on/25% off pulsed current (**II-IV**) and 50% on:50% off alternating current (**III**) – were used in the iontophoretic experiments (current density 0.5 mA/cm^2, pulsing frequency 500 Hz). For determining the relationship between the current density and steady-state flux, current densities in the range of 0 - 0.5 mA/cm^2 where utilized (**I, III**). The current profiles were adjusted by CFG253 function generator and TDS210 oscilloscope (Tektronix Inc., Beaverton, OR, USA) and monitored by Fluke 8808A multimeter (Hewlett Packard, WA, USA).

Data analysis (I-IV):
On the basis of the sample concentrations from the permeation experiments, the cumulative amount of drug permeated across the full-thickness skin or epidermis was calculated and plotted against time. The linear part of the curve was used for calculating the steady-state flux values [(nmol/h*cm^2 (**I, III, IV**) or µg/h*cm^2 (**II**)].

Iontophoretic enhancement factors were calculated accordingly (**I-IV**):

$$E = \frac{J_{iontophoresis}}{J_{passive}} \quad \text{(Eq. 10)}$$

where $J_{iontophoresis}$ and $J_{passive}$ are the iontophoretic and passive steady-state flux of the drug, respectively.

Transport numbers were calculated using an equation (**I-IV**):

$$T_n = \frac{z*F*dQ/dt}{MW*I} \quad \text{(Eq. 11)}$$

where *z* is the valence of the drug, *F* is the Faraday`s constant, *dQ/dt* is the linear slope of the iontophoretic phase (in mass units per time), *MW* is the molecular weight and *I* is the total current passed through the skin.

To determine whether clinically relevant steady-state concentration of a drug in the plasma (c_{ss}, ng/ml) during transdermal delivery could be achieved, c_{ss} was calculated followingly (**I-II**):

$$c_{ss} = \frac{A*J_{ss}}{CL} \quad \text{(Eq. 12)}$$

where *A* is the surface area for drug absorption, J_{ss} is the steady-state flux, and *CL* is the clearance of the drug from the body.

4.2.9 Cryosectioning and imaging (III)

Cryosectioning of the skin was performed immediately after the permeation experiments. The surface of the skin was gently cleaned from drug residues with deionized water and cotton. Discs of 6 mm in diameter were punched out of skin and sections (30 µm thick) were cut at -20°C using a Leica CM3050 cryostat (Leica Microsystems, Wetzlar, Germany). On cryosectioning, placement of the skin punch was not parallel to the cutting blade of the cryotome to avoid dislocation of the particles from outside into the deeper skin layers or vice versa, but in a perpendicular position limiting sectioning artefacts (Labouta et al., 2011). The sections were mounted in Vectashield Antifade Mounting Medium (Vectorlabs, Burlingame, CA, USA) prior to the imaging and observed using confocal laser scanning microscope Leica TCS SP5II HCS (Leica Microsystems, Wetzlar, Germany).

4.2.10 Analysis of the drugs (I-IV)

HPLC assays (I-IV)

Apomorphine hydrochloride (**I**), acetaminophen (**II**), flufenamic acid (**III**) and diclofenac sodium (**IV**) concentrations were analysed by high performance liquid chromatography (HPLC) instrument by Agilent 1100 Series (Agilent Technologies, Germany). The specific parameters are shown in Table 8.

Table 8. HPLC parameters for the quantification of the drugs.

Drug	Column	Mobile phase	Λ (nm)
Apomorphine HCl	Gemini NX C18 3 µm 110 Å, 100 x 4.6 mm (Phenomenex Co., USA)	0.1% TFA pH2.0/ ACN (85:15)	273
Paracetamol	Discovery® C18 5 µm, 150 x 4.6 mm (Supelco Analytical, USA)	0.1% TFA pH2.0/ ACN (90:10)	249
Flufenamic acid	LiChrospher 100 RP-18, 5 µm, 125*4 mm (Merck, Germany)	McIlvaine buffer pH2.2/ MeOH (20:80)	284
Diclofenac sodium	Discovery® C18 5 µm, 150x4.6 mm (Supelco Analytical, USA)	Phosphate buffer pH3.0/ MeOH (30:70)	284

UPLC-ESI-MS assays (II):

For the quantification of leuprorelin acetate concentrations, a method based on ultra-performance liquid chromatography combined with electrospray ionization mass spectrometry (UPLC-ESI-MS) was developed. Chromatographic separation was performed with a Waters Acquity UPLC instrument (Waters, MA, USA) and Waters Acquity UPLC BEH300 C18 (2.1 x 100 mm, 1.7 µm) column (Waters, MA, USA) at 50 °C. The mobile phase consisted of 0.01% TFA in deionized water (A) and 0.01 % TFA in acetonitrile (B). The gradient elution consisted of 5-100% B at 0-2.5 min, 100% B at 2.5-3 min, then a reduction to 5% B at 3.1 min; 3.1-5 min, 5% B for equilibration of column. The flow-rate was 0.45 ml/min and injection volume 0.1 µl. After every sample two blank injections (isopropanol) were made to prevent the peptide carryover. The linear concentration range of leuprorelin acetate was established in the range of 0.1-50 µg/ml (R2=0.9979). LOQ=0.1 µg/ml, %RSD was 0.3% and 3% for retention times and peak areas, respectively. Mass spectral experiments were carried out using a Xevo triplequadrupole mass spectrometer (TQ-S) equipped with an ESI source (Waters, MA, USA). The ESI source was operated in positive ionization mode. The optimal ESI source parameters were as follows: capillary voltage 3.2 kV, cone voltage 26 V, source temperature 150 °C, desolvation temperature 500 °C. Nitrogen was used as the desolvation gas (800 L h^{-1}) and cone gas (200 L h^{-1}). The multiple reaction monitoring (MRM) mode was employed (quantifier 605.47 → 249.10, CE 26 eV and qualifier 605.47 → 110.10, CE 52 eV) for quantification.

5 RESULTS AND DISCUSSION

5.1 Combined use of ion-exchange fibers and iontophoresis for transdermal drug delivery (I-II)

5.1.1 Drug binding into cation-exchange fibers (I-II)

The potential of cation-exchange fibers with strong ion-exchange groups (Smopex®-101, sulphonic acid groups) and weak ion-exchange groups (Smopex®-102, carboxylic acid groups) as drug reservoirs in transdermal iontophoresis was tested. The properties and scanning electron microscope images of the fibers are presented in Table 9 and Figure 6.

Table 9. Characteristics of cation-exchange fibers.

Cation-exchange fiber	Framework	Functional groups	Binding capacity (mmol/g)	pKa
Smopex®-101	polypropylene	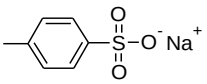	4.1	0-1
Smopex®-102	polypropylene	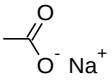	6.4	3-5

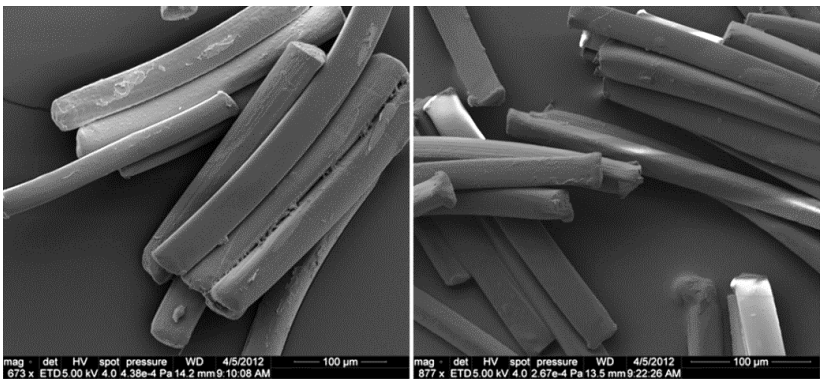

Fig. 6. Scanning electron microscope images of Smopex®-101 (left) and Smopex®-102 (right) cation-exchange fibers.

With both the tested drugs – apomorphine and leuprorelin acetate – similar loading was obtained with Smopex®-101 and Smopex®-102 cation-exchange fibers. The reason for that may be that too low amounts of the compounds were used for

loading, which were not sufficient to bring out the differences in the loading extent. For apomorphine (**I**), no differences in loading efficacy were seen between the two fiber types in the case of either 0.1% or 0.25% loading solution (Table 10). Higher apomorphine concentration in the loading solution increased the molar amount of loading and relative occupancy in both the fibers, but, at the same time, slightly decreased the loading efficiency (*i.e.* % of apomorphine extracted from the loading solution). Leuprorelin acetate (**II**) loading of ≈0.074 mmol per g of fiber was obtained with both the cation-exchange fibers, *i.e.* about 1-2% of the ionic binding sites in the fibers were occupied by the peptide.

Table 10. The molar amount (mmol/g) / percentage of loading capacity (%) of apomorphine loaded into the cation-exchange fibers after the first and the second loading periods (mean, n=10*). Both loading periods were 24 h.

Conc. of loading solution	Smopex®-101		Smopex®-102	
	After I loading	After II loading	After I loading	After II loading
0.1%	0.160/ 3.91%	0.325/ 7.94%	0.155/ 2.42%	0.313/ 4.89%
0.25%	0.413/ 10.06%	0.827/ 20.16%	0.394/ 6.16%	0.796/ 12.43%

* Ten fiber bundles were immersed in the same loading solution.

pH of the loading solution (I-II):

The pH of the external solution determines the ionization state of both the ion-exchanger and the drug, and therefore the extent of the ion-exchange process during loading or release (Kankkunen et al., 2002a). The ionization degrees of the cation-exchangers during drug loadings were calculated according to the Henderson–Hasselbalch equation, $I\% = 100/[1 + \text{antilog}(pK_a - pH)]$. Apomorphine loading solutions were prepared at pH 3.0, at which 99% of the sulphonic acid groups of the Smopex®-101 ($pK_a<1$) and only 9.09% of the carboxylic acid groups of Smopex®-102 ($pK_a\approx4$) were ionized (**I**) (Florence and Attwood, 2011). Although the difference in the degree of ionization between the two fiber types should result in different loading extents, the huge shift in the pH of loading solution of Smopex®-102 probably diminished this effect and by the end of the loading all the carboxylic acid groups were ionized (I%=100% at pH 8-8.5). Fiber loading with leuprorelin acetate was performed at pH 7.4, at which 100% of the cation-exchange groups in both the fiber types were ionized (**II**).

The degradation rate of easily oxidizing drugs like apomorphine **(I)** is highly dependent on the pH of the solution. Therefore, different pH values and antioxidant ascorbic acid concentrations were tested to find out the most stable loading solution. The amount of intact drug and pH shifts in the loading solution were measured during a two week storage test at room temperature. The turn in the color of the solution of apomorphine into green or yellow (depending on the vehicle) indicated the formation of oxidation product. The best stability and the smallest pH shift were observed in the apomorphine solution at pH 3.0 with no antioxidant. The solutions

with Smopex®-101 fibers remained stable during the whole period of the loading and no degradation products were detected visually. At the same time the loading solutions of Smopex®-102 and the fibers themselves had a strong green colour after 24 hours of loading and the pH of the solution had risen to 8-8.5.

The pre-treatment of fibers (I):

The nature of the preloaded counter-ion may affect the binding of drug into the ion-exchanger (Jaskari et al., 2001). Therefore, the effect of pre-treatment with NaCl or HCl on subsequent loading with apomorphine was determined (**I**). The pre-treatment of cation-exchange fibers with NaCl solution did not increase apomorphine loading to either fiber type, as all of the ion-exchange groups had been already occupied with sodium ions prior to that. At the same time, when the fiber bundles were pre-treated with HCl (especially in the case of Smopex®-102), the amount of drug loaded into the fibers was also changed (Fig. 7), together with improvement in drug stability during the loading procedure. In the case of Smopex®-101, the acid pre-treatment slightly increased the loading degree. On the contrary, an enormous decrease in loading was seen after the Smopex®-102 fibers were pre-treated with HCl. It seemed that in Smopex®-102 fibers, H^+ ions in the HCl solution were quickly exchanged with Na^+-ions. Later during the loading of drug, the exchange between H^+ and apomorphine$^+$-ions in the fiber seemed to be very slow and only a small fraction of apomorphine was bound to Smopex®-102 during the 48 hour loading period.

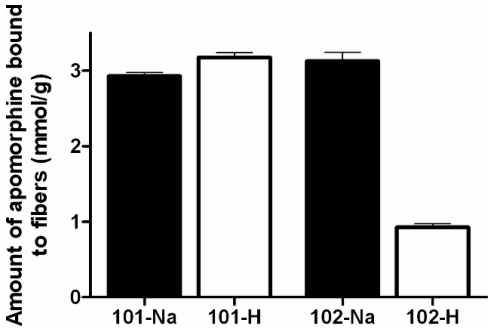

Fig. 7. The molar amount (mmol/g) of apomorphine bound to cation-exchange fibers without (101-Na and 102-Na) or with (101-H and 102-H) 100 mM HCl pre-treatment (mean ± SEM, n=3).

In summary, the extent of drug loading and the stability were dependent on the ion-exchange groups of the fiber, the preloaded counter-ions attached to the ion-exchange groups and pH of the loading solution.

5.1.2 Drug release from ion-exchange fibers (I)

The effect of counter-ion concentration and valence:

The interchange of drug bound to the cation-exchange fibers and the counter-ions of the external solution is dependent on the electrical potential difference (Donnan potential) between the two phases (Helfferich, 1995). Increase in the concentration of counter-ions in the solution (*i.e.* the ionic strength) or in the valence of counter-ion leads to a decrease in the Donnan potential (Hänninen et al., 2007; Jaskari et al., 2001; Kankkunen et al., 2002a). Lower Donnan potential means that the interaction between the drug and the ion-exchange groups is weaker, allowing more extensive release of the drug from the fiber. The rate and extent of the release of apomorphine was clearly higher when the concentration of the counter-ion in the surrounding solution was increased (Fig. 8). Also, at equimolar amounts, divalent Ca^{2+} was more efficient in releasing apomorphine from both the cation-exchange fibers than monovalent Na^{+}. In addition to reduced Donnan potential, significantly higher charge density of Ca^{2+} compared to Na^{+} contributed to the process.

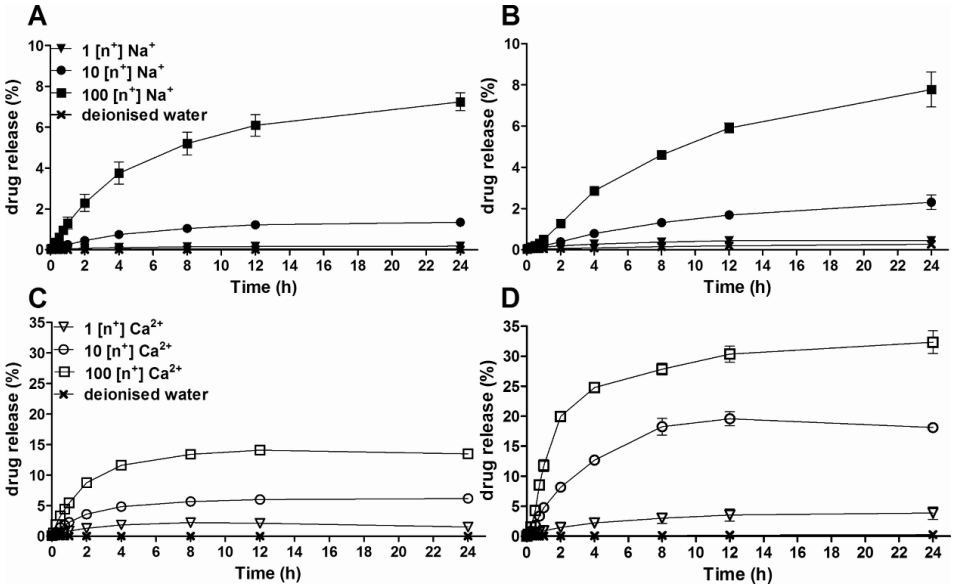

Fig. 8. The release profiles of apomorphine from Smopex®-101 (A and C) and Smopex®-102 (B and D) cation-exchange fiber bundles during 24 h (mean ± SEM, n=3). The molar amount of extracting sodium- (closed symbols) or calcium-ions (open symbols) in the release media was equal (1[n^{+}]), 10 fold (10[n^{+}]) or 100 fold (100[n^{+}]) compared to the loaded apomorphine amount.

The effect of the cation-exchange groups:

The studied cation-exchange fibers share the same polymeric framework – polypropylene – but different cation-exchange groups (sulphonic or carboxylic acid in Smopex®-101 or Smopex®-102, respectively). The results demonstrated that more apomorphine was released from the fiber with weak carboxylic acid groups than from the fiber with strong sulphonic acid groups (Fig. 8). Different release profiles

between the fiber types were seen only when using $CaCl_2$ as the extracting electrolyte. In the case of Smopex®-102, the strongest extracting solution used (100[n^+] $CaCl_2$) released about 30% of bound apomorphine during 24 h, while from Smopex®-101 fibers the corresponding value did not exceed 15%. Since the specific interactions between apomorphine and the fibers seemed to be strong, the release from the fibers remained quite low at all the electrolyte concentrations. Thus, apomorphine acted similarly to other lipophilic drugs, such as propranolol or tacrine, that are bound more strongly to the strong sulphonic acid groups than to the weaker carboxylic acid groups (Jaskari et al., 2001; Vuorio et al., 2003). The different impact of Ca^{+2} on the cationic drug release between the fibers with sulphonic acid or carboxylic acid groups has been claimed to be due to the strong binding of Ca^{+2} to the carboxylic groups (Charman et al., 1991).

In conclusion, the drug release from the cation-exchange fibers could be controlled by modifying either the fiber type or the ionic composition of the external solution.

5.1.3 Drug permeation from solution formulations (I-II)

Apomorphine permeation (I):
Apomorphine permeation experiments were conducted with donor solutions at pH5 due to an increase in the rate of degradation of the drug at higher pH values. The application of the iontophoresis significantly enhanced the *in vitro* permeation of apomorphine across the full-thickness porcine skin (Fig. 9A and Table 11). A steady-state flux was attained in all protocols after approximately three hours and the lag-time for the highest current density (0.5 mA/cm^2, 5 mg/ml donor solution) was 134 minutes.

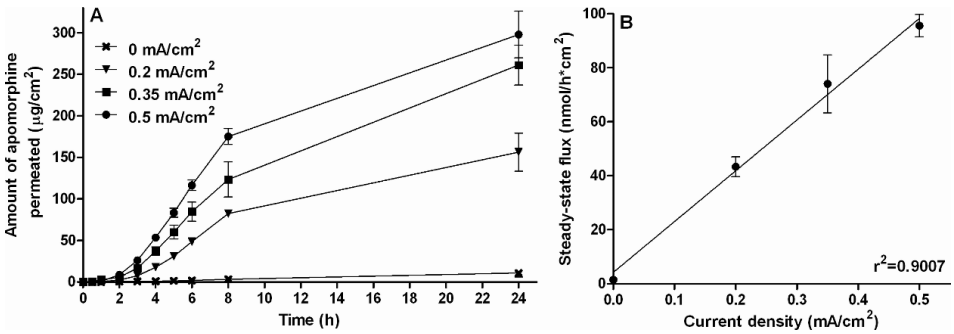

Fig. 9. **A.** The cumulative amount of apomorphine (µg/cm^2) permeated into the receiver compartment across the porcine skin passively and at different current densities. **B.** Relationship between current density and steady-state flux of apomorphine. The donor solution contained 5 mg/ml of apomorphine. The current was on for 8 h, whereafter passive drug permeation was followed for up to 24 h. Mean ± SEM, n=3-5.

Integrity of the skin and reversibility of the permeability increase were tested by measuring the passive flux after switching off the current at 8 h. The post-iontophoretic flux remained at a higher level compared to the normal passive flux of apomorphine. The relationship between the current density and steady state flux was determined at 5 mg/ml apomorphine donor solution concentration and at a current density range of 0-0.5 mA/cm^2 (Figure 9B). A linear relationship (r^2=0.9007) between these two parameters was established.

Table 11. Passive and iontophoretic fluxes (J_{ss}) and enhancement factors (E) of apomorphine across porcine skin from donor solutions at two different drug concentrations. Mean ± SEM. n=3-5.

Current density (mA/cm²)	1 mg/ml		5 mg/ml	
	J_{ss} (nmol/h*cm^2)	E	J_{ss} (nmol/h*cm^2)	E
0	0.47 ± 0.23	1	1.50 ± 0.13	1
0.20	20.41 ± 1.92	43	43.36 ± 3.72	29
0.35	-	-	74.11 ± 10.73	50
0.50	50.93 ± 6.50	108	95.64 ± 4.17	64

Therapeutic plasma levels of apomorphine range between 1.4-10.7 ng/ml (Neef and van Laar, 1999) and CL = 40.4 ± 15 ml/min/kg (van der Geest et al., 1998). Assuming a direct correlation between the *in vitro* and *in vivo* permeation and utilizing an Eq. 12 (Page 37), steady-state plasma concentrations c_{ss} was calculated. Iontophoretic delivery from the 5 mg/ml solution at the maximum current density from a 25 cm^2-sized permeation area (typical size of the patch) would result in a plasma level of 4.41 ng/ml of apomorphine. Thus, transdermal iontophoretic delivery of apomorphine can be therapeutically significant at our experimental parameters.

Leuprorelin permeation (II):

The permeation experiments with leuprorelin acetate (Fig. 10 and Table 12) were conducted with donor solutions at pH 7.4, where the peptide possesses a net charge ≈+1 (Hoogstraate et al., 1994). This pH was utilized as it has been proposed that the iontophoretic delivery of monovalent leuprorelin (at pH 7-8) is more efficient compared to divalent leuprorelin (at pH 4.5-5), as the divalent ions migrate slowly and may interact more with the charged sites in the skin (Lu et al., 1993). Passive permeability values were in agreement with those reported earlier (Kochhar and Imanidis, 2003, 2004) and rather small due to the large molecular weight and charge of the compound. The application of the iontophoresis significantly enhanced the *in vitro* delivery of the peptide across the porcine epidermis.

The pulsed current (PC) was slightly more efficient in carrying leuprorelin across the epidermis than constant current. Although, the results failed to show statistical difference by unpaired t-test, about 15% increase in the mean value of steady-state flux and about 22% increase in the cumulative amount of peptide delivered during 12 h of iontophoretic treatment were obtained with the pulsed current compared to 100% constant direct current. The total amount of current passed through the

epidermis in pulsed current profile was 25% smaller than in 100% DC profile. When normalizing 75% PC flux values to the same current amount as in 100% of DC profile, the transport of the peptide would be far more effective (≈50% increase in effective flux and ≈60% increase in amount of peptide delivered in 12 h). Furthermore, when comparing the transport numbers of the two iontophoretic current treatments by unpaired t-test, a statistically higher value was obtained with the pulsed current compared to constant current.

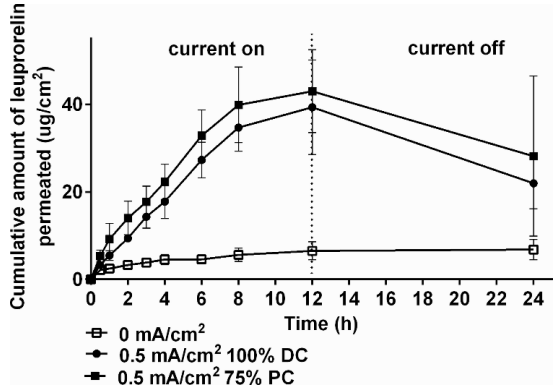

Fig. 10. The cumulative amount of leuprorelin (μg/cm^2) permeated into the receiver compartment across the porcine epidermis passively (0 mA/cm^2) and with the 100% constant (0.5 mA/cm^2 100% DC) and 75%on:25%off pulsed current (0.5 mA/cm^2 75% PC). Mean ± SD, n=5-6.

After iontophoretic current termination, leuprorelin acetate amounts in the receiver compartment of the diffusion cells decreased rapidly, most probably due to the adsorption of the peptide onto skin. Although the proteolytic activity of skin is much lower compared to mucosal routes (Steinstrasser and Merkle, 1995), we also cannot fully exclude the possibility of degradation of the peptide during the permeation experiments, as metabolism during transdermal delivery has been reported for a number of LHRH analogues (Delgado-Charro and Guy, 1995; Miller et al., 1990). The donor solution peptide concentrations were stable when kept at 37°C for 24 h

Table 12. Steady-state fluxes (J_{ss}), cumulative amounts (Q) of peptide delivered in 12 h, transport numbers (T_n) and iontophoretic enhancement factors (E) of leuprorelin delivered passively or by different iontophoretic current profiles. Mean ± SD. n=4-6.

Current profile	J_{ss} (μg/h*cm^2)	Q in 12 h (μg/cm²)	T_n	E
0 mA/cm²	0.47 ± 0.286	6.54 ± 2.063	-	-
100% DC	3.81 ± 0.820	35.26 ± 13.900	$1.70 \times 10^{-4} \pm 3.64 \times 10^{-5}$	8.1
75% PC	4.36 ± 0.758^{ns}	43.07 ± 9.407^{ns}	$2.59 \times 10^{-4} \pm 4.45 \times 10^{-5}$**	9.3

^{ns} not significant ($p>0.05$) J_{ss} and Q 75% PC vs 100% DC; ** $p<0.01$ T_n 75% PC vs 100% DC (unpaired t-test).

5.1.4 Electroosmotic transport of leuprorelin (II)

In order to estimate the magnitude of electroosmotic transport of the peptidic drug leuprorelin, a neutral polar molecule acetaminophen was included into the donor formulations. Transdermal transport of neutral molecule during anodal iontophoresis is mainly driven by electroosmosis (plus passive diffusion) and, hence, it gives a good estimation about the changes in the contribution of the electroosmosis as a transport mechanism for the molecule of interest (Fig. 11). Surprisingly, in the presence of the peptide in the donor formulation, the passive but not the iontophoretic flux of the marker compound was hindered during the 100% constant current treatment ($p<0.05$ by unpaired t-test). As the electroosmotic flux of compound is directly related to the amount of current passed across the epidermis, the pulsed current profile resulted in lower acetaminophen flux compared to the constant current profile when acetaminophen was iontophoresed alone. About 20% decrease was observed both in steady-state flux and amount of the marker compound permeated in 12 h with 75%on:25%off pulsed current treatment. Curiously, in the presence of leuprorelin in the donor formulation, the pulsed current treatment slightly increased the total acetaminophen flux compared to the constant current treatment although the results failed to demonstrate the statistical difference because of high variation.

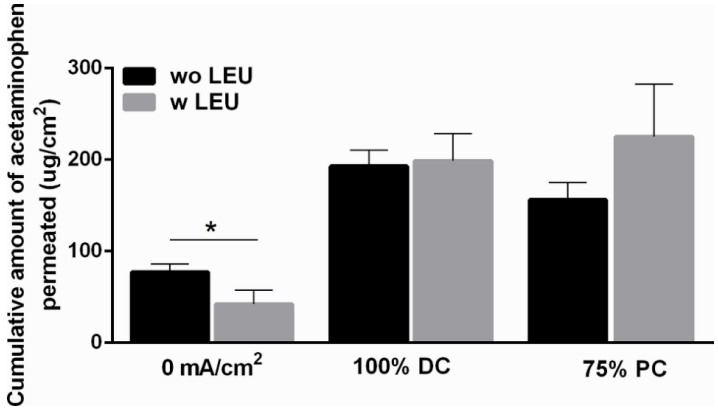

Fig. 11. Cumulative amounts of electroosmotic marker acetaminophen delivered across porcine epidermis during 12 h passively and with iontophoresis with (w LEU) and without (wo LEU) leuprorelin acetate at 100% constant (100% DC) and 75%on:25%off pulsed current (75% PC). Mean ± SD, * $p<0.05$ passive wo LEU vs passive w LEU (unpaired t-test).

Naturally, several assumptions are prerequisites to such analysis (Schuetz et al., 2005a). Firstly, the marker and the drug should be transported in a similar fashion by convective solvent flow. Secondly, there should be no interaction between these two substances. And thirdly, the electroosmotic flux of the marker should be proportional to its donor concentration.

The fractions of both transport mechanisms involved in acetaminophen delivery − passive diffusion and electroosmosis – from its total flux under constant and pulsed iontophoretic delivery − have been demonstrated in Fig 12. Electroosmotic component of the flux (J_{EO}) has been calculated according to the Eq. 9 (Page 36). To eliminate the differences in flux values due to the amount of current delivered, electroosmotic fluxes obtained with 75%on:25% off pulsed current (75% of the time the current was on) have been normalized to the total amount of current delivered during the 12 h of constant current treatment at the current density of 0.5 mA/cm^2 (100% of the time the current was on). Under constant current, the presence of the peptide had no effect on the total flux of acetaminophen. As the passive transport of the compound was inhibited, we believe that higher electroosmotic transport compensated for that part, so that the total flux remained the same as without the peptide in donor solution. The situation under pulsed current was different. As in the presence of the peptide, the total flux of acetaminophen was significantly higher than without the peptide, we suggest that this change was caused by the combined effects of enhanced electroosmotic transport and reduced inhibition of passive diffusion.

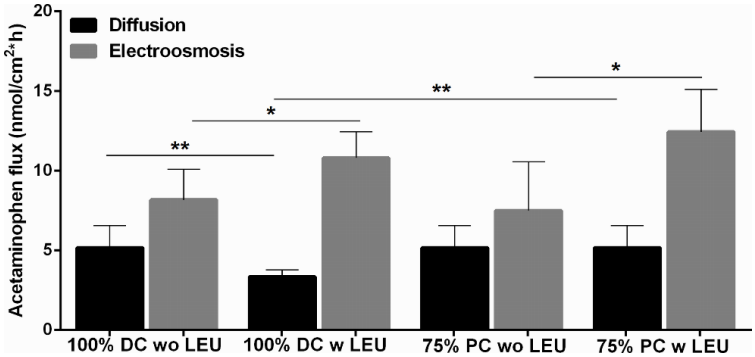

Fig. 12. The estimated proportions of diffusion (D) and electroosmosis (EO) from the total flux of acetaminophen delivered without (wo) and with (w) leuprorelin acetate. Electroosmotic flux values from 75% PC iontophoresis have been normalized to the total amount of current delivered at 100% DC treatment. Mean ± SD. * p<0.05 100% DC EO and 75% PC EO wo LEU vs w LEU; ** p<0.01 100% DC D wo LEU vs w LEU and D w LEU 100% DC vs 75% PC.

Based on these results we can conclude that pulsed current may offer significant benefits over constant current in the transdermal iontophoretic delivery of therapeutic peptides that have a tendency to adsorb into the skin and inhibit electroosmosis as their main transport mechanism. The significantly higher transport number obtained by the pulsed current demonstrated improved transport efficiency due to the more pronounced electroosmotic solvent flow.

5.1.5 Drug permeation from ion-exchange fibers (I-II)

Transdermal *in vitro* permeation of leuprorelin (**II**) was investigated from both of the cation-exchange fibers − Smopex®-101 and Smopex®-102 (Fig. 14), while only Smopex®-101 cation-exchange fibers were chosen as drug reservoirs for

apomorphine (**I**), as degradation of the drug was observed when it was loaded into Smopex®-102 fibers (Fig. 13). When the cation-exchange fibers loaded with either apomorphine or leuprorelin were used in the donor compartment of the diffusion cells, a gradual drug release from the fibers was observed during the application period of iontophoresis and then the concentration in the donor compartment remained almost constant. Different release profiles of leuprorelin were observed from the Smopex®-101 and Smopex®-102 fibers (**II**). From Smopex®-101 fibers that possess stronger sulphonic acid as the ion-exchange groups, the release remained slower and more limited compared to Smopex®-102 fibers with weaker carboxylic acid as ion-exchange groups. In general, as only a small fraction of the total drug inside the fibers was released during the 24 h of the permeation studies, the drug fluxes from the fibers remained lower compared to those from drug solutions (**I-II;** Table 13 and 14).

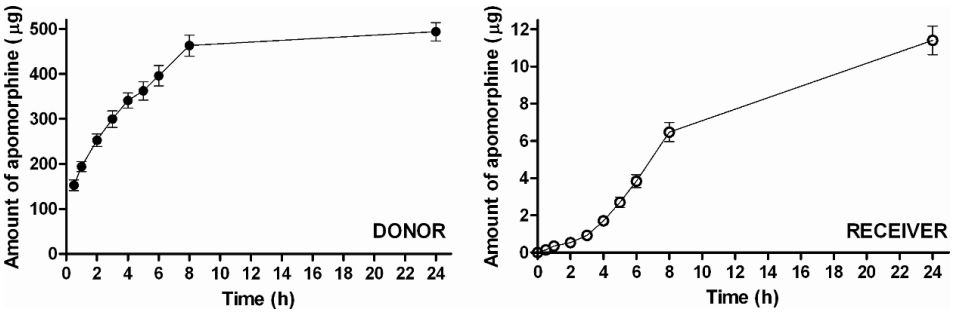

Fig. 13. The amounts of apomorphine in the donor and receiver compartments during iontophoretic delivery (0.5 mA/cm^2) across the porcine skin from Smopex-101 ion-exchange fiber (containing 24.66 ± 0.26 mg of apomorphine). The current was on for 8 h (mean ± SEM. n=6).

Table 13. Apomorphine release from Smopex®-101 ion-exchange fibers and passive and iontophoretic fluxes (J_{ss}) across porcine skin (mean ± SEM, n=6).

Current density (mA/cm²)	Amount of drug released in 24 h (%)	J_{ss} (nmol/h*cm^2)
0	1.7	0.07 ± 0.01
0.20	2.2	0.95 ± 0.09
0.50	2.0	4.30 ± 0.32

Despite of significantly lower fluxes from the cation-exchange fibers (compared to peptide flux from solution), one must take into account that leuprorelin acetate is a very potent drug (**II**). Taking into account the plasma clearance of the peptide (Sennello et al., 1986), a continuous delivery rate of 8.4 µg/h for 24 h has been calculated to be necessary for therapeutic effect (Kochhar and Imanidis, 2004). With the steady-state fluxes obtained from Smopex®-101 and Smopex®-102 fibers, 27.1 cm^2 and 12 cm^2 permeation areas were calculated as sufficient to achieve therapeutically effective delivery rate of leuprorelin, respectively. So the delivery of LHRH analogue leuprorelin acetate is feasible in therapeutic amounts from a drug reservoir based on cation-exchange fibers.

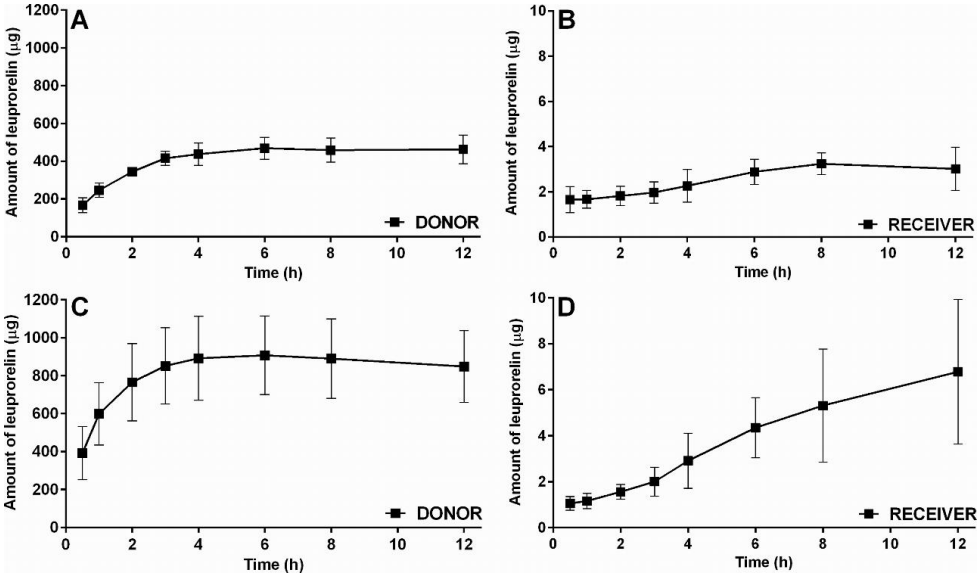

Fig. 14. The cumulative amounts of leuprorelin acetate in the donor and receiver compartments during 12 h iontophoretic delivery (0.5 mA/cm^2 constant current) across the porcine epidermis from Smopex®-101 (A and B) Smopex®-102 (C and D) ion-exchange fibers (containing 9.12 and 8.91 mg of peptide, respectively). Mean ± SD, n=4.

Table 14. The release of leuprorelin acetate from Smopex®-101 and Smopex®-102 cation-exchange fibers and iontophoretic fluxes (J_{ss}) across porcine epidermis (mean ± SD, n=4).

Fiber	Amount of peptide released in 12 h (%)	J_{ss} (µg/h*cm^2)
Smopex®-101	5.1 ± 0.6	0.31 ± 0.18
Smopex®-102	12.9 ± 6.0	0.71 ± 0.28

5.1.6 The effect of cations in the donor solution (I)

In experiments with apomorphine-loaded Smopex®-101 fibers, the impact of the cation (Na^+) concentration and nature of the cation were investigated (Table 15). In addition to the monovalent Na^+, the effect of divalent Ca^{2+}, trivalent Al^{3+} as well as of two organic cations with higher molecule masses − TEA^+ (tetraethylammonium) and BA^+ (benzalkonium) − were studied. As the iontophoretic mobility of a compound is inversely related to its molecular weight (Yoshida and Roberts, 1993), TEA^+ and BA^+ carry less current due to their lower mobility. Cations other than Na^+ were all used as chloride salts at a concentration of 154 mM, except for benzalkonium chloride (15.4 mM) that possesses surfactant properties and would be toxic at such a high concentration. Results from these experiments demonstrated that both the Na^+ concentration and the cation type in the donor solution exerted statistically significant effects on transdermal steady-state flux of apomorphine ($p<0.001$).

Table 15. The effect of Na^+ concentration and different cations in the donor buffer on the release and iontophoretic flux (J_{ss}) of apomorphine at a current of 0.5 mA/cm^2 (mean ± SEM. n=6).

Cation in the donor	pH of donor	Amount of drug released in 24 h (%)	J_{ss} (nmol/h*cm^2)	T_n
15.4 mM Na^+	5.00	0.9	6.09 ± 0.80	$3.26 \times 10^{-4} \pm 4.27 \times 10^{-5}$
154 mM Na^+	5.00	2.0	4.30 ± 0.32	$2.30 \times 10^{-4} \pm 1.70 \times 10^{-5}$
1540 mM Na^+	5.00	3.8	0.56 ± 0.08 ***	$0.30 \times 10^{-4} \pm 0.43 \times 10^{-5}$
154 mM Ca^{2+}	3.18	5.8	1.23 ± 0.01 ***	$0.66 \times 10^{-4} \pm 0.06 \times 10^{-5}$
154 mM Al^{3+}	2.94	7.5	0.21 ± 0.09 ***	$0.11 \times 10^{-4} \pm 0.46 \times 10^{-5}$
154 mM TEA^+	5.00	3.6	4.79 ± 0.49	$2.57 \times 10^{-4} \pm 2.65 \times 10^{-5}$
15.4 mM BA^+	5.00	3.7	2.15 ± 0.29 **	$1.15 \times 10^{-4} \pm 1.58 \times 10^{-5}$

** $p < 0.01$ 15.4 mM BA^+ vs 154 mM Na^+; *** $p < 0.001$ 1540 mM Na^+, 154 mM Ca^{2+} and 154 mM Al^{3+} vs 154 mM Na^+ (One-way ANOVA following Bonferroni`s multiple comparison test).

The concentration of cation:

When using a 1540 mM Na^+ in the donor buffer, the release of the drug was improved compared to that of 154 mM Na^+, but the flux across the skin remained significantly lower. At the same time, when 15.4 mM Na^+ was used in the donor, the flux was increased, despite of the smaller release of the drug from the fibers. On one hand, higher concentration of Na^+ would result in a decrease in Donnan potential leading to more extensive drug release from the ion-exchanger. At the same time it means more competition for the drug in the iontophoretic flux because of the presence of higher amounts of smaller and more mobile cations. Also, higher salt concentration in the donor formulations creates a water gradient over skin and thus, less hydrated tissue that could result in decreased transdermal drug fluxes (Bjorklund et al., 2010). Therefore, aiming for the highest fluxes possible, the amount of competing co-ions should be kept as low as possible as it affects the iontophoretic flux more than the actual drug concentration in the donor compartment. As expected, the 15.4 mM Na^+ provided also the highest transport number for the drug as the presence of competitive ions was the smallest.

The nature of cation:

As expected, the multivalent cations released more apomorphine from the cation-exchange fibers compared to Na^+ at the same molar concentration, and the release was increased with the increasing cation valence. At the same time, the iontophoretic transdermal fluxes of apomorphine from these donor solutions remained very low. The reason for that is the higher competition for the drug in the iontophoretic flux as cations with higher valence also carry higher fraction of the total current. Also, as the pH of the solutions of these chlorides ($CaCl_2$ and $AlCl_3$) was below the isoelectric point of the porcine skin, the negative charge of the skin was reversed and the cation transport suppressed. The solutions of organic cations released more apomorphine from the fibers compared to 154 mM Na^+, but at the same time, no

improvement in transdermal flux was observed. Overall, the amount of drug released into the donor compartment and the corresponding transdermal steady-state flux of apomorphine did not correlate to each other when different cations were used in the donor compartment.

In summary, cation-exchange fibers can be regarded as suitable reservoir materials to be combined with iontophoresis in order to retard the release of small or large molecular therapeutics and to provide additional control in their transport across the skin. By a suitable choice of the ionic composition of the donor formulation the release and flux kinetics can me modified to meet the required needs.

5.2 Combined use of nanocarriers and iontophoresis for transdermal drug delivery (III-IV)

5.2.1 Properties of the nanocarriers (III-IV)

In this part of the study, we aimed at producing drug-loaded nanocarriers (polymeric nanoparticles and liposomes) possessing a surface charge of the same sign as the drug loaded inside the carriers. Thereby, the benefit from the iontophoretic treatment to the transdermal drug delivery would be two-fold. According to our hypothesis, firstly, the electric current would push the liposomes into hair follicles, that has been recognized as one of the possible routes in transdermal absorption of drugs (Lauer et al., 1995). Thereafter, iontophoresis would pump the drug released from the depot in the skin or on the surface of the skin further into the bloodstream.

FA-PLGA nanoparticles (III):
Hydrophobic model drug – flufenamic acid (FFA) − was loaded into FA-PLGA nanoparticles (Fig. 15). The properties of the prepared drug-loaded and respective drug free FA-PLGA nanoparticles are presented in Table 16.

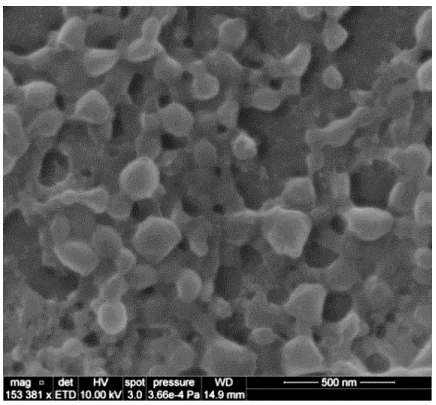

Fig. 15. Scanning electron microscope image of flufenamic acid-loaded FA-PLGA nanoparticles.

Table 16. Properties of flufenamic acid-loaded and respective drug-free FA-PLGA nanoparticles (mean ± SD, n=3).

	FFA loaded particles	Blank particles
Mean diameter (nm)	174.2 ± 1.8	179.0 ± 2.6
PDI	0.074 ± 0.004	0.072 ± 0.026
Zeta-potential (mV)	-8.50 ± 0.14	-17.80 ± 0.20
Drug content (w/w%)*	5.6 ± 0.2	-

* Grams of FFA in 100 g of lyophilized nanoparticles

Liposomes (IV):

Four different types of liposomes (conventional, pegylated, ultradeformable and ethosomes) were prepared and loaded with a hydrophilic model drug – diclofenac sodium (DS) (compositions are found in Table 7 in Section 4.2.3). The properties of the developed drug-loaded lipid vehicles are summarized in Table 17.

Table 17. Particle size, polydispersity index (PDI), charge (zeta potential) and mean encapsulation efficiency (EE%) of the prepared DS lipid vesicles.

Formulation and code	Size (nm)	PDI	Charge (mV)	Mean EE%
Conventional liposomes (F1)	147.0 ± 1.5	0.085 ± 0.013	-34.3 ± 1.7	67.5
Pegylated liposomes (F2)	144.2 ± 0.1	0.079 ± 0.029	-27.7 ± 1.0	60.4
Transfersomes (F3)	117.7 ± 0.5	0.073 ± 0.028	-29.8 ± 1.6	79.9
Ethosomes (F4)	116.5 ± 0.6	0.104 ± 0.005	-26.7 ±1.9	49.6

5.2.2 Stability of the nanocarriers

Prior to the permeation experiments, the electrochemical stabilities of the drug-loaded nanocarriers were evaluated under different iontophoretic current modes (**III-IV**). The stability of the FFA-loaded FA-PLGA nanoparticles was also determined when in contact with human epidermis or porcine full-thickness skin (**III**). All the results are presented as a change in hydrodynamic diameter and polydispersity index (PDI).

With the FFA-loaded FA-PLGA nanoparticles (**III**), no changes in hydrodynamic diameter or PDI were detected during the 72 h incubation of the particles in buffer without iontophoretic current or during the 8 h under constant, pulsed or alternating current (Fig. 16). At the same time, a significant increases both in hydrodynamic

diameter and PDI were observed after the FFA-loaded FA-PLGA nanoparticles had been in contact with the lower (dermal) side of human epidermis and full-thickness porcine skin for 24 h. This was not evident when the nanoparticle dispersion was placed on the upper (*stratum corneum*) side of the skin. Most likely the reason for such results was the separation/diffusion of skin components into the nanoparticle dispersion (and/or subsequent aggregation of the particles) during incubation. The degradation of the nanospheres is highly unlikely considering that short incubation times and fresh formulations were always used (Wu and Wang, 2001).

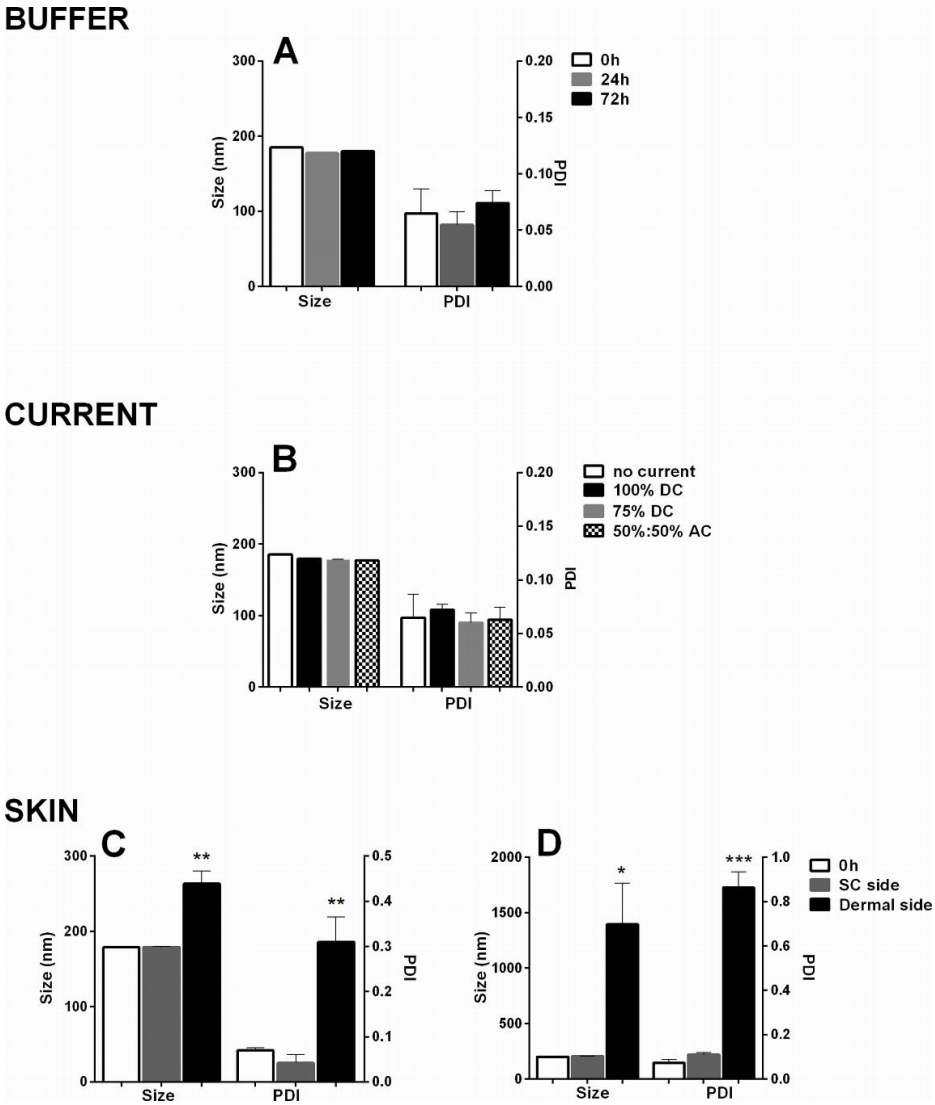

Fig. 16. Stability of FFA FA-PLGA nanoparticles expressed as a change in hydrodynamic diameter and PDI in 25 mM Hepes buffered saline pH=7.4 for 72 h (A), under different iontophoretic current profiles for 8 h (B) and in contact with *stratum corneum* (SC) or dermal side of human epidermis (C) or full-thickness porcine skin for 24 (D). Mean ± SD, n=3; * $p < 0.05$, ** $p < 0.01$, *** $p < 0.001$ (One-way ANOVA following Bonferroni`s multiple comparison test).

With liposomes (**IV**), no changes in hydrodynamic diameters were detected after 8 h of incubation of any vesicle formulation under constant or pulsed current (Fig. 17). The PDIs of formulations F1, F2 and F3 had increased slightly, but these changes did not reach statistical significance ($p>0.05$ when compared with unpaired t-test before and after current treatment). Although pore widening of lipid bilayers under electric field has been associated with breakdown of liposomes and leakage of loaded drug, the magnitude of current used in typical transdermal iontophoretic treatment regimens is too small to cause such rupture of vesicles. Furthermore, under electric current field the fusion of charged vesicles is inhibited, so it can contribute to better colloidal stability of the study formulations.

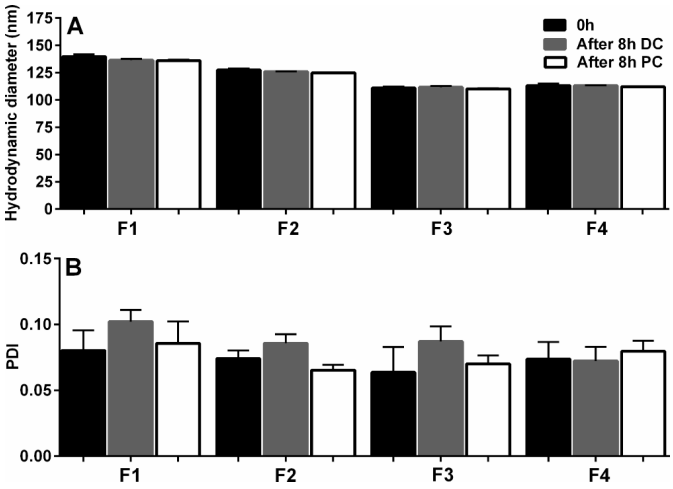

Fig. 17. Electrochemical stability of liposomes under iontophoretic current for 8 h expressed as a change in hydrodynamic diameter and PDI. Mean ± SD, n=3.

5.2.3 Drug release from nanocarriers

The drug formulation to be utilized in combination with transdermal iontophoresis should preferably avoid immediate/burst drug release and deliver the drug to the permeation site in a gradual yet continuous manner. In this way, more predictable and controlled drug transport could be achieved, resulting in transdermal drug transport less dependent on skin variables. The release kinetics of drugs from the nanocarriers was studied in a similar setting as the *in vitro* transdermal permeation tests – at 32 °C (**III**) or 37°C (**IV**) in static Franz diffusion cells, using a synthetic dialysis membrane to separate the donor compartment from the receiver compartment. From FA-PLGA nanoparticles the drug release was also determined under different iontophoretic current modes (**III**).

In experiments with FFA-loaded PLGA nanoparticles, the amount of FFA gradually increased in the receiver compartment upto 8 h, followed by a plateau at ≈50% of encapsulated drug amount released (Fig. 18). The application of

iontophoretic current – constant, pulsed or alternating – did not have any effect on the release of FFA from the nanoparticles. This result is supported by an earlier study where the release of peptidic drug triptorelin from PLGA nanospheres was also found not to be affected by iontophoretic current (Nicoli et al., 2001).

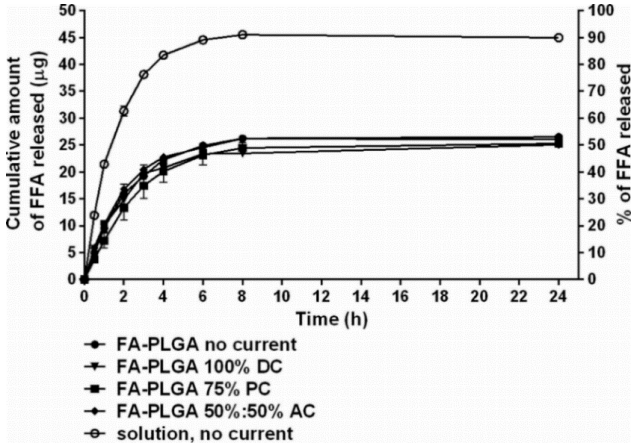

Fig. 18. Release of FFA from FA-PLGA nanoparticles passively and under different current modes. Current was on for 8 h. The total amount of FFA in nanoparticles was 50 µg. Mean ± SD, n=3).

From all the liposome formulations DS was released at a similar rate, resulting in ≈50% of the encapsulated drug released in 24 h (Fig. 19). In general, the most important factors affecting drug release from liposomes are the physicochemical properties of the liposome membrane and the therapeutic agent, and the vesicle size (Lindner and Hossann, 2010). All our formulations possessed similar vesicle size and drug-to-lipid ratio (data not shown) and the effects of differences in composition (inclusion of surfactant, ethanol or cholesterol) on release were not evident in this study. Thus, all the formulations demonstrated suitable release kinetics to be used in transdermal delivery purposes and any changes in transport efficiency of DS from different lippid vesicle formulations across the skin could only be attributed to the differences in liposome-skin-iontophoretic current interactions − not in drug release rate.

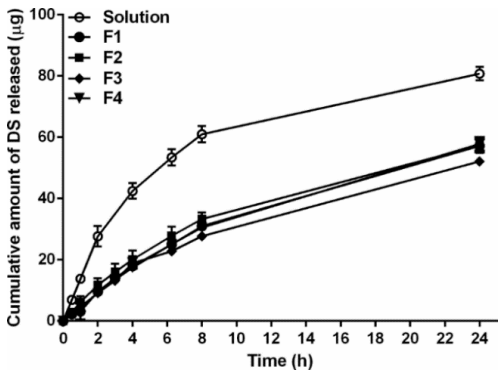

Fig. 19. Release of diclofenac sodium (DS) from different liposome formulations (F1-F4). The total amount of DS in liposomes was 100 µg. Mean ± SD, n=3.

In summary, all the prepared nanocarriers were deemed suitable for transdermal iontophoretic administration, regarding the colloidal properties, stability under iontophoretic current and release kinetics.

5.2.4 Drug permeation from solution

Permeation studies with flufenamic acid (FFA; **III;** Fig. 20 and Table 18) and diclofenac sodium (DS; **IV;** Fig. 21 and Table 19) were conducted at pH 7.4, where they carry a negative charge and can therefore be administered under a negatively charged electrode (cathode). According to the Henderson–Hasselbalch equation, at pH 7.4 practically all FFA and DS are ionized state (99.97% and 99.94% for FFA and DS, respectively) and can therefore maximally benefit from the iontophoretic current. As is evident from experiments with drug solutions, the application of iontophoresis significantly increased the permeation of both the drugs across the skin. As the iontophoretic flux of compounds is typically directly related to the amount of current passed through the skin, the constant current was the most effective protocol in enhancing the *in vitro* transdermal delivery of FFA and DS (**III-IV**). As expected, the pulsed current profile resulted in ≈25% lower steady-state flux values compared to the constant current as the current was on only 75% of the time. The application of alternating current was quite inefficient in transporting negatively charged FFA across the skin and the steady-state flux values remained only slightly superior to passive delivery (**III**).

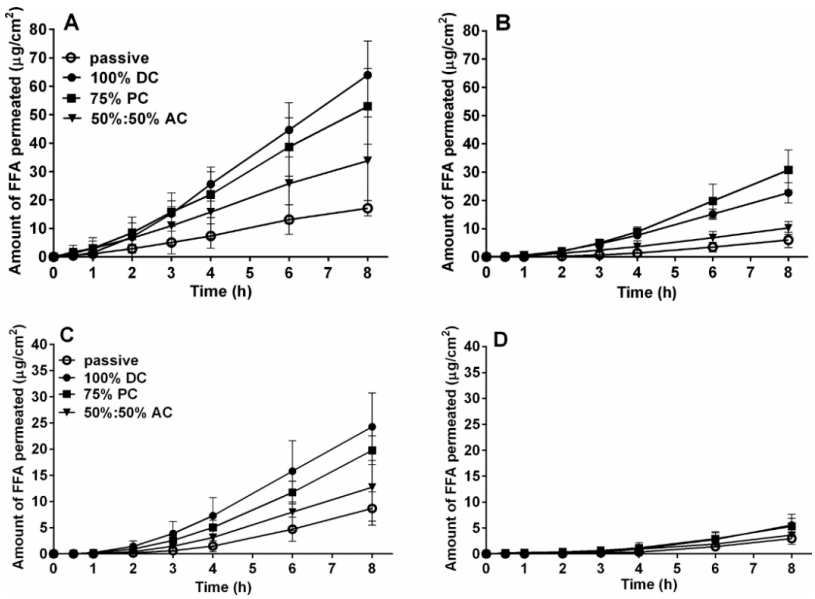

Fig. 20. The permeation curves of FFA without (passive) and with different iontophoretic current modes across human epidermis from solution (A) and FA-PLGA nanoparticulate formulation (B) and across porcine full-thickness skin from solution (C) and FA-PLGA nanoparticulate formulation (D). 100 % DC – constant direct current 0.5 mA/cm^2; 75% PC – 75% on:25% off pulsed current; 50%:50% AC – 50% cathodal:50% anodal alternating current (mean ± SD, n=4-6).

For FFA, a linear relationship with r^2= 0.8241 between the current density and steady-state flux values was established in experiments with human epidermis as a permeation membrane at a donor concentration of 1 mg/ml of FFA over a constant current density range of 0 - 0.5 mA/cm^2 (**III**). Therefore, increasing the current density of the donor solution resulted in higher steady-state fluxes.

Table 18. The descriptive values calculated from FFA permeation curves (mean ± SD, n=4-7).

	Current type	J_{ss} [a] (nmol/h*cm^2)	E [b]	Q_{8h} (µg) [c]	T_n [d]
Human epidermis	**FFA solution**				
	Passive	9.29 ± 1.67	-	30.0 ± 4.6	-
	100% DC	33.56 ± 5.72	3.8	101.6 ± 30.4	1.79 x 10^{-3} ± 3.06 x 10^{-4}
	75% PC	25.73 ± 6.95	2.8	93.2 ± 23.4	1.84 x 10^{-3} ± 4.96 x 10^{-4}
	50%:50% AC	11.06 ± 2.76	1.2	59.5 ± 27.2	0.87 x 10^{-3} ± 4.92 x 10^{-4}
	FFA FA-PLGA nanoparticles				
	Passive	3.07 ± 1.39	-	10.5 ± 4.9	-
	100% DC	11.59 ± 2.11	3.8	39.9 ± 6.3	6.21 x 10^{-4} ± 1.13 x 10^{-5}
	75% PC	15.13 ± 13.86 [ns]	4.9	54.1 ± 12.62 *	9.41 x 10^{-4} ± 3.68 x 10^{-4} [ns]
	50%:50% AC	5.02 ± 0.33	1.6	18.0 ±4.1	2.69 x 10^{-4} ± 4.32 x 10^{-5}
Porcine skin	**FFA solution**				
	Passive	4.37 ± 1.73	-	20.9 ± 7.7	-
	100% DC	12.75 ± 3.57	2.9	58.5 ± 15.6	1.66 x 10^{-3} ± 7.43 x 10^{-4}
	75% PC	10.21 ± 3.73	2.3	47.7 ± 16.3	7.29 x 10^{-4} ± 2.67 x 10^{-4}
	50%:50% AC	6.67 ± 3.43	1.5	30.7 ±15.6	3.57 x 10^{-4} ± 1.84 x 10^{-4}
	FFA FA-PLGA nanoparticles				
	Passive	1.28 ± 0.65	-	7.1 ± 2.8	-
	100% DC	2.76 ± 1.14	2.2	13.4 ± 5.1	1.48 x 10^{-4} ± 6.09 x 10^{-5}
	75% PC	2.46 ± 0.76	1.9	11.2 ± 4.9	1.62 x 10^{-4} ± 7.02 x 10^{-5}
	50%:50% AC	1.77 ± 0.21	1.4	8.8 ± 0.7	9.46 x 10^{-5} ± 1.13 x 10^{-5}

[a] steady-state flux; [b] enhancement factor; [c] cumulative amount of drug permeated in 8h; [d] transport numbers. [ns] not significant ($p>0.05$) J_{ss} and T_n 75% PC vs 100% DC; * $p<0.05$ Q_{8h} 75% PC vs 100% DC (unpaired t-test).

5.2.5 Drug permeation from nanocarriers

In general, the use of nanocarrier formulations in the donor compartments of diffusion cells resulted in decreased steady-state flux values and increased lag-times compared to the FFA (**III**) or DS (**IV**) delivery from solutions. This was caused by the gradual and limited release of the model compound from the nanoparticles or liposomes during the time frame of permeation experiments. It is possible that this incubation time was too short to demonstrate the potential superiority of nanoencapsulation of tested model drugs permeation across the skin. As iontophoretic treatment periods for more than 8 h are not practical and applicable in most clinical settings, we did not consider longer delivery times here.

Surface charge of the nanocarrier (IV):

One of the aims of this study was to investigate the effect of surface charge of the nanocarrier on model drug transport under iontophoretic current. For that purpose, we compared the drug transport from pegylated liposomes with reduced negative zeta potential value to that from highly negatively charged conventional liposomes. As expected, the highly negatively charged conventional liposomes (F1) led to slightly more efficient iontophoretic delivery of DS than pegylated liposomes with reduced surface charge (F2), indicating that the liposome charge can affect the outcome of iontophoretic treatment. Also, the enhancement factors and transport numbers of F2 were lower than that of F1. At the same time, passive drug fluxes from both the formulations were identical. This indicates that the higher iontophoretic flux of F1 liposomes could have only be related directly to the more pronounced mobility of the nanocarrier under electric current (electrorepulsion of liposome), not to changes in skin-liposome interaction, leading to improved diffusion of liposomes.

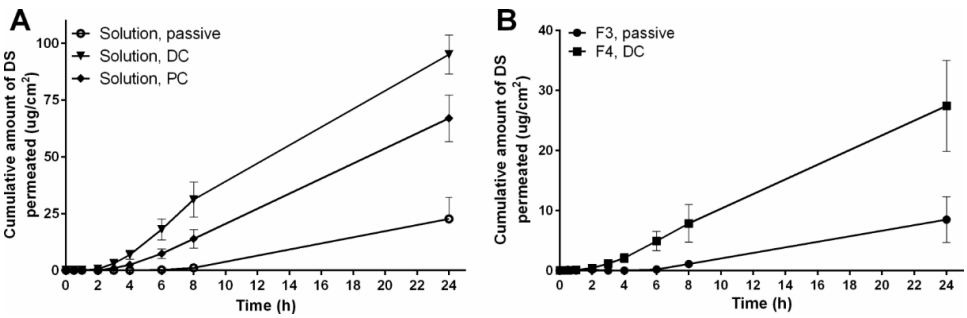

Fig. 21. The *in vitro* transdermal permeation of DS across porcine full-thickness skin. **A**. The permeation curves of DS from solution formulation passively and under direct constant (DC) or pulsed current (PC). **B**. The liposome formulations with the highest passive (F3, passive) or iontophoretic flux (F4, DC). Mean ± SD, n=5-6.

Type of the lipid vesicle (III):

In a study of DS-loaded liposomes, the impact of the type of the vesicular system was determined on the permeation of loaded model drug under iontophoretic delivery. Thus, the drug permeation from conventional liposomes and two special vesicular systems, ultradeformable liposomes and ethosomes was compared. From all the tested lipid vesicle formulations, ultradeformable liposomes (F3) resulted in the highest passive flux but not the highest iontophoretic flux (Fig. 21B). At the same time, the highest iontophoretic flux was obtained with ethosomes (F4) under direct constant current (E_{DC}=6.4 and E_{DC}=2.4 for F4 and F3, respectively), although the passive transport of DS from ethosomes was inferior to the one from transfersomes. For transfersomes, open (non-occluded) administration has been proposed to be prerequisite to obtain maximum permeation enhancing effect as the driving force for penetration – transdermal hydration gradient – is eliminated by occlusive conditions (Cevc and Blume, 1992). At the same time as the application of iontophoretic current requires aqueous media around the electrodes, all our

permeation experiments were conducted under occlusion to prevent the evaporation of the buffer from the donor compartment. Interestingly, in our study occlusion did not abolish totally the penetration enhancing effects of the transfersomes compared to other tested lipid vesicles. Similar results were obtained when estradiol transport from transfersomes under occlusion was studied (Essa et al., 2004).

Table 19. The results from the permeation experiments with DS solution and different lipid vesicle formulations (F1-F4). Mean, n=5-6.

	Treatment	J_{ss}[a] (nmol/h*cm^3)	T_n[b]	E[c]	% of J_{PC} of J_{DC}[d]
	Passive	2.78 ± 1.31	-	-	-
Solution	*DC*	14.21 ± 7.51	$8.13 \times 10^{-4} \pm 3.81 \times 10^{-4}$	5.1	-
	PC	10.45 ± 4.27	$7.47 \times 10^{-4} \pm 2.86 \times 10^{-4}$	3.8	73.5
	Passive	1.11 ± 0.43	-	-	-
F1	*DC*	3.98 ± 1.78	$2.13 \times 10^{-4} \pm 9.53 \times 10^{-5}$	3.6	-
	PC	2.94 ± 0.90	$2.10 \times 10^{-4} \pm 6.46 \times 10^{-5}$	2.6	73.9
	Passive	1.11 ± 0.56	-	-	-
F2	*DC*	3.64 ± 1.12	$1.95 \times 10^{-4} \pm 7.47 \times 10^{-5}$	3.3	-
	PC	1.78 ± 0.72	$1.27 \times 10^{-4} \pm 5.09 \times 10^{-5}$	1.6	48.6
	Passive	1.44 ± 0.30	-	-	-
F3	*DC*	3.47 ± 1.23	$1.86 \times 10^{-4} \pm 6.72 \times 10^{-5}$	2.4	-
	PC	2.38 ± 0.64	$1.70 \times 10^{-4} \pm 3.98 \times 10^{-5}$	1.7	68.6
	Passive	0.71 ± 0.18	-	-	-
F4	*DC*	4.53 ± 1.59	$2.43 \times 10^{-4} \pm 1.04 \times 10^{-4}$	6.4	-
	PC	2.87 ± 1.82	$2.05 \times 10^{-4} \pm 1.39 \times 10^{-4}$	4.1	63.4

[a] steady-state flux; [b] transport number; [c] enhancement factor; [d] % of J_{PC} of J_{DC} – percent of steady-state flux of pulsed current treatment from steady-state flux of constant current treatment

Effect of current type (III-IV):

In addition, the effect of current type was studied on the transdermal delivery of a drug loaded into nanocarriers. Constant current (DC) treatment is typically the most efficient in enhancing transdermal delivery of charged or ionic drugs, although it has some limitations, especially in long-term continuous use (see Section 2.2.2). Interestingly, in contrast to free drug delivery from solution, when using dispersions of FFA-loaded nanoparticles in the donor compartment, the application of pulsed current (PC) was equal or more efficient in carrying the FFA across the skin compared to the constant current (**III**). The cumulative amount of FFA delivered from the FA-PLGA nanoparticles across human epidermis with pulsed current was significantly higher than the amount transported with constant current ($p<0.05$). However, we were not able to detect any remarkable differences either in the intensity or depth of the fluorescence signal in the cryo-sectioned porcine full-thickness skin after permeation studies without or with iontophoresis by the different current profiles (Fig. 22.). On the contrary, pulsed current treatment had no clear advantage over constant current treatment in combination with any liposome formulation (**IV**). The treatment was especially ineffective with liposomes with

lower surface charge such as pegylated or ultradeformable liposomes, as seen from the % of J_{PC} of J_{DC} value (that show the percent of steady-state flux of pulsed current treatment from the steady-state flux of constant current treatment). Under alternating current (AC), model drug FFA was transported from nanoparticle dispersions across the skin similarly to solution formulation, with fluxes only slightly higher than with passive delivery (**III**).

Skin type (III):

The transdermal transport of free and nanoencapsulated FFA under passive and iontophoretic conditions was investigated in two skin barrier models of "golden standard" − human epidermis and full-thickness porcine skin. Both these skin models are histologically and biochemically very similar and the fluxes have been repeatedly demonstrated to correlate well (Godin and Touitou, 2007). However, when studying *in vitro* penetration of substances through the follicular route, the properties of porcine skin are believed to be superior to excised human skin, mainly due to the fact that the follicular reservoir of the human skin is significantly reduced after excision (Patzelt et al., 2008). Our study did not reveal any major differences in results with human epidermis and porcine full-thickness skin, but obviously the flux values remained lower and lag-times longer when delivering the hydrophobic FFA across full-thickness skin compared to the epidermal layer only.

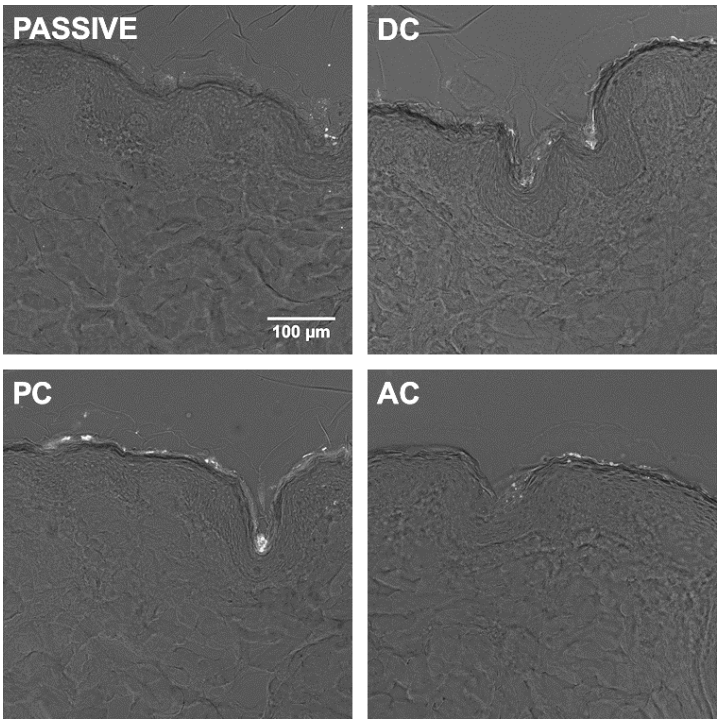

Fig. 22. Confocal laser scanning images of cross sections of porcine skin after permeability study without iontophoresis and with different iontophoretic current treatments. Fluorescence from FA-PLGA nanoparticles is represented in white colour.

Overall, in this study we did not establish any clear advantage from nanoencapsulation of drugs into nanocarriers with respect to drug permeation across the skin compared to free drug formulation, both in passive delivery or with any tested iontophoretic protocols. Nevertheless, it cannot be excluded that similar systems of combining nanocarriers and iontophoresis could have potential in other therapeutic regimens, *e.g.* aiming at depot formation in the skin after short-term (1-2 h) iontophoresis, followed by sustained release of drugs into the systemic blood circulation over longer periods of time.

CONCLUSIONS

In this study novel systems combining iontophoresis and ion-exchange fibers or drug-loaded nanocarriers were developed and tested for the controlled transdermal delivery of various therapeutics. The main conclusions are:

1. Ion-exchange fibers are promising drug reservoir materials to retard the drug release and provide additional control into transdermal transport of small molecular weight drugs and peptides. The drug release from the fibers and the following transdermal flux can be controlled by modifying either the fiber type or the ionic composition of the external solution. Due to the high affinity of tested model drugs towards the ion-exchanger, the transdermal fluxes from the fibers remained lower compared to the respective fluxes from solution formulations.

2. The use of pulsed current may offer significant benefit over constant current in the transdermal iontophoretic delivery of therapeutic peptides that have a tendency to adsorb into skin and inhibit electroosmosis as their main transport mechanism. Although the application of pulsed current did not result in the increase of transdermal flux of the cationic hydrophobic peptide leuprorelin across porcine epidermis compared to constant current, the significantly higher transport number demonstrated improved transport efficiency due to elimination of the inhibition of electroosmotic solvent flow.

3. Although the tested drug-loaded nanocarriers – PLGA nanoparticles and lipid vesicles – were suitable for transdermal iontophoretic administration, regarding the colloidal properties, stability under iontophoretic current and drug release kinetics, no clear advantage was observed with respect to drug permeation from free drug formulations. Nanoencapsulation of model drugs led to reduced transdermal steady-state fluxes and longer lag-times, both in passive and iontophoretic delivery regimens.

4. This is the first study to systematically investigate the effect of iontophoretic current type on the transdermal permeation of a drugs loaded into nanocarriers. Based on our findings, polymeric nanoparticle-based formulations for transdermal iontophoretic delivery could benefit from the use of pulsed current instead of the traditional constant current. In contrast, traditional constant current iontophoresis should be applied in combination with the drug-loaded lipid vesicular nanocarriers.

5. Several crucial formulation parameters have to be carefully considered when developing ion-exchanger or nanocarrier-based systems intended for transdermal iontophoretic drug delivery. Both the release and flux of drugs from the ion-exchange reservoir are highly dependent on the ionic composition of the donor formulation. In our study, the presence of competing co-ions in the donor solution had a dominating impact on drug fluxes over the amount of the drug molecules

released from the fibers into the donor formulation. Iontophoretic drug transport from lipid vesicular nanocarriers is significantly affected by the composition and charge of the lipid bilayer.

The major challenge in the development of new iontophoretic systems is to design relatively inexpensive and patient-friendly systems, while still maintaining the stability of drugs and providing efficient drug delivery. In this thesis, we demonstrated that ion-exchanger or nanocarrier-based drug reservoir systems are suitable to be combined with iontophoresis and that several of the above problems could be overcome by these systems. Although groundwork has been laid for the application of such combined approaches, there is a long way to determine the full potential of these systems in transdermal drug delivery.

Today, ion-exchange materials are still mainly used for the purification and separation of compounds. More detailed and exhaustive studies are required to explore the benefits of such materials in drug delivery applications, including in iontophoretic drug delivery for drug release control, competing counter-ion removal or drug flux enhancement. In order to optimize iontophoretic drug delivery from systems based on ion-exchange materials, precise impact of all the physicochemical properties of the drug and electric current on drug release kinetics from ion-exchangers has to be determined. Modeling and simulation to build predictive tools on the interactions between drug/ion-exchanger/external conditions, could be applied to facilitate the research in further realizing the utilization of these materials as drug carriers.

The combined use of nanotechnology and active enhancement techniques such as iontophoresis is predicted to be one of the future strategies in further increasing the drug transport for dermal or transdermal administration. Combined with nanotechnology, iontophoresis could open up the transcutaneous route to new therapeutic areas and the range of drugs to be delivered by skin could be expanded to electrically neutral, hydrophilic, large or unstable molecules. Still further studies are needed to investigate the potential of follicular route for delivering therapeutics in nanocarriers into viable skin or systemic circulation. Also, as nanocarriers represent a heterogeneous group of drug vehicles with typically complex and multiple modes of drug transport, more investigations are warranted to fully understand the exact transport mechanism from each nanocarrier category, either in passive or iontophoretic delivery. Finally, the efficacy and safety of all such combined systems in humans requires thorough evaluation.

REFERENCES

Abrego, G., Alvarado, H., Souto, E.B., Guevara, B., Bellowa, L.H., Garduno, M.L., Garcia, M.L., Calpena, A.C., 2016. Biopharmaceutical profile of hydrogels containing pranoprofen-loaded PLGA nanoparticles for skin administration: In vitro, ex vivo and in vivo characterization. Int J Pharm 501, 350-361.

Akerman, S., Viinikka, P., Svarfvar, B., Jarvinen, K., Kontturi, K., Nasman, J., Urtti, A., Paronen, P., 1998. Transport of drugs across porous ion exchange membranes. J Control Release 50, 153-166.

Akimoto, T., Kawahara, K., Nagase, Y., Aoyagi, T., 2001. Polymeric transdermal drug penetration enhancer: The enhancing effect of oligodimethylsiloxane containing a glucopyranosyl end group. J Control Release 77, 49-57.

Anand, V., Kandarapu, R., Garg, S., 2001. Ion-exchange resins: carrying drug delivery forward. Drug Discov Today 6, 905-914.

Azagury, A., Khoury, L., Enden, G., Kost, J., 2014. Ultrasound mediated transdermal drug delivery. Adv Drug Deliv Rev 72, 127-143.

Atyabi, F., Sharma, H.L., Mohammad, H.A.H., Fell, J.T., 1996. Controlled drug release from coated floating ion exchange resin beads. J Control Release 42, 25-28.

Aulton, M.E., Taylor, K.M.G., 2013. Aulton's Pharmaceutics: The Design and Manufacture of Medicines. Elsevier Health Sciences UK.

Bamrungsap, S., Zhao, Z., Chen, T., Wang, L., Li, C., Fu, T., Tan, W., 2012. Nanotechnology in therapeutics: a focus on nanoparticles as a drug delivery system. Nanomedicine (Lond) 7, 1253-1271.

Banga, A.K., 2002. Electrically Assisted Transdermal And Topical Drug Delivery. CRC Press.

Berti, J.J., Lipsky, J.J., 1995. Transcutaneous Drug Delivery: A Practical Review. Mayo Clin Proc 70, 581-586.

Bhise, K., Shaikh, S., Bora, D., 2008. Taste Mask, Design and Evaluation of an Oral Formulation Using Ion Exchange Resin as Drug Carrier. AAPS PharmSciTech 9, 557-562.

Biswajit, M., Niladri, S.D., Ruma, M., Priyanka, B., Pranab, J.D., Paramita, P., 2014. Current Status and Future Scope for Nanomaterials in Drug Delivery, in: Ali Demir Sezer (Ed.), Application of Nanotechnology in Drug Delivery. InTech.

Bjorklund, S., Engblom, J., Thuresson, K., Sparr, E., 2010. A water gradient can be used to regulate drug transport across skin. J Control Release 143, 191-200.

Bodde, H.E., Verhoef, J.C., Ponec, M., 1989. Transdermal peptide delivery. Biochemical Society transactions 17, 943-945.

Boinpally, R.R., Zhou, S.L., Devraj, G., Anne, P.K., Poondru, S., Jasti, B.R., 2004. Iontophoresis of lecithin vesicles of cyclosporin A. Int J Pharm 274, 185-190.

Bouchard, F.E., Friedman, I.J., Taylor, R.J., 1958. Vitamin b12 products and preparation thereof, A61K31/00 ed. Pfizer & Co

Brand, R.M., Guy, R.H., 1995. Iontophoresis of nicotine in vitro: pulsatile drug delivery across the skin? J Control Release 33, 285-292.

Burnette, R.R., Ongpipattanakul, B., 1987. Characterization of the permselective properties of excised human skin during iontophoresis. J Pharm Sci 76, 765-773.

Cevc, G., Blume, G., 1992. Lipid vesicles penetrate into intact skin owing to the transdermal osmotic gradients and hydration force. BBA - Biomembranes 1104, 226-232.

Cevc, G., Schatzlein, A., Richardsen, H., 2002. Ultradeformable lipid vesicles can penetrate the skin and other semi-permeable barriers unfragmented. Evidence from double label CLSM experiments and direct size measurements. Biochim Biophys Acta 1564, 21-30.

Cevc, G., Vierl, U., 2010. Nanotechnology and the transdermal route: A state of the art review and critical appraisal. J Control Release 141, 277-299.

Charman, W.N., Christy, D.P., Geunin, E.P., Monkhouse, D.C., 1991. Interaction between calcium, a model divalent cation, and a range of poly (acrylic acid) resins as a function of solution pH. Drug Dev Ind Pharm 17, 271-280.

Charoenputtakun, P., Li, S.K., Ngawhirunpat, T., 2015. Iontophoretic delivery of lipophilic and hydrophilic drugs from lipid nanoparticles across human skin. Int J Pharm 495, 318-328.

Chen, H., Zhu, H., Zheng, J., Mou, D., Wan, J., Zhang, J., Shi, T., Zhao, Y., Xu, H., Yang, X., 2009. Iontophoresis-driven penetration of nanovesicles through microneedle-induced skin microchannels for enhancing transdermal delivery of insulin. J Control Release 139, 63-72.

Cheng, Y., Man, N., Xu, T., Fu, R., Wang, X., Wang, X., Wen, L., 2007. Transdermal delivery of nonsteroidal anti-inflammatory drugs mediated by polyamidoamine (PAMAM) dendrimers. J Pharm Sci 96, 595-602.

Cheng, Y.H., Watts, P., Hinchcliffe, M., Hotchkiss, R., Nankervis, R., Faraj, N.F., Smith, A., Davis, S.S., Illum, L., 2002. Development of a novel nasal nicotine formulation comprising an optimal pulsatile and sustained plasma nicotine profile for smoking cessation. J Control Release 79, 243-254.

Chereddy, K.K., Coco, R., Memvanga, P.B., Ucakar, B., des Rieux, A., Vandermeulen, G., Preat, V., 2013. Combined effect of PLGA and curcumin on wound healing activity. J Control Release 171, 208-215.

Chien, Y.W., Siddiqui, O., Shi, W.M., Lelawongs, P., Liu, J.C., 1989. Direct current iontophoretic transdermal delivery of peptide and protein drugs. J Pharm Sci 78, 376-383.

Christy, D.P., Kim, S.W., Petersen, R.V., 1979. Effect of temperature and an ion-exchange resin on cation diffusion through silicone polymer tubing. J Pharm Sci 68, 1102-1105.

Conaghey, O.M., Corish, J., Corrigan, O.I., 1998. The release of nicotine from a hydrogel containing ion exchange resins. Int J Pharm 170, 215-224.

Craane-van Hinsberg, W.H., Verhoef, J.C., Bax, L.J., Junginger, H.E., Bodde, H.E., 1995. Role of appendages in skin resistance and iontophoretic peptide flux: human versus snake skin. Pharm Res 12, 1506-1512.

Curdy, C., Kalia, Y.N., Guy, R.H., 2001. Non-invasive assessment of the effects of iontophoresis on human skin in-vivo. J Pharm Pharmacol 53, 769-777.

da Silva, C.L., Del Ciampo, J.O., Rossetti, F.C., Bentley, M.V., Pierre, M.B., 2013. Improved in vitro and in vivo cutaneous delivery of protoporphyrin IX from PLGA-based nanoparticles. Photochem Photobiol 89, 1176-1184.

Danhier, F., Ansorena, E., Silva, J.M., Coco, R., Le Breton, A., Preat, V., 2012. PLGA-based nanoparticles: an overview of biomedical applications. J Control Release 161, 505-522.

Delgado-Charro, M.B., Guy, R.H., 1995. Iontophoretic delivery of nafarelin across the skin. Int J Pharm 117, 165-172.

Delgado-Charro, M.B., Guy, R.H., 2003. Iontophoresis - Applications in drug Delivery and Noninvasive Monitoring, in: Guy, R.H., Hadgraft, J. (Eds.), Transdermal Drug Delivery. Marcel Dekker, New York, pp. 199-227.

Delgado-Charro, M.B., Rodriguez-Bayon, A.M., Guy, R.H., 1995. Iontophoresis of Nafarelin - Effects of Current-Density and Concentration on Electrotransport in-Vitro. J Control Release 35, 35-40.

Denet, A.R., Vanbever, R., Preat, V., 2004. Skin electroporation for transdermal and topical delivery. Adv Drug Deliv Rev 56, 659-674.

Dragicevic-Curic, N., Scheglmann, D., Albrecht, V., Fahr, A., 2008. Temoporfin-loaded invasomes: Development, characterization and in vitro skin penetration studies. J Control Release 127, 59-69.

Drayton, C.J., Hansch, C., Sammes, P.G., Taylor, J.B., 1990. Cumulative subject index & drug compendium, Pergamon, Oxford.

Drugbank, www.drugbank.ca.

EC, 2008. On Regulatory Aspects of Nanomaterials, in: Committee on the Environment, P.H.a.F.S. (Ed.).

Economy, J., Dominguez, L., Mangun, C.L., 2002. Polymeric Ion-Exchange Fibers. Ind Eng Chem Res 41, 6436-6442.

Ekman, K., 1994. Applied Radiation Processing of Polyolefins. Åbo Akademi University.

Elder, D.P., 2005. Pharmaceutical Applications of Ion-Exchange Resins. J Chem Educ 82, 575.

Essa, E.A., Bonner, M.C., Barry, B.W., 2002a. Human skin sandwich for assessing shunt route penetration during passive and iontophoretic drug and liposome delivery. J Pharm Pharmacol 54, 1481-1490.

Essa, E.A., Bonner, M.C., Barry, B.W., 2002b. Iontophoretic estradiol skin delivery and tritium exchange in ultradeformable liposomes. Int J Pharm 240, 55-66.

Essa, E.A., Bonner, M.C., Barry, B.W., 2004. Electrically assisted skin delivery of liposomal estradiol; phospholipid as damage retardant. J Control Release 95, 535-546.

Fang, J.Y., Sung, K.C., Lin, H.H., Fang, C.L., 1999. Transdermal iontophoretic delivery of enoxacin from various liposome-encapsulated formulations. J Control Release 60, 1-10.

Farahmand, S., Maibach, H.I., 2009. Estimating skin permeability from physicochemical characteristics of drugs: A comparison between conventional models and an in vivo-based approach. Int J Pharm 375, 41-47.

Finkelstein, A., Mauro, A., 2011. Physical Principles and Formalisms of Electrical Excitability, Comprehensive Physiology. John Wiley & Sons, Inc.

Florence, A.T., Attwood, A.D., 2011. Physicochemical Principles of Pharmacy. Pharmaceutical Press, London.

Gao, Y., Yuan, J., Liu, H., Yang, Y., Hou, Y., Li, S., 2014. Tramadol loading, release and iontophoretic characteristics of ion-exchange fiber. Int J Pharm 465, 102-111.

Godin, B., Touitou, E., 2007. Transdermal skin delivery: predictions for humans from in vivo, ex vivo and animal models. Adv Drug Deliv Rev 59, 1152-1161.
Goodman, L.S., Gilman, A., Brunton, L.L., Lazo, J.S., Parker, K.L., 2006. Goodman & Gilman's the pharmacological basis of therapeutics. McGraw-Hill, New York.
Gratieri, T., Alberti, I., Lapteva, M., Kalia, Y.N., 2013. Next generation intra- and transdermal therapeutic systems: using non- and minimally-invasive technologies to increase drug delivery into and across the skin. Eur J Pharm Sci 50, 609-622.
Gratieri, T., Kalaria, D., Kalia, Y.N., 2011. Non-invasive iontophoretic delivery of peptides and proteins across the skin. Expert Opin Drug Deliv 8, 645-663.
Gratieri, T., Kalia, Y.N., 2013. Mathematical models to describe iontophoretic transport in vitro and in vivo and the effect of current application on the skin barrier. Adv Drug Deliv Rev 65, 315-329.
Green, P.G., 1996. Iontophoretic delivery of peptide drugs. J Control Release 41, 33-48.
Gregor, H.P., 1951. Gibbs-Donnan Equilibria in Ion Exchange Resin Systems. J Am Chem Soc 73, 642-650.
Guo, X., Chang, R.K., Hussain, M.A., 2009. Ion-exchange resins as drug delivery carriers. J Pharm Sci 98, 3886-3902.
Guy, R.H., 1996. Current status and future prospects of transdermal drug delivery. Pharm Res 13, 1765-1769.
Guy, R.H., 2010. Transdermal Drug Delivery, in: Schäfer-Korting, M. (Ed.), Drug Deliv. Springer Berlin Heidelberg, Berlin, Heidelberg, pp. 399-410.
Guy, R.H., Hadgraft, J., 1992. Rate control in transdermal drug delivery? Int J Pharm 82, R1-R6.
Guy, R.H., Hadgraft, J., 2002. Transdermal Drug Delivery Systems: Revised and Expanded. Taylor & Francis.
Guy, R.H., Kalia, Y.N., Delgado-Charro, M.B., Merino, V., Lopez, A., Marro, D., 2000. Iontophoresis: electrorepulsion and electroosmosis. J Control Release 64, 129-132.
Hadgraft, J., Guy, R.H., 2002. Feasibility assessment in topical and transdermal delivery: mathematical models and in vitro studies, in: Hadgraft, J., Guy, R.H. (Eds.), Transdermal Drug Delivery. Informa Health Care, New York, pp. 1-25.
Han, I., Kim, M., Kim, J., 2004. Enhanced transfollicular delivery of adriamycin with a liposome and iontophoresis. Exp Dermatol 13, 86-92.
Harland, C.E., 1994. Ion exchange: theory and practice. Royal Society of Chemistry, Cambridge.
Helfferich, F., 1995. Ion exchange. Dover Publications Inc., New York.
Helmstadter, A., 2001. The history of electrically-assisted transdermal drug delivery ("iontophoresis"). Die Pharmazie 56, 583-587.
Herwadkar, A., Banga, A.K., 2011. Transdermal Delivery of Peptides and Proteins, in: Van der Walle, C. (Ed.), Peptide and Protein Delivery. Academic Press, China.
Herwadkar, A., Banga, A.K., 2012. An update on the application of physical technologies to enhance intradermal and transdermal drug delivery. Ther Deliv 3, 339-355.
Hirvonen, J., 2005. Topical iontophoretic delivery. Am J Drug Deliv 3, 67-81.

Hirvonen, J., Kalia, Y.N., Guy, R.H., 1996. Transdermal delivery of peptides by iontophoresis. Nat Biotechnol 14, 1710-1713.
Hogan, N.C., Taberner, A.J., Jones, L.A., Hunter, I.W., 2015. Needle-free delivery of macromolecules through the skin using controllable jet injectors. Expert Opin Drug Deliv 12, 1637-1648.
Hoogstraate, A.J., Srinivasan, V., Sims, S.M., Higuchi, W.I., 1994. Iontophoretic Enhancement of Peptides - Behavior of Leuprolide Versus Model Permeants. J Control Release 31, 41-47.
Howard, J.P., Drake, T.R., Kellogg, D.L., Jr., 1995. Effects of alternating current iontophoresis on drug delivery. Arch Phys Med Rehabil 76, 463-466.
Hussain, M.A., DiLuccio, R.C., Shefter, E., 1989. Hollow fibers as an oral sustained-release delivery system. Pharm Res 6, 49-52.
Hänninen, K., 2008. Characterization of Ion-Exchange Fibers for Controlled Drug Delivery, Faculty of Pharmacy. University of Helsinki, Helsinki.
Hänninen, K.R., Murtomäki, L.S., Kaukonen, A.M., Hirvonen, J.T., 2007. The effect of valence on the ion-exchange process: theoretical and experimental aspects on compound binding/release. J Pharm Sci 96, 117-131.
Ita, K., 2015. Transdermal Delivery of Drugs with Microneedles-Potential and Challenges. Pharmaceutics 7, 90-105.
Ito, Y., Casolaro, M., Kono, K., Imanishi, Y., 1989. An insulin-releasing system that is responsive to glucose. J Control Release 10, 195-203.
Jackson, S.J., Bush, D., Perkins, A.C., 2001. Comparative scintigraphic assessment of the intragastric distribution and residence of cholestyramine, Carbopol 934P and sucralfate. Int J Pharm 212, 55-62.
Jani, R., Gan, O., Ali, Y., Rodstrom, R., Hancock, S., 1994. Ion exchange resins for ophthalmic delivery. J Ocul Pharmacol 10, 57-67.
Jaskari, T., Vuorio, M., Kontturi, K., Manzanares, J.A., Hirvonen, J., 2001. Ion-exchange fibers and drugs: an equilibrium study. J Control Release 70, 219-229.
Jaskari, T., Vuorio, M., Kontturi, K., Urtti, A., Manzanares, J.A., Hirvonen, J., 2000. Controlled transdermal iontophoresis by ion-exchange fiber. J Control Release 67, 179-190.
Joshi, N., Lemke, J., Danesi, H., 2016. Design and functionality of a smart fentanyl iontophoretic transdermal system for the treatment of moderate-to-severe postoperative pain. Pain Manag 6, 137-145.
Junyaprasert, V.B., Manwiwattanakul, G., 2008. Release profile comparison and stability of diltiazem-resin microcapsules in sustained release suspensions. Int J Pharm 352, 81-91.
Kajimoto, K., Yamamoto, M., Watanabe, M., Kigasawa, K., Kanamura, K., Harashima, H., Kogure, K., 2011. Noninvasive and persistent transfollicular drug delivery system using a combination of liposomes and iontophoresis. Int J Pharm 403, 57-65.
Kalia, Y.N., Naik, A., Garrison, J., Guy, R.H., 2004. Iontophoretic drug delivery. Adv Drug Deliv Rev 56, 619-658.
Kankkunen, T., 2002. Controlled Transdermal Drug Delivery by Iontophoresis and Ion-exchange Fiber, Faculty of Science, Department of Pharmacy. University of Helsinki, Helsinki.
Kankkunen, T., Huupponen, I., Lahtinen, K., Sundell, M., Ekman, K., Kontturi, K., Hirvonen, J., 2002a. Improved stability and release control of levodopa and

metaraminol using ion-exchange fibers and transdermal iontophoresis. Eur J Pharm Sci 16, 273-280.
Kankkunen, T., Sulkava, R., Vuorio, M., Kontturi, K., Hirvonen, J., 2002b. Transdermal iontophoresis of tacrine in vivo. Pharm Res 19, 704-707.
Kantaria, S., Rees, G.D., Lawrence, M.J., 1999. Gelatin-stabilised microemulsion-based organogels: rheology and application in iontophoretic transdermal drug delivery. J Control Release 60, 355-365.
Karande, P., Jain, A., Ergun, K., Kispersky, V., Mitragotri, S., 2005. Design principles of chemical penetration enhancers for transdermal drug delivery. Proc Natl Acad Sci U S A 102, 4688-4693.
Khan, K.A., Rhodes, C.T., 1975. Water-sorption properties of tablet disintegrants. J Pharm Sci 64, 447-451.
Khan, N.R., Harun, M.S., Nawaz, A., Harjoh, N., Wong, T.W., 2015. Nanocarriers and their Actions to Improve Skin Permeability and Transdermal Drug Delivery. Curr Pharm Des 21, 2848-2866.
Kigasawa, K., Miyashita, M., Kajimoto, K., Kanamura, K., Harashima, H., Kogure, K., 2012. Efficient intradermal delivery of superoxide dismutase using a combination of liposomes and iontophoresis for protection against UV-induced skin damage. Biol Pharm Bull 35, 781-785.
Knoblauch, P., Moll, F., 1993. In vitro pulsatile and continuous transdermal delivery of buserelin by iontophoresis. J Control Release 26, 203-212.
Knorr, F., Lademann, J., Patzelt, A., Sterry, W., Blume-Peytavi, U., Vogt, A., 2009. Follicular transport route--research progress and future perspectives. Eur J Pharm Biopharm 71, 173-180.
Kochhar, C., Imanidis, G., 2003. In vitro transdermal iontophoretic delivery of leuprolide-mechanisms under constant voltage application. J Pharm Sci 92, 84-96.
Kochhar, C., Imanidis, G., 2004. In vitro transdermal iontophoretic delivery of leuprolide under constant current application. J Control Release 98, 25-35.
Kogan, A., Garti, N., 2006. Microemulsions as transdermal drug delivery vehicles. Adv Colloid Interface Sci 123–126, 369-385.
Kosandrovich, E.G., Soldatov, V.S., 2012. Fibrous Ion Exchangers, in: Dr, I., Luqman, M. (Eds.), Ion Exchange Technology I: Theory and Materials. Springer Netherlands, Dordrecht, pp. 299-371.
Kulkarni, S.B., Banga, A.K., Betageri, G.V., 1996. Transdermal lontophoretic delivery of colchicine encapsulated in liposomes. Drug Deliv 3, 245-250.
Labouta, H.I., Kraus, T., El-Khordagui, L.K., Schneider, M., 2011. Combined multiphoton imaging-pixel analysis for semiquantitation of skin penetration of gold nanoparticles. Int J Pharm 413, 279-282.
Lademann, J., Patzelt, A., Richter, H., Antoniou, C., Sterry, W., Knorr, F., 2009. Determination of the cuticula thickness of human and porcine hairs and their potential influence on the penetration of nanoparticles into the hair follicles. J Biomed Opt 14, 021014.
Lademann, J., Richter, H., Teichmann, A., Otberg, N., Blume-Peytavi, U., Luengo, J., Weiß, B., Schaefer, U.F., Lehr, C.-M., Wepf, R., Sterry, W., 2007. Nanoparticles – An efficient carrier for drug delivery into the hair follicles. Eur J Pharm Biopharm 66, 159-164.
Lai, P., Daear, W., Lobenberg, R., Prenner, E.J., 2014. Overview of the preparation of organic polymeric nanoparticles for drug delivery based on gelatine,

chitosan, poly(d,l-lactide-co-glycolic acid) and polyalkylcyanoacrylate. Colloids Surf B Biointerfaces 118, 154-163.
Lau, D.T., Sharkey, J.W., Petryk, L., Mancuso, F.A., Yu, Z., Tse, F.L., 1994. Effect of current magnitude and drug concentration on iontophoretic delivery of octreotide acetate (Sandostatin) in the rabbit. Pharm Res 11, 1742-1746.
Lauer, A.C., Lieb, L.M., Ramachandran, C., Flynn, G.L., Weiner, N.D., 1995. Transfollicular drug delivery. Pharm Res 12, 179-186.
Lawler, J.C., Davis, M.J., Griffith, E.C., 1960. Electrical characteristics of the skin. The impedance of the surface sheath and deep tissues. J Invest Dermatol 34, 301-308.
Lee, P.W., Hsu, S.H., Tsai, J.S., Chen, F.R., Huang, P.J., Ke, C.J., Liao, Z.X., Hsiao, C.W., Lin, H.J., Sung, H.W., 2010. Multifunctional core-shell polymeric nanoparticles for transdermal DNA delivery and epidermal Langerhans cells tracking. Biomaterials 31, 2425-2434.
Levin, G., Gershonowitz, A., Sacks, H., Stern, M., Sherman, A., Rudaev, S., Zivin, I., Phillip, M., 2005. Transdermal delivery of human growth hormone through RF-microchannels. Pharm Res 22, 550-555.
Li, S.K., Zhu, H., Higuchi, W.I., 2006. Enhanced transscleral iontophoretic transport with ion-exchange membrane. Pharm Res 23, 1857-1867.
Lindner, L.H., Hossann, M., 2010. Factors affecting drug release from liposomes. Curr Opin Drug Discov Devel 13, 111-123.
Lito, P.F., Cardoso, S.P., Loureiro, J.M., Silva, C.M., 2012. Ion Exchange Equilibria and Kinetics, in: Dr, I., Luqman, M. (Eds.), Ion Exchange Technology I: Theory and Materials. Springer Netherlands, Dordrecht, pp. 51-120.
Liu, W., Hu, M., Liu, W., Xue, C., Xu, H., Yang, X., 2008. Investigation of the carbopol gel of solid lipid nanoparticles for the transdermal iontophoretic delivery of triamcinolone acetonide acetate. Int J Pharm 364, 135-141.
Losi, P., Briganti, E., Errico, C., Lisella, A., Sanguinetti, E., Chiellini, F., Soldani, G., 2013. Fibrin-based scaffold incorporating VEGF- and bFGF-loaded nanoparticles stimulates wound healing in diabetic mice. Acta Biomater 9, 7814-7821.
Lu, J.M., Wang, X., Marin-Muller, C., Wang, H., Lin, P.H., Yao, Q., Chen, C., 2009. Current advances in research and clinical applications of PLGA-based nanotechnology. Expert Rev Mol Diagn 9, 325-341.
Lu, M.F., Lee, D., Carlson, R., Rao, G.S., Hui, H.W., Adjei, L., Herrin, M., Sundberg, D., Hsu, L., 1993. The Effects of Formulation Variables on Iontophoretic Transdermal Delivery of Leuprolide to Humans. Drug Dev Ind Pharm 19, 1557-1571.
Lu, M.Y., Borodkin, S., Woodward, L., Li, P., Diesner, C., Hernandez, L., Vadnere, M., 1991. A polymer carrier system for taste masking of macrolide antibiotics. Pharm Res 8, 706-712.
Luengo, J., Weiss, B., Schneider, M., Ehlers, A., Stracke, F., Konig, K., Kostka, K.H., Lehr, C.M., Schaefer, U.F., 2006. Influence of nanoencapsulation on human skin transport of flufenamic acid. Skin Pharmacol Physiol 19, 190-197.
Marro, D., Guy, R.H., Delgado-Charro, M.B., 2001. Characterization of the iontophoretic permselectivity properties of human and pig skin. J Control Release 70, 213-217.
McCrudden, M.T., Singh, T.R., Migalska, K., Donnelly, R.F., 2013. Strategies for enhanced peptide and protein delivery. Ther Deliv 4, 593-614.

Michinaka, Y., Mitragotri, S., 2011. Delivery of polymeric particles into skin using needle-free liquid jet injectors. J Control Release 153, 249-254.
Miller, L.L., Kolaskie, C.J., Smith, G.A., Rivier, J., 1990. Transdermal iontophoresis of gonadotropin releasing hormone (LHRH) and two analogues. J Pharm Sci 79, 490-493.
Mitragotri, S., 2013. Devices for overcoming biological barriers: the use of physical forces to disrupt the barriers. Adv Drug Deliv Rev 65, 100-103.
Mittal, A., Raber, A.S., Schaefer, U.F., Weissmann, S., Ebensen, T., Schulze, K., Guzman, C.A., Lehr, C.M., Hansen, S., 2013. Non-invasive delivery of nanoparticles to hair follicles: a perspective for transcutaneous immunization. Vaccine 31, 3442-3451.
Moffat, A.C., 1986. Clarke's Isolation and Identification of Drugs. Pharmaceutical Press, London.
Mutalik, S., Parekh, H.S., Anissimov, Y.G., Grice, J.E., Roberts, M.S., 2013. Iontophoresis-mediated transdermal permeation of peptide dendrimers across human epidermis. Skin Pharmacol Physiol 26, 127-138.
Naik, A., Kalia, Y.N., Guy, R.H., 2000. Transdermal drug delivery: overcoming the skin's barrier function. Pharm Sci Technolo Today 3, 318-326.
Neef, C., van Laar, T., 1999. Pharmacokinetic-pharmacodynamic relationships of apomorphine in patients with Parkinson's disease. Clin Pharmacokinet 37, 257-271.
Neubert, R.H., 2011. Potentials of new nanocarriers for dermal and transdermal drug delivery. Eur J Pharm Biopharm 77, 1-2.
Nicoli, S., Santi, P., Couvreur, P., Couarraze, G., Colombo, P., Fattal, E., 2001. Design of triptorelin loaded nanospheres for transdermal iontophoretic administration. Int J Pharm 214, 31-35.
Oberli, M.A., Schoellhammer, C.M., Langer, R., Blankschtein, D., 2014. Ultrasound-enhanced transdermal delivery: recent advances and future challenges. Ther Deliv 5, 843-857.
Ozcan, I., Azizoglu, E., Senyigit, T., Ozyazici, M., Ozer, O., 2013. Comparison of PLGA and lecithin/chitosan nanoparticles for dermal targeting of betamethasone valerate. J Drug Target 21, 542-550.
Parhi, R., Suresh, P., Mondal, S., Kumar, P.M., 2012. Novel penetration enhancers for skin applications: a review. Curr Drug Deliv 9, 219-230.
Parra, A., Clares, B., Rossello, A., Garduno-Ramirez, M.L., Abrego, G., Garcia, M.L., Calpena, A.C., 2016. Ex vivo permeation of carprofen from nanoparticles: A comprehensive study through human, porcine and bovine skin as anti-inflammatory agent. Int J Pharm 501, 10-17.
Pastore, M.N., Kalia, Y.N., Horstmann, M., Roberts, M.S., 2015. Transdermal patches: history, development and pharmacology. Br J Pharmacol 172, 2179-2209.
Patzelt, A., Richter, H., Buettemeyer, R., Huber, H.J., Blume-Peytavi, U., Sterry, W., Lademann, J., 2008. Differential stripping demonstrates a significant reduction of the hair follicle reservoir in vitro compared to in vivo. Eur J Pharm Biopharm 70, 234-238.
Payne, W.W., 1956. Ion-exchange resins in clinical medicine. J Pharm Pharmacol 8, 397-402.

Philipse, A., Vrij, A., 2011. The Donnan equilibrium: I. On the thermodynamic foundation of the Donnan equation of state. J Phys Condens Matter 23, 194106.
Phipps, B.J., Gyory, J.R., 1992. Transdermal ion migration. Adv Drug Deliv Rev 9, 137-176.
Pierre, M.B., Dos Santos Miranda Costa, I., 2011. Liposomal systems as drug delivery vehicles for dermal and transdermal applications. Arch Dermatol Res 303, 607-621.
Pikal, M.J., 2001. The role of electroosmotic flow in transdermal iontophoresis. Adv Drug Deliv Rev 46, 281-305.
Prausnitz, M.R., 1999. A practical assessment of transdermal drug delivery by skin electroporation. Adv Drug Deliv Rev 35, 61-76.
Prausnitz, M.R., 2004. Microneedles for transdermal drug delivery. Adv Drug Deliv Rev 56, 581-587.
Prausnitz, M.R., Langer, R., 2008. Transdermal drug delivery. Nat Biotechnol 26, 1261-1268.
Prescrire, 2009. Fentanyl transdermal system: market withdrawal. Exposes patients to a risk of overdose. The market withdrawal, due to a manufacturing defect, is more than welcome. Prescrire international 18, 110.
Prow, T.W., Grice, J.E., Lin, L.L., Faye, R., Butler, M., Becker, W., Wurm, E.M., Yoong, C., Robertson, T.A., Soyer, H.P., Roberts, M.S., 2011. Nanoparticles and microparticles for skin drug delivery. Adv Drug Deliv Rev 63, 470-491.
Raber, A.S., Mittal, A., Schafer, J., Bakowsky, U., Reichrath, J., Vogt, T., Schaefer, U.F., Hansen, S., Lehr, C.M., 2014. Quantification of nanoparticle uptake into hair follicles in pig ear and human forearm. J Control Release 179, 25-32.
Raghunathan, Y., 1980. Prolonged release pharmaceutical preparations. Google Patents.
Raiman, J., Koljonen, M., Huikko, K., Kostiainen, R., Hirvonen, J., 2004. Delivery and stability of LHRH and Nafarelin in human skin: the effect of constant/pulsed iontophoresis. Eur J Pharm Sci 21, 371-377.
Ramirez, Patricio, Alcaraz, A., Mafé, S., Pellicer, J., 2002. Donnan Equilibrium of Ionic Drugs in pH-Dependent Fixed Charge Membranes: Theoretical Modeling. J Colloid Interface Sci 253, 171-179.
Rastogi, R., Anand, S., Koul, V., 2009. Flexible polymerosomes—An alternative vehicle for topical delivery. Colloids Surf B Biointerfaces 72, 161-166.
Roustit, M., Blaise, S., Cracowski, J.-L., 2014. Trials and tribulations of skin iontophoresis in therapeutics. Br J Clin Pharmacol 77, 63-71.
Sarveiya, V., Templeton, J.F., Benson, H.A.E., 2004. Ion-pairs of ibuprofen: increased membrane diffusion. J Pharm Pharmacol 56, 717-724.
Schroeter, A., Engelbrecht, T., Neubert, R.H., Goebel, A.S., 2010. New nanosized technologies for dermal and transdermal drug delivery. A review. J Biomed Nanotechnol 6, 511-528.
Schuetz, Y.B., Naik, A., Guy, R.H., Kalia, Y.N., 2005a. Effect of amino acid sequence on transdermal iontophoretic peptide delivery. Eur J Pharm Sci 26, 429-437.
Schuetz, Y.B., Naik, A., Guy, R.H., Vuaridel, E., Kalia, Y.N., 2005b. Transdermal iontophoretic delivery of vapreotide acetate across porcine skin in vitro. Pharm Res 22, 1305-1312.

Schuetz, Y.B., Naik, A., Guy, R.H., Vuaridel, E., Kalia, Y.N., 2005c. Transdermal iontophoretic delivery of vapreotide acetate across porcine skin in vitro. Pharm. Res. 22, 1305-1312.

Sekkat, N., Kalia, Y.N., Guy, R.H., 2001. Control of drug delivery across an impaired skin barrier by iontophoresis, Proceed. Int'l. Symp. Control. Rel. Bioact. Mater., San Diego (USA), pp. 185-186.

Sennello, L.T., Finley, R.A., Chu, S.Y., Jagst, C., Max, D., Rollins, D.E., Tolman, K.G., 1986. Single-dose pharmacokinetics of leuprolide in humans following intravenous and subcutaneous administration. J Pharm Sci 75, 158-160.

Shahzad, Y., Louw, R., Gerber, M., du Plessis, J., 2015. Breaching the skin barrier through temperature modulations. J Control Release 202, 1-13.

Shaw, J., Urquhart, J., 1979. Programmed, systemic drug delivery by the transdermal route. Trends Pharmacol Sci 1, 208-211.

Shaw, J.E., Chandrasekaran, S.K., Campbell, P., 1976. Percutaneous Absorption: Controlled Drug Delivery For Topical or Systemic Therapy. J Invest Dermatol 67, 677-678.

Shaw, J.E., Theeuwes, F., 1985. Transdermal dosage forms, in: Prescott, L.F., Nimmo, W.S. (Eds.), Rate control in drug therapy. Churchill Livingstone, New York, pp. 65-70.

Sieg, A., Wascotte, V., 2009. Diagnostic and therapeutic applications of iontophoresis. J Drug Target 17, 690-700.

Sinatra, R., 2005. The fentanyl HCl patient-controlled transdermal system (PCTS): an alternative to intravenous patient-controlled analgesia in the postoperative setting. Clin Pharmacokinet 44 Suppl 1, 1-6.

Singh, P., Puchun, L., Dinh, S.M., 1998. in: Bronaugh, R.L., Maibach, H.I. (Eds.), Percutaneous Absorption: Drugs--Cosmetics--Mechanisms--Methods, 3rd ed. Marcel Dekker Inc., New York.

Singh, P., Roberts, M.S., Maibach, H.I., 1995. Modelling of plasma levels of drugs following transdermal iontophoresis. J Control Release 33, 293-298.

Sintov, A.C., Brandys-Sitton, R., 2006. Facilitated skin penetration of lidocaine: combination of a short-term iontophoresis and microemulsion formulation. Int J Pharm 316, 58-67.

Sintov, A.C., Krymberk, I., Daniel, D., Hannan, T., Sohn, Z., Levin, G., 2003. Radiofrequency-driven skin microchanneling as a new way for electrically assisted transdermal delivery of hydrophilic drugs. J Control Release 89, 311-320.

Sklar, L.R., Burnett, C.T., Waibel, J.S., Moy, R.L., Ozog, D.M., 2014. Laser assisted drug delivery: a review of an evolving technology. Lasers Surg Med 46, 249-262.

Sloan, K.B., Wasdo, S., 2003. Designing for topical delivery: Prodrugs can make the difference. Med Res Rev 23, 763-793.

Sloan, K.B., Wasdo, S.C., 2007. Topical Delivery Using Prodrugs, in: Stella, V.J., Borchardt, R.T., Hageman, M.J., Oliyai, R., Maag, H., Tilley, J.W. (Eds.), Prodrugs: Challenges and Rewards Part 1. Springer New York, New York, NY, pp. 83-123.

Stachowiak, J.C., Li, T.H., Arora, A., Mitragotri, S., Fletcher, D.A., 2009. Dynamic control of needle-free jet injection. J Control Release 135, 104-112.

Steinstrasser, I., Merkle, H.P., 1995. Dermal metabolism of topically applied drugs: pathways and models reconsidered. Pharm Acta Helv 70, 3-24.

Sundell, M.J., Ekman, K.B., Svarfvar, B.L., Näsman, J.H., 1995. Preparation of poly[ethylene-g-(vinylbenzyl chloride)] and functionalization with bis(phosphonic acid) derivatives. Reactive Polymers 25, 1-16.

Zakzewski, C., Amory, D., Jasaitis, D., Li, J.-J., 1992. Iontophoretically enhanced transdermal delivery of an ACE inhibitor in induced hypertensive rabbits: Preliminary report. Cardiovasc Drug Ther 6, 589-595.

Zhai, Y., Zhai, G., 2014. Advances in lipid-based colloid systems as drug carrier for topic delivery. J Control Release 193, 90-99.

Zhang, Z., Tsai, P.-C., Ramezanli, T., Michniak-Kohn, B.B., 2013. Polymeric nanoparticles-based topical delivery systems for the treatment of dermatological diseases. Wiley Interdiscip Rev Nanomed Nanobiotechnol 5, 205-218.

Zhang, W., Gao, J., Zhu, Q., Zhang, M., Ding, X., Wang, X., Hou, X., Fan, W., Ding, B., Wu, X., Wang, X., Gao, S., 2010. Penetration and distribution of PLGA nanoparticles in the human skin treated with microneedles. Int J Pharm 402, 205-212.

Zhu, H., Li, S.K., Peck, K.D., Miller, D.J., Higuchi, W.I., 2002. Improvement on conventional constant current DC iontophoresis: a study using constant conductance AC iontophoresis. J Control Release 82, 249-261.

Thomas, B.J., Finnin, B.C., 2004. The transdermal revolution. Drug Discov Today 9, 697-703.

Thong, H.Y., Zhai, H., Maibach, H.I., 2007. Percutaneous penetration enhancers: an overview. Skin Pharmacol Physiol 20, 272-282.

Tinkle, S.S., Antonini, J.M., Rich, B.A., Roberts, J.R., Salmen, R., DePree, K., Adkins, E.J., 2003. Skin as a route of exposure and sensitization in chronic beryllium disease. Environ Health Perspect 111, 1202-1208.

Tomoda, K., Terashima, H., Suzuki, K., Inagi, T., Terada, H., Makino, K., 2011. Enhanced transdermal delivery of indomethacin-loaded PLGA nanoparticles by iontophoresis. Colloids Surf B Biointerfaces 88, 706-710.

Tomoda, K., Terashima, H., Suzuki, K., Inagi, T., Terada, H., Makino, K., 2012a. Enhanced transdermal delivery of indomethacin using combination of PLGA nanoparticles and iontophoresis in vivo. Colloids Surf B Biointerfaces 92, 50-54.

Tomoda, K., Watanabe, A., Suzuki, K., Inagi, T., Terada, H., Makino, K., 2012b. Enhanced transdermal permeability of estradiol using combination of PLGA nanoparticles system and iontophoresis. Colloids Surf B Biointerfaces 97, 84-89.

Touitou, E., Dayan, N., Bergelson, L., Godin, B., Eliaz, M., 2000. Ethosomes - novel vesicular carriers for enhanced delivery: characterization and skin penetration properties. J Control Release 65, 403-418.

Tsujimoto, H., Hara, K., Tsukada, Y., Huang, C.C., Kawashima, Y., Arakaki, M., Okayasu, H., Mimura, H., Miwa, N., 2007. Evaluation of the permeability of hair growing ingredient encapsulated PLGA nanospheres to hair follicles and their hair growing effects. Bioorg Med Chem Lett 17, 4771-4777.

Uchegbu, I.F., Vyas, S.P., 1998. Non-ionic surfactant based vesicles (niosomes) in drug delivery. Int J Pharm 172, 33-70.

Walters, K.A., Hadgraft, J., 1993. Pharmaceutical Skin Penetration Enhancement. Taylor & Francis.

van der Geest, R., van Laar, T., Kruger, P.P., Gubbens-Stibbe, J.M., Bodde, H.E., Roos, R.A., Danhof, M., 1998. Pharmacokinetics, enantiomer interconversion, and metabolism of R-apomorphine in patients with idiopathic Parkinson's disease. Clin Neuropharmacol 21, 159-168.

van der Maaden, K., Jiskoot, W., Bouwstra, J., 2012. Microneedle technologies for (trans)dermal drug and vaccine delivery. J Control Release 161, 645-655.

Vecchia, B.E., Bunge, A.L., 2002. Evaluating the transdermal permeability of chemicals, in: Hadgraft, J., Guy, R.H. (Eds.), Transdermal Drug Delivery. Marcel Dekker, New York, pp. 25-57.

Vega, E., Egea, M.A., Garduno-Ramirez, M.L., Garcia, M.L., Sanchez, E., Espina, M., Calpena, A.C., 2013. Flurbiprofen PLGA-PEG nanospheres: role of hydroxy-beta-cyclodextrin on ex vivo human skin permeation and in vivo topical anti-inflammatory efficacy. Colloids Surf B Biointerfaces 110, 339-346.

Weiner, N., Lieb, L., Niemiec, S., Ramachandran, C., Hu, Z., Egbaria, K., 1994. Liposomes: a novel topical delivery system for pharmaceutical and cosmetic applications. J Drug Target 2, 405-410.

Weiss, R., Hessenberger, M., Kitzmüller, S., Bach, D., Weinberger, E.E., Krautgartner, W.D., Hauser-Kronberger, C., Malissen, B., Boehler, C., Kalia, Y.N., Thalhamer, J., Scheiblhofer, S., 2012. Transcutaneous vaccination via laser microporation. J Control Release 162, 391-399.

Wiedersberg, S., Guy, R.H., 2014. Transdermal drug delivery: 30+ years of war and still fighting! J Control Release 190, 150-156.

Williams, A., 2003. Transdermal and Topical Drug Delivery: from Theory to Clinical Practice. Pharmaceutical Press, London.

Wu, X.S., Wang, N., 2001. Synthesis, characterization, biodegradation, and drug delivery application of biodegradable lactic/glycolic acid polymers. Part II: biodegradation. J Biomater Sci Polym Ed 12, 21-34.

Vuorio, M., 2004. The Use of Ion-Exchange Fibers in Controlled Transdermal Iontophoretic Drug Delivery, Department of Chemical Technology. Helsinki University of Technology, Espoo, Finland.

Vuorio, M., Manzanares, J.A., Murtomaki, L., Hirvonen, J., Kankkunen, T., Kontturi, K., 2003. Ion-exchange fibers and drugs: a transient study. J Control Release 91, 439-448.

Vutla, N.B., Betageri, G.V., Banga, A.K., 1996. Transdermal iontophoretic delivery of enkephalin formulated in liposomes. J Pharm Sci 85, 5-8.

Xin, C., Li-Hong, W., Yue, Y., Ya-Nan, G., Qi-Fang, W., Yang, Y., San-Ming, L., 2012. A novel method to enhance the efficiency of drug transdermal iontophoresis delivery by using complexes of drug and ion-exchange fibers. Int J Pharm 428, 68-75.

Xin, C., Lihong, W., Fei, H., Yan, W., Qifang, W., Yang, Y., Yue, Y., San-ming, L., 2014. To enhance the efficiency of nefopam transdermal iontophoresis by using a novel method based on ion-exchange fiber. Drug Dev Ind Pharm 40, 9-16.

Xu, Q., Ibrahim, S.A., Higuchi, W.I., Li, S.K., 2009. Ion-exchange membrane assisted transdermal iontophoretic delivery of salicylate and acyclovir. Int J Pharm 369, 105-113.

Yoshida, N.H., Roberts, M.S., 1993. Solute molecular size and transdermal iontophoresis across excised human skin. J Control Release 25, 177-195.

Yu, J., Kalaria, D.R., Kalia, Y.N., 2011. Erbium:YAG fractional laser ablation for the percutaneous delivery of intact functional therapeutic antibodies. J Control Release 156, 53-59.

Yu, L., Li, S., Yuan, Y., Dai, Y., Liu, H., 2006. The delivery of ketoprofen from a system containing ion-exchange fibers. Int J Pharm 319, 107-113.

Yuan, J., Gao, Y., Wang, X., Liu, H., Che, X., Xu, L., Yang, Y., Wang, Q., Wang, Y., Li, S., 2014. The load and release characteristics on a strong cationic ion-exchange fiber: kinetics, thermodynamics, and influences. Drug Des Devel Ther 8, 945-955.